Electronic Supplementary Material (ESI) for Chemical Science.
This journal is © The Royal Society of Chemistry 2021

Supplementary Materials for

Introduction of Plumbole to f-Element Chemistry

Luca Münzfeld,‡[a] Xiaofei Sun,‡[a] Sören Schlittenhardt,[b] Christoph Schoo,[a] Adrian Hauser,[a] Sebastian Gillhuber,[c] Florian Weigend,[d] Mario Ruben,*[b,e,f] Peter W. Roesky*[a]

[a] L. Münzfeld, X. Sun, Dr. C. Schoo, A. Hauser, Prof. Dr. P. W. Roesky
Institute of Inorganic Chemistry, Karlsruhe Institute of Technology (KIT), Engesserstraße 15, D-76131 Karlsruhe, Germany.
E-mail: roesky@kit.edu
[b] S. Schlittenhardt, Prof. Dr. M. Ruben
Institute of Nanotechnology, Karlsruhe Institute of Technology (KIT), Hermann-von-Helmholtz-Platz 1, D-76344 Eggenstein-Leopoldshafen, Germany.
[c] S. Gillhuber
Institute of Physical Chemistry, Karlsruhe Institute of Technology (KIT), Engesserstraße 15, D-76131 Karlsruhe, Germany.
[d] Prof. Dr. F. Weigend
Fachbereich Chemie, Philipps-Universität Marburg, Hans-Meerwein-Straße 4, D-35032 Marburg, Germany.
[e] Prof. Dr. M. Ruben
Centre Européen de Science Quantique (CESQ); Institut de Science et d'Ingénierie Supramoléculaires (ISIS, UMR 7006), CNRS-Université de Strasbourg, 8 allée Gaspard Monge BP 70028 67083 Strasbourg Cedex, France.
[f] Prof. Dr. M. Ruben
Institute of Quantum Materials and Technologies (IQMT), Karlsruhe Institute of Technology, Hermann-von-Helmholtz-Platz 1, 76344 Eggenstein-Leopoldshafen, Germany.

Table of Contents

Supplementary Methods

General Considerations: All manipulations of air-sensitive materials were performed under rigorous exclusion of oxygen and moisture in flame-dried Schlenk-type glassware either on a dual manifold Schlenk line, interfaced to a high vacuum (10^{-3} torr) pump, or in an argon-filled *MBraun* glove box. Hydrocarbon solvents were pre-dried using an *MBraun* solvent purification system (*SPS-800*), degassed and stored *in vacuo* over $LiAlH_4$. Tetrahydrofuran was additionally distilled under nitrogen over potassium before storage *in vacuo* over $LiAlH_4$. C_6D_6 and THF-d_8 were dried over Na-K alloy and degassed by freeze-pump-thaw cycles.

Elemental analyses were carried out with an *Elementar Vario MICRO Cube*. NMR spectra were recorded on *Bruker* spectrometers (*Avance II* 300 MHz, *Avance* 400 MHz, or *Avance III* 400 MHz). Chemical shifts are referenced internally using signals of the residual protio solvent (^1H) or the solvent (^{13}C) and are reported relative to tetramethylsilane (^1H, $^{13}C\{^1H\}$), or externally relative to tetramethylsilane (^{29}Si) or 1.0 M LiCl(aq) (^7Li). All NMR spectra were measured at 298 K, unless otherwise specified. The multiplicity of the signals is indicated as s = singlet, d = doublet, dd = doublet of doublets, t = triplet, q = quartet, m = multiplet and br = broad. Assignments were determined based on unambiguous chemical shifts, coupling patterns, ^{13}C-DEPT experiments or 2D correlation experiments (^1H-^1H COSY, ^1H-^{13}C HMQC, ^1H-^{13}C HMBC and ^1H-^{29}Si HMBC).

Infrared (IR) spectra were recorded in the region 4000–400 cm^{-1} on a *Bruker Tensor 37 FTIR* spectrometer equipped with a room temperature DLaTGS detector, a diamond attenuated total reflection (ATR) unit and a nitrogen-flushed chamber. In terms of their intensity, the signals were classified into different categories (vs = very strong, s = strong, m = medium, w = weak).

Raman spectra were recorded in the region 4000-20 cm^{-1} on a *Bruker MultiRam* spectrometer equipped with a Nd:YAG laser (λ = 1064 nm) and a germanium detector at a resolution of 2 cm^{-1}. The powdered crystalline sample materials were flame sealed in a glass tube. The laser energy was adjusted to values between 20 and 200 mW depending on the FID amplitude and laser focusing. In terms of their intensity, the signals were classified into different categories (vs = very strong, s = strong, m = medium, w = weak).

HR-EI-MS spectra were recorded with a *Thermo Fisher Scientific DFS–Magnetic Sector GC/MS* instrument using powdered crystalline samples.

$[Ln(BH_4)(thf)_3]$ (Ln = La, Ce, Sm, Er), $[Li_2(thf)_2(L^{Pb})]$ (L^{Pb} = 1,4-bis-tert-butyl-dimethylsilyl-2,3-bis-phenyl-plumbolyl) and H_2COT^{TIPS} (TIPS = 1,4-bis-triisopropylsilyl-cyclooctatetraenyl) were prepared according to literature procedures.[1,2,3] All other chemicals were obtained from commercial sources and used without further purification.

Note: To ensure the best possible purity and reliability of all compounds, only crystalline material was isolated. Hence all yields and analytics refer to isolated crystalline samples, whereas yields are generally lower compared to bulk samples. Elemental analysis gave

reproducibly low C and H values for all compounds discussed here. In the case of compounds **1-4** this might mislead to the assumption, that the coordinated THF molecules are completely removed upon drying *in vacuo*. However, NMR experiments of the dried crystalline samples unambiguously proof that some amounts of THF-H_8 stemming from the dissolved compounds is still abundant. Since we could not determine the exact amount of residual THF in the samples, the theoretical values of **1-4** were calculated for the THF free species. The low C and H values are probably caused by carbide formation, e.g. caused by silicon or the lanthanide ions in **1-4**. HR-EI-MS spectra of compounds **1-4** were recorded to proof the suggested composition of the isolated crystalline material.

For compounds **5-10** a similar behavior is observed, however much less pronounced. We assume that this is caused by the lower mass percentage of the silicon and the corresponding lanthanide in complexes **5-10** compared to **1-4**, caused by the relatively high molar weight of the incorporated lead atom. This leads to C/H-values in the expected- to lower expected range.

Synthetic protocols

Synthesis of [$K_2(COT^{TIPS})$]

The deprotonation of H_2COT^{TIPS} was conducted in a modified procedure.[3] A mixture of H_2COT^{TIPS} (10.0 g, 24.0 mmol, 1.00 eq) and potassium *tert*-butoxide (5.38 g, 48.0 mmol, 2.00 eq) was suspended in 300 mL *n*-heptane. Afterwards *n*-BuLi (2.5 M in hexanes, 19.2 mL, 48.0 mmol, 2.00 eq) was added dropwise to the reaction mixture at room temperature under vigorous stirring. After complete addition, the reaction mixture turned dark red and the formation of an off-white solid was observed. The resultant suspension was stirred for 12 h at room temperature. Subsequently, precipitated [K_2COT^{TIPS}] was collected by filtration and washed with approximately 200 mL *n*-heptane until the washing solution remained colorless. After drying *in vacuo* [K_2COT^{TIPS}] was isolated as an off-white powder. Yield: 9.16 g (18.5 mmol, 77%).
^{1}H NMR in agreement with literature.[3]

Synthesis of [Ln(η^8-COT^{TIPS})BH_4] (1-4)

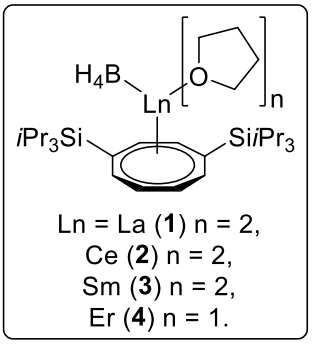

Ln = La (**1**) n = 2,
Ce (**2**) n = 2,
Sm (**3**) n = 2,
Er (**4**) n = 1.

In a general procedure THF was added at -78°C to a mixture of [$K_2(COT^{TIPS})$] (1.00 g, 2.02 mmol, 1.00 eq) and the corresponding [$Ln(BH4)_3(thf)_3$] (2.02 mmol, 1.00 eq, Ln = La: 801 mg, Ce: 804mg, Sm: 825 mg, Er: 859 mg). The resulting suspension was slowly warmed to room temperature and vigorously stirred for 12 h. During this time, the reaction mixture adopted a characteristic color depending on the corresponding lanthanide ion (La: light orange, Ce: yellow-green, Sm: purple, Er: orange) and the formation of an off-white solid was observed. Afterwards all volatiles were removed *in vacuo.* The residual solid was extracted with hot toluene (40 mL) and filtered over celite on a medium porosity sintered glass frit. The filtrate was stripped to dryness and washed with *n*-pentane until the washing solution remained colorless. The remaining solids were dried under reduced pressure and dissolved in hot toluene. Subsequently the obtained saturated solutions were stored at room temperature until the formation of crystalline material was observable. After this initial crystallization the samples were stored at -30 °C for one week to maximize the crystalline yields. The pure compounds were then isolated as crystalline solids (La: colorless, Ce: yellow, Sm: purple, Er: pink) by decantation of the mother liquor and drying *in vacuo* for 1 h. Further concentration of the mother liquor did not yield significant amounts of additional product. Single crystals suitable for X-ray diffraction were obtained by slow evaporation of a THF solution (**1**-**3**) or recrystallization from hot toluene (**4**). Elemental analysis indicates removal of THF from the complexes upon drying *in vacuo* for compounds **1**-**4**. Thus, above depiction of compounds **1**-**4**

reflects their molecular structure in the solid state as determined by SCXRD, since the exact structure of the isolated solvate-free compounds was not investigated.

[La(η^8-COT^{TIPS})BH_4] (1): Yield: 1.02 g (1.79 mmol), 89%. Anal. Calcd for $C_{26}H_{52}BSi_2La$ (570.59): C, 54.73; H, 9.19. Found: C, 54.77; H, 8.93. **HR-EI - MS**: (70 eV, QT = 180 °C): m/z [%] = 570.274 $[M]^+$ (25.75), 555.234 $[M\text{-}BH_4]^+$ (14.49); 513.185 $[M\text{-}BH_4\text{-}C_3H_6]^+$ (100). **^{1}H NMR** (400.30 MHz, THF-d_8): δ [ppm]: 6.77 (s, 2H, CH_{COT}); 6.66-6.59 (m, 2H, CH_{COT}); 6.55-6.49 (m, 2H, CH_{COT}); 3.64-3.60 (m, 4H, C$H_{2\ thf}$); 1.79-1.75 (m, 4H, C$H_{2\ thf}$); 1.63 (sept, $^3J_{HH}$ = 7.5 Hz, 6H, Si(CH(CH_3)$_2$)$_3$); 1.21, 1.17 (two sets of d, $^3J_{HH}$ = 7.5 Hz, 36H, Si(CH(CH_3)$_2$)$_3$); 0.20 (br q, $^1J_{HB}$ = 85 Hz, 4H, BH_4). **^{11}B NMR** (128.43 MHz, THF-d_8): δ [ppm]: -26.6 (q,$^1J_{HB}$ = 85 Hz, BH$_4$). **^{13}C{^{1}H} NMR** (100.67 MHz, THF-d_8): δ [ppm]: 106.8 (C_{COT}); 104.6 (C_{COT}); 101.3 (C_{COT}); 99.3 (C_{COT}); 68.4 (C_{thf}); 26.5 (C_{thf}); 20.0 (Si(CH(CH$_3$)$_2$)$_3$); 13.4 (Si(CH(CH$_3$)$_2$)$_3$). **^{29}Si{^{1}H} NMR** (79.52 MHz, THF-d_8): δ [ppm]: 6.7 (SiiPr$_3$). **Raman**: $\tilde{\nu}$ [cm^{-1}] = 3056 (w), 3014 (w), 2972 (m), 2943 (m), 2865 (vs), 2750 (w), 2708 (w), 2388 (w), 2329 (w), 2242 (w), 2165 (w), 1532 (w), 1493 (m), 1473 (m), 1445 (w), 1369 (w), 1343 (w), 1297 (w), 1252 (w), 1234 (w), 1159 (w), 1072 (w), 1035 (w), 1015 (w), 1003 (w), 971 (w), 926 (w), 883 (m), 812 (w), 787 (w), 754 (s), 738 (w), 670 (w), 640 (w), 609 (w), 571 (w), 517 (m), 454 (m), 422 (w), 388 (w), 362 (w), 316 (w), 256 (m), 238 (m), 178 (w), 100 (m), 67 (m). **IR (ATR)**: $\tilde{\nu}$ (cm^{-1}) = 2941 (vs), 2889 (vs), 2863 (vs), 2413 (w), 2242 (w), 1462 (s), 1380 (w), 1367 (w), 1343 (w), 1250 (w), 1212 (w), 1135 (w), 1070 (m), 1031 (m), 1012 (s), 957 (w), 931 (m), 881 (s), 834 (w), 792 (m), 735 (m), 667 (m), 637 (s), 607 (w), 583 (m), 525 (w), 465 (w).

[Ce(η^8-COT^{TIPS})BH_4] (2): Yield: 809 mg (1.41 mmol), 70%, Anal. Calcd for $C_{26}H_{52}BSi_2Ce$ (571.80): C, 54.61; H, 9.17. Found: C, 53.68; H, 8.65. **HR-EI - MS**: (70 eV, QT = 250 °C): m/z [%] = 571.216 $[M]^+$ (27.14), 556.178 $[M\text{-}BH_4]^+$ (14.49); 514.110 $[M\text{-}BH_4\text{-}C_3H_6]^+$ (100). **^{1}H NMR** (300.13 MHz, THF-d_8): δ [ppm]: 25.82 (br s, 4H, BH_4); 11.23 (br s, 2H, CH_{COT}); 7.21 (br s, 2H, CH_{COT}); 3.64-3.60 (m, C$H_{2\ thf}$); 1.79-1.75 (m, C$H_{2\ thf}$); 1.36 (br s, 6H, Si(CH(CH$_3$)$_2$)$_3$); 1.04 (d, $^3J_{HH}$ = 5.7 Hz, 18H; Si(CH(CH_3)$_2$)$_3$); 0.17 (d, $^3J_{HH}$ = 5.7 Hz, 18H; Si(CH(CH_3)$_2$)$_3$); -5.86 (br s, 2H, CH_{COT}). **^{13}C{^{1}H} NMR** (75.48 MHz, THF-d_8): δ [ppm]: 136.8 (C_{COT}); 117.6 (C_{COT}); 108.4 (C_{COT}); 108.2 (C_{COT}); 68.4 (C_{thf}); 26.6 (C_{thf}); 19.4 (Si(CH(CH$_3$)$_2$)$_3$); 18.5 (Si(CH(CH$_3$)$_2$)$_3$); 13.8 (Si(CH(CH$_3$)$_2$)$_3$). **^{29}Si{^{1}H} NMR** (59.63 MHz, THF-d_8): δ [ppm]: -3.0 (SiiPr$_3$).**^{11}B NMR** (96.29 MHz, THF-d_8): δ [ppm]: 17.8 (br, BH$_4$). **Raman**: $\tilde{\nu}$ (cm^{-1}) = 3037 (w), 3006 (w), 2942 (m), 2864 (vs), 2752 (w), 2710 (w), 2428 (w), 2308 (w), 2240 (m), 2160 (m), 2132 (w), 2113 (w), 1532 (m), 1490 (w), 1470 (w), 1447 (w), 1383 (w), 1295 (w), 1232 (w), 1158 (w), 1074 (w), 1017 (w), 996 (w), 971 (w), 920 (s), 883 (m), 825 (w), 755 (s), 668 (w), 643 (w), 610 (w), 558 (w), 516 (w), 452 (m), 363 (w), 280 (m), 249 (m), 97 (s). **IR (ATR)**: $\tilde{\nu}$ (cm^{-1}) = 2998 (w), 2942 (vs), 2889 (s), 2864 (vs), 2428 (w), 2241 (w), 1581 (w), 1462 (m), 1385 (w), 1364 (w), 1306 (m), 1236 (vs), 1207 (s), 1147 (s), 1035 (m), 985 (s), 922 (w), 882 (s), 855 (w), 822 (w), 746 (m), 666 (s), 642 (s), 581 (w); 516 (w).

[Sm(η^8-COT^{TIPS})BH_4] (3): Yield: 856 mg (1.47 mmol) 73% Anal. Calcd for $C_{26}H_{52}BSi_2Sm$ (582.04): C, 53.65; H, 9.01. Found: C, 53.61; H, 8.46. **HR-EI - MS**: (70 eV, QT = 250 °C): m/z

[%] = 583.189 $[M]^+$ (8.00), 568.154 $[M\text{-}BH_4]^+$ (3.59); 526.124 $[M\text{-}BH_4\text{-}C_3H_6]^+$ (8.98). **^{1}H NMR** (300.13 MHz, THF-d_8): δ [ppm]: 13.11 (br s, 2H, CH_{COT}); 12.12 (br s, 2H, CH_{COT}); 10.56 (br s, 2H, CH_{COT}); 3.64-3.59 (m, C$H_{2\ thf}$); 2.37 (sept, 6H, $^3J_{HH}$ = 7.4 Hz, Si(CH(CH_3)$_2$)$_3$)); 1.86 (d, $^3J_{HH}$ = 7.4 Hz, 18H; Si(CH(CH_3)$_2$)$_3$)); 1.79-1.75 (m, C$H_{2\ thf}$); 1.68 (d, $^3J_{HH}$ = 7.5 Hz, 18H, Si(CH(CH_3)$_2$)$_3$)); -21.71 (br, 4H, BH_4). **^{13}C{^{1}H} NMR** (75.47 MHz, THF-d_8): δ [ppm]: 87.7 (C_{COT}); 84.9 (C_{COT}) 83.1 (C_{COT}); 77.4 (C_{COT}); 68.4 (C_{thf}); 26.5 (C_{thf}); 20.4 (Si(CH(CH$_3$)$_2$)$_3$); 12.1 (Si(CH(CH$_3$)$_2$)$_3$). **^{29}Si{^{1}H} NMR** (59.63 MHz, THF-d_8): δ [ppm]: 22.3 (*Sii*Pr$_3$).**^{11}B NMR** (96.29 MHz, THF-d_8): δ [ppm]: -64.6 (s, BH$_4$). **Raman**: $\tilde{\nu}$ (cm^{-1}) = 3030 (w), 3003 (w), 2924 (m), 2865 (vs), 2754 (w), 2712 (w), 2437 (w), 2330 (w), 2241 (w), 2197 (w), 2159 (w), 2132 (w), 1491 (m), 1470 (w), 1447 (w), 1293 (w), 1234 (w), 1157 (w), 1072 (w), 1017 (w), 993 (w), 970 (w), 921 (s), 882 (m), 819 (m), 756 (s), 670 (w), 639 (w), 605 (w), 562 (w), 518 (m), 452 (m), 364 (m), 279 (m), 235 (s), 181 (m), 108 (s), 97 (s). **IR (ATR)**: $\tilde{\nu}$ (cm^{-1}) = 3018 (s), 2942 (vs), 2888 (s), 2863 (vs), 2430 (m), 2257 (m), 1462 (s), 1380 (w), 1287 (w), 1250 (w), 1216 (w), 1100 (w), 1071 (w), 1031 (m), 1011 (m) 959 (w), 934 (m), 881 (m), 858 (w), 833 (w), 802 (w), 742 (m), 668 (m), 637 (s), 609 (w), 584 (m), 526 (w), 464 (w).

[Er(η^8-COT^{TIPS})BH$_4$] (4): Due to the strong paramagnetic behavior of **4**, not all expected resonances could be observed in the ^{1}H-NMR spectrum. Additionally, the resonance assignment could not be performed unambiguously. Moreover, the ^{13}C-NMR remained silent. Yield: 703 mg (1.17 mmol) 58% Anal. Calcd for $C_{26}H_{52}BSi_2Er$ (598.94): C, 52.14; H, 8.75. Found: C, 52.31; H, 8.62. **HR-EI-MS**: (70 eV, QT = 200°C): m/z [%] = 597.297 $[M+H]^+$ (21.27), 582.250 $[M\text{-}BH_4]^+$ (3.78); 540.182 $[M\text{-}BH_4\text{-}C_3H_6]^+$ (86.19). **^{1}H NMR** (300.12 MHz, THF-d_8): δ [ppm]: 3.60 (s, C$H_{2\ thf}$); 1.80 (s, C$H_{2\ thf}$); 0.98 (m, CH_{COT} or BH_4); -16.30 (s, 18H, Si(CH(CH_3)$_2$)$_3$)); -18.73 (s, 18H, Si(CH(CH_3)$_2$)$_3$)); -28.06 (s, 6H, Si(CH(CH$_3$)$_2$)$_3$)); -51.79 (br s, CH_{COT} or BH_4); -61.28 (br s, CH_{COT} or BH_4). **^{29}Si{^{1}H} NMR** (59.63 MHz, THF-d_8): δ [ppm]: 59.0 (*Sii*Pr$_3$).**^{11}B NMR** (96.29 MHz, THF-d_8): δ [ppm]: -193.5 (br s, BH$_4$). **Raman**: $\tilde{\nu}$ (cm^{-1}) = 3043 (w), 3027 (w), 2997 (m), 2943 (s), 2888 (m), 2861 (vs), 2772 (w), 2750 (w), 2708 (w), 2467 (m), 2372 (w), 2241 (w), 2201 (w), 2136 (w), 1524 (w), 1485 (m), 1470 (m), 1445 (m), 1381 (w), 1367 (w), 1295 (w), 1250 (w), 1231 (w), 1156 (w), 1073 (w), 1043 (w), 1015 (w), 997 (w), 969 (w), 928 (w), 880 (s), 823 (w), 777 (w), 760 (m), 669 (w), 646 (w), 606 (w), 570 (w), 517 (m), 454 (m), 421 (w), 390 (w), 363 (w), 315 (m) 277 (m), 243 (s), 210 (w), 165 (m), 116 (s), 75 (s). **IR (ATR)**: $\tilde{\nu}$ (cm^{-1}) = 2998 (w), 2940 (vs), 2921 (vs), 2888 (s), 2862 (vs), 2465 (m), 2240 (w), 2202 (w), 2136 (m), 1462 (s), 1383 (w), 1366 (w), 1251 (w), 1211 (w), 1186 (m), 1071 (w), 1037 (m), 1014 (s), 993 (w), 931 (m), 880 (m), 859 (w), 752 (m), 667 (m), 641 (s), 604 (w), 580 (m), 525 (m), 478 (w).

Synthesis of [Li(thf)(η^5-L^{Pb})La(η^8-COT^{TIPS})] (5)

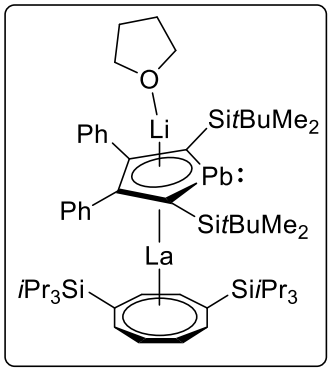

To a mixture of $[Li_2(thf)_2(L^{Pb})]$ (120 mg, 0.150 mmol, 1.00 eq) and **1** (86 mg, 0.150 mmol, 1.00 eq) was condensed THF (10 mL) at -88 °C. The resulting brownish-red solution was slowly warmed up to room temperature and stirred 12 h at room temperature, during which time the solution became orange-brown. All volatiles were removed under reduced pressure and the solid residue was extracted with hot *n*-heptane (10 mL). Subsequently, the ^{n}heptane extract was concentrated until the formation of a brown solid was observed. The resulting suspension was gently heated until all solids were redissolved and storage of the saturated solution at room temperature for 12 h led to the formation of single crystals suitable for X-ray diffraction. After removing approximately 5 mg of crystals for SCXRD experiments, each batch was further stored at -10 °C for one week to induce crystallization of the residual product. Separation from the mother liquor and drying *in vacuo* for 1 h gave **5** as orange-green crystalline material.

Yield (based on crystals): 103 mg (0.081 mmol), 54%. Anal. Calcd for $C_{58}H_{96}LiOSi_4LaPb$ (1274.79): C, 54.65; H, 7.59. Found: C, 55.08; H, 7.05. **^{1}H NMR** (400.30 MHz, THF-d_8): δ [ppm]: 6.84 (t, $^3J_{HH}$ = 7.4 Hz, 4H, *o*-CH_{Ph}); 6.75-6.71 (m, 2H, *p*-CH_{Ph}); 6.63-6.65 (m, 4H, *m*-CH_{Ph}); 6.58-6.53 (m, 2H, CH_{COT}); 6.41-6.36 (m, 4H, CH_{COT}); 3.63-3.60 (m, 4H, C$H_{2\,thf}$); 1.79-1.76 (m, 4H, C$H_{2\,thf}$; 1.55 (sept, $^3J_{HH}$ = 7.4 Hz, 6H, Si(CHMe$_2$)$_3$); 1.13, 1.12 (two sets of d, $^3J_{HH}$ = 7.4 Hz, 36H, Si(CH(CH_3)$_2$)$_3$); 0.59 (s, 18H, SiC(CH_3)$_3$Me$_2$); 0.42 (s, 6H, Si*t*Bu(CH_3)$_2$); -0.36 (s, 6H, Si*t*Bu(CH_3)$_2$). **^{13}C{^{1}H} NMR** (100.67 MHz, THF-d_8): δ [ppm]: 228.0 ($C_{\alpha,Pb}$); 163.0 ($C_{quart,Ph}$); 161.7 ($C_{\beta,Pb}$); 130.8 (C_{Ph}); 126.7 (C_{Ph}) ; 124.1 (C_{Ph}) ; 103.4 (C_{COT}); 101.7 (C_{COT}); 99.1 (C_{COT}); 97.5 ($C_{quart,COT}$); 68.4 (C_{thf}); 29.7 (SiC(CH$_3$)$_3$(CH$_3$)$_2$); 26.6 (C_{thf}); 20.9 (Si(CH(CH$_3$)$_2$)$_3$); 18.6 (SiC(CH$_3$)$_3$(CH$_3$)$_2$); 13.5 (Si(CH(CH$_3$)$_2$)$_3$) ; 5.9 (Si*t*Bu(CH$_3$)$_2$); 3.7 (Si*t*Bu(CH$_3$)$_2$). **^{7}Li{^{1}H} NMR** (116.64 MHz, THF-d_8): δ [ppm]: -0.51. **^{29}Si{^{1}H} NMR** (79.52 MHz, THF-d_8): δ [ppm]: 7.3 (*Sii*Pr$_3$); 0.7 (*Sit*BuMe$_2$). **IR (ATR)**: $\tilde{\nu}$ (cm^{-1}) = 3058 (w), 2930 (vs), 2888 (w), 2861 (vs), 1595 (w), 1555 (w), 1490 (w), 1463 (vs), 1384 (w), 1361 (w), 1316 (w), 1244 (s), 1208 (w), 1183 (w), 1072 (w), 1029 (m), 953 (m), 932 (w), 881 (s), 855 (w), 824 (s), 803 (w), 762 (m), 736 (w), 697 (m), 642 (s), 585 (m), 514 (w), 441 (w).

Synthesis of [Li(thf)(η^5-L^{Pb})Ce(η^8-COT^{TIPS})] (6)

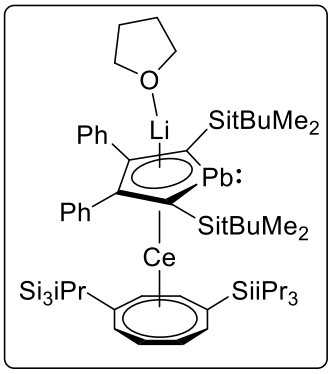

To a mixture of $[Li_2(thf)_2(L^{Pb})]$ (115 mg, 0.144 mmol, 1.00 eq) and **2** (82 mg, 0.144 mmol, 1.00 eq) was condensed THF (10 mL) at -88 °C. The resulting brownish-red solution was slowly warmed up to room temperature and stirred 12 h at room temperature, during which time the solution became orange-brown. All volatiles were removed under reduced pressure and the solid residue was extracted with hot *n*-heptane (10 mL). Subsequently, the *n*heptane extract was concentrated until the formation of a brown solid was observed. The resulting suspension was gently heated until all solids were redissolved and storage of the saturated solution at room temperature for 12 h led to the formation of single crystals suitable for X-ray diffraction. After removing approximately 5 mg of crystals for SCXRD experiments, each batch was further stored at -10 °C for one week to induce crystallization of the residual product. Separation from the mother liquor and drying *in vacuo* for 1 h gave **5** as orange-green crystalline material. The paramagnetic behavior of **6** did not allow recording meaningful NMR-spectra.

Yield (based on crystals): 90 mg (0.070 mmol), 49%. Anal. Calcd for $C_{58}H_{96}LiOSi_4CePb$ (1274.79): C, 54.60; H, 7.58. Found: C, 54.61; H, 7.38. **IR (ATR)**: $\tilde{\nu}$ (cm^{-1}) = 3065 (w), 2929 (vs), 2888 (w), 2862 (vs), 1595 (w), 1555 (m), 1489 (w),1463 (s), 1385 (w), 1362 (w), 1310 (w), 1245 (s), 1182 (w), 1071 (w), 1010 (m), 952 (w), 920 (w), 882 (m), 854 (w), 824 (vs), 805 (w), 760 (m), 719 (w), 670 (w), 646 (m), 582 (w), 512 (w), 431 (w).

Synthesis of [Li(thf)(η^5-L^{Pb})Sm(η^8-COT^{TIPS})] (7)

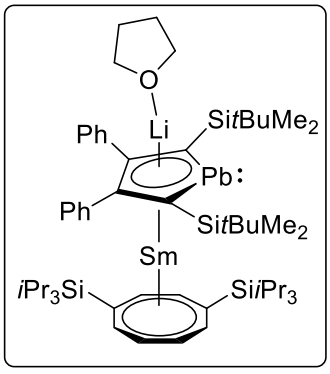

To a mixture of $[Li_2(thf)_2(L^{Pb})]$ (120 mg, 0.150 mmol, 1.00 eq) and **3** (88 mg, 0.150 mmol, 1.00 eq) was condensed THF (10 mL) at -88 °C. The resulting brownish-red solution was slowly warmed up to room temperature and stirred 12 h at room temperature, during which time the solution became orange-brown. All volatiles were removed under reduced pressure. The solid residue was extracted with toluene (10 mL). Afterwards, the toluene solution was concentrated until the formation of a brown solid was observed. The resulting suspension was gently heated until all solids were redissolved. Subsequently, single crystals suitable for X-ray diffraction analysis were obtained from the concentrated toluene solution after storage at 5 °C for one week. After removing approximately 5 mg of crystals for SCXRD experiments, each batch was separated from the mother liquor to give **7** as orange-green crystalline material after drying *in vacuo* for 1h.

Yield (based on crystals): 87 mg (0.068 mmol), 45%. Anal. Calcd for $C_{58}H_{96}LiSi_4Sm$ (1286.25): C, 54.16; H, 7.52. Found: C, 54.19; H, 7.17. Due to the paramagnetic behavior of **7**, one of the

CH_{Ph} resonances is not visible in the ^{1}H-NMR and the $^{13}C\{^{1}H\}$-NMR spectrum. **^{1}H NMR** (400.30 MHz, THF-d_8): δ [ppm]: 10.86 (s, 2H, CH_{COT}); 8.62 (br s, 2H, CH_{COT}); 7.20-7.06 (m, 3H, CH_{tol}); 6.34 (m, 2H, CH_{Ph}); 6.14 (br s, 4H, CH_{Ph}); 5.93 (br s, 2H, CH_{COT}); 3.63-3.60 (m, 4H, $CH_{2\ thf}$); 2.30 (s, 1.8H, $CH_{3\ tol}$); 1.79-1.76 (m, 4H, $CH_{2\ thf}$); 1.22 (s, 18H, $SiC(CH_3)_3Me_2$); 0.93 (sept, $^{3}J_{HH}$ = 7.4 Hz, 6H, $Si(CHMe_2)_3$); 0.74 (d, $^{3}J_{HH}$ = 7.4 Hz, 18H, $Si(CH(CH_3)_2)_3$); 0.65 (d, $^{3}J_{HH}$ = 7.4 Hz, 18H, $Si(CH(CH_3)_2)_3$); 0.53 (s, 6H, $SitBu(CH_3)_2$); -0.60 (s, 6H, $SitBu(CH_3)_2$). **$^{13}C\{^{1}H\}$ NMR** (100.67 MHz, THF-d_8): δ [ppm]: 169.3 ($C_{\alpha,Pb}$); 169.0 ($C_{\beta,Pb}$); 138.6 ($C_{quart,tol}$); 129.8 (C_{tol}); 129.1 (C_{tol}); 128.5 ($C_{quart,Ph}$); 126.2 (C_{tol}); 125.3 (C_{Ph}); 123.5 (C_{Ph}); 94.2 (C_{COT}); 86.9 (C_{COT}); 85.4 (C_{COT}); 79.2 (C_{COT}); 68.4 (C_{thf}); 29.6 ($SiC(CH_3)_3Me_2$); 26.0 (C_{thf}); 21.7 ($CH_{3\ tol}$); 20.2 ($Si(CH(CH_3)_2)_3$); 20.1 ($Si(CH(CH_3)_2)_3$); 16.4 ($SiC(CH_3)_3Me_2$); 11.3 ($Si(CHMe_2)_3$); 4.8 ($SitBu(CH_3)_2$); 4.1 ($SitBu(CH_3)_2$). **$^{29}Si\{^{1}H\}$ NMR** (79.52 MHz, THF-d_8): δ [ppm]: 15.6 ($SiiPr_3$); 5.0 ($SitBuMe_2$). **IR (ATR):** $\tilde{\nu}$ (cm^{-1}) = 2945 (vs), 2861 (vs), 1596 (w), 1556 (w), 1491 (w), 1463 (s), 1385 (w), 1360 (w), 1315 (w), 1244 (s), 1209 (w), 1179 (w), 1072 (w), 1026 (m), 953 (m), 935 (w), 920 (w), 881 (m), 855 (w), 824 (w), 800 (m), 763 (m), 742 (w), 698 (m), 643 (m), 585 (m), 511 (w), 2887 (w), 444 (w), 477 (w).

Synthesis of [Li(thf)(η^5-L^{Pb})Er(η^8-COT^{TIPS})] (8)

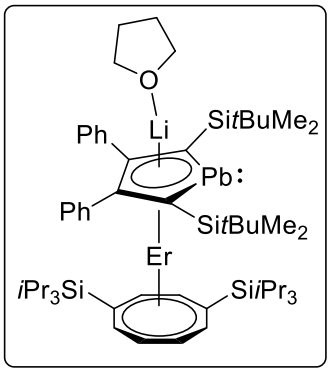

To a mixture of [$Li_2(thf)_2(L^{Pb})$] (122 g, 0.153mmol, 1.00 eq) and **4** (92 mg, 0.153 mmol, 1.00 eq) was condensed THF (10 mL) at -88 °C. The resulting brownish-red solution was slowly warmed up to room temperature and stirred 12 h at room temperature, during which time the solution became orange-brown. All volatiles were removed under reduced pressure and the solid residue was extracted with hot *n*-heptane (10 mL). Subsequently, the ^{n}heptane extract was concentrated until the formation of a brown solid was observed. The resulting suspension was gently heated until all solids were redissolved and storage of the saturated solution at room temperature for 12 h led to the formation of single crystals suitable for X-ray diffraction. After removing approximately 5 mg of crystals for SCXRD experiments, each batch was further stored at -10 °C for one week to induce crystallization of the residual product. Separation from the mother liquor and drying *in vacuo* for 1 h gave **5** as orange-green crystalline material. The paramagnetic behavior of **8** did not allow recording meaningful NMR-spectra.

Yield (based on crystals): 78 mg (0.060 mmol), 39%. Anal. Calcd. for $C_{58}H_{96}ErLiOPbSi_4$ (1303.14): C, 53.46; H, 7.43. Found: C, 53.08; H, 6.73. **IR (ATR):** $\tilde{\nu}$ (cm^{-1}) = 2944 (s), 2886 (w), 2862 (vs), 1596 (w), 1556 (w), 1489 (w), 1464 (s), 1385 (m), 1362 (w), 1312 (w), 1244 (s), 1209 (w), 1187 (w), 1152 (w), 1028 (m), 956 (m), 934 (w), 882 (s), 855 (w), 822 (w), 804 (vs), 763 (m), 736 (w), 701 (m), 637 (s), 583 (m), 511 (w).

Synthesis of $[Li(Et_2O)_{3.4}(thf)_{0.6}][(\eta^5\text{-}L^{Pb})Er(\eta^8\text{-}COT^{TIPS})]$ (9)

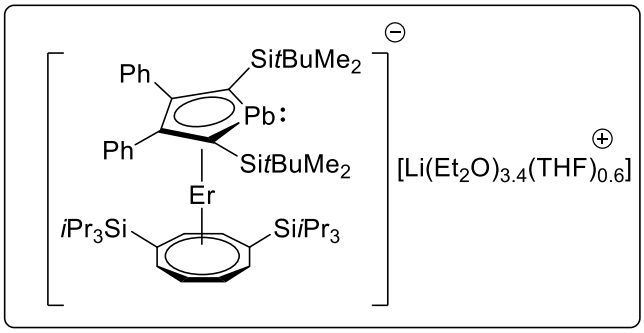

To a mixture of $[Li_2(thf)_2(L^{Pb})]$ (143 mg, 0.180 mmol, 1.00 eq) and **4** (107 mg, 0.180 mmol, 1.00 eq) was condensed THF (10 mL) at -88 °C. The resulting brownish-red solution was slowly warmed up to room temperature and stirred 12 h at room temperature upon which the mixture became orange-brown. All volatiles were removed under reduced pressure. The solid residue was extracted with toluene (10 mL). After removal of the solvent *in vacuo*, the solid residue was dissolved in Et_2O (10 mL) upon which the solution became dark red. Crystals suitable for X-ray diffraction analysis were obtained by slow evaporation of the Et_2O solution at room temperature. After removing approximately 5 mg of crystalline material from the sample for SCXRD experiments, the residual material was washed with cold Et_2O and dried *in vacuo* at room temperature for 30 min to give compound **9** as dark red crystalline material.

Yield (based on crystals): 78 mg (0.073 mmol), 41%.

Note: elemental analysis of compound **9** indicated partial removal of the Li-coordinated solvents after drying of **9** *in vacuo* (30 min, room temperature). This tentatively results in a compound similar to **8**. Found: C, 52.80; H, 6.82. However, elemental analysis does not allow to distinguish between Li-coordinated Et_2O or THF as the elemental composition of these two only differs by two hydrogen atoms: Anal. Calcd. for $C_{54}H_{88}ErLiPbSi_4$ (C_4H_8O) (1303.14): C, 53.46; H, 7.43. for $C_{54}H_{88}ErLiPbSi_4$ ($C_4H_{10}O$). Thus, the exact composition of the isolated material could not be determined. **IR (ATR):** $\tilde{\nu}$ (cm^{-1}) = 2943 (vs), 2928 (vs), 2891 (s), 2862 (vs), 1559 (w), 1488 (w), 1463 (s), 1386 (m), 1361 (m), 1306 (w), 1247 (m), 1133 (s), 1099 (m), 1071 (m), 1017 (m), 918 (m), 883 (m), 850 (w), 825 (s), 807 (w), 758 (m), 702 (w), 669 (w), 645 (m), 579 (w), 523 (w). The IR spectrum of 9 was recorded again after sufficient drying under vacuum: **IR (ATR):** $\tilde{\nu}$ (cm^{-1}) = 2924 (vs), 2888 (vs), 2860 (vs), 1595 (w), 1487 (w), 1463 (s), 1384 (w), 1362 (s), 1305 (w), 1290 (m), 1245 (s), 1134 (s), 1097 (vs), 1071 (m), 1024 (vs), 956 (m), 921 (s), 882 (s), 854 (m), 823 (m), 805 (s), 767 (m), 737 (v), 725 (m), 700 (m), 665 (m), 578 (s), 523 (m).

Synthesis of [Li(12-c-4)$_2$][(η^5-L^{Pb})Er(η^8-COT^{TIPS})] (10)

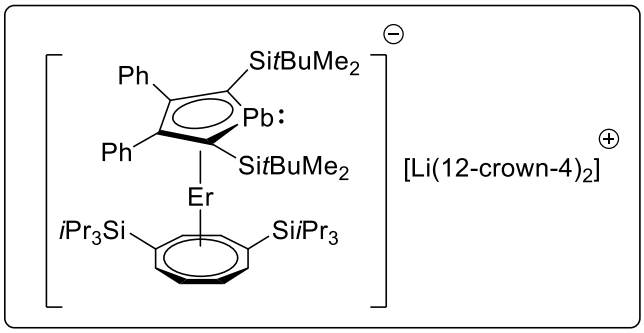

To a mixture of [Li$_2$(thf)$_2$(L^{Pb})] (110 mg, 0.138 mmol; 1.00 eq) and **4** (86 mg, 0.138 mmol; 1.00 eq) was condensed THF (10 mL) at -88 °C. The resulting brownish-red solution was slowly warmed up to room temperature and stirred 12 h at room temperature, during which time the solution became orange-brown. All volatiles were removed under reduced pressure. The solid residue was extracted with toluene (10 mL). To the toluene solution was added 12-crown-4 (0.050 g, 0.284 mmol). The color of the solution changed from dark brown to dark red immediately and the solution was stirred for 2 h at room temperature. Afterwards the solvent was removed until crystallization was imminent and small amounts of precipitated solids were redissolved by gentle heating. Subsequent storage at -30 °C for two days led to the formation of a dark red crystalline material. Afterwards, the mother liquor was removed and after drying residue *in vacuo* for 1 h compound **10** was obtained as dark red, crystalline material. Crystals suitable for X-ray diffraction analysis were obtained by redissolving the isolated crystalline material in hot toluene and subsequent storage of the saturated solution at room temperature for 12 h. The paramagnetic behavior of **10** did not allow recording meaningful NMR-spectra.

Yield (based on crystals): 90 mg (0.057 mmol), 41%. Anal. Calcd. for $C_{70}H_{120}ErLiO_8Si_4Pb$ (1583.46): C, 53.10; H, 7.64. Found: C, 52.75; H, 7.63. IR (ATR): $\tilde{\nu}$ (cm^{-1}) = 2943 (s), 2890 (m), 2861 (vs), 1595 (w), 1555 (w), 1463 (m), 1385 (m), 1361 (w), 1306 (w), 1291 (m), 1246 (m), 1133 (s), 1097 (s), 1071 (m), 1019 (m), 917 (m), 882 (m), 844 (m), 824 (m), 805 (m), 765 (w), 720 (w), 701 (w), 665 (w), 611 (w), 576 (w), 514 (w).

NMR Spectra

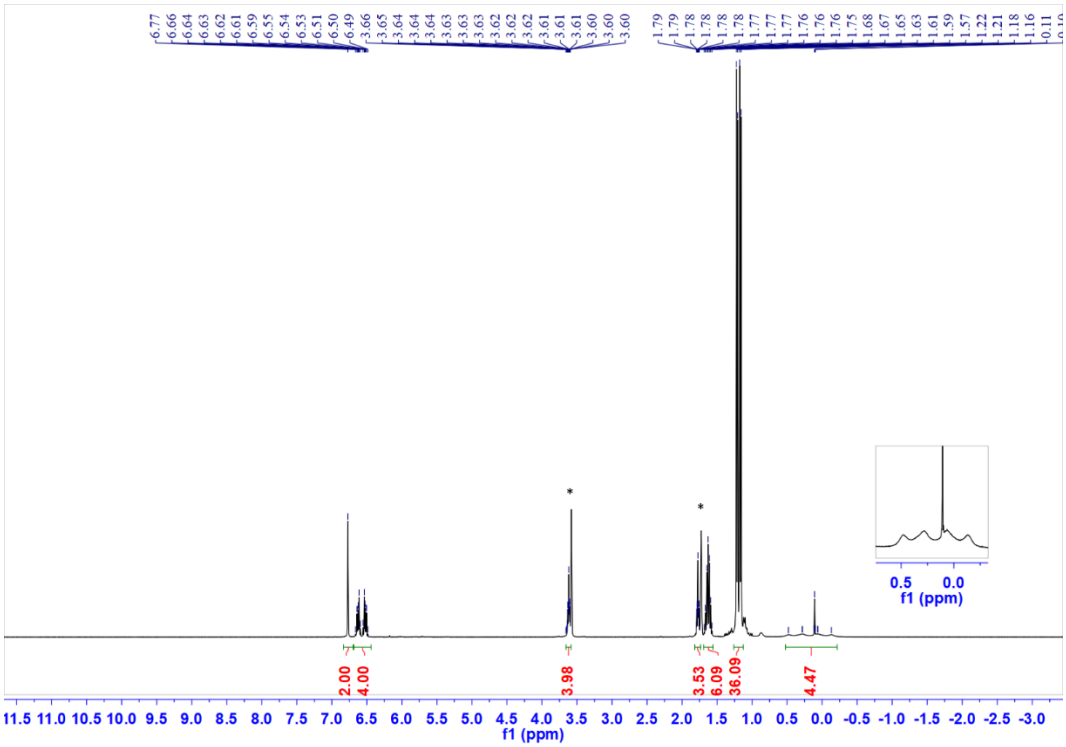

Figure S1. ^{1}H NMR spectrum of [La(η^{8}-COT^{TIPS})BH$_4$] (**1**) in THF-d_8: *, residual protio solvent signal.

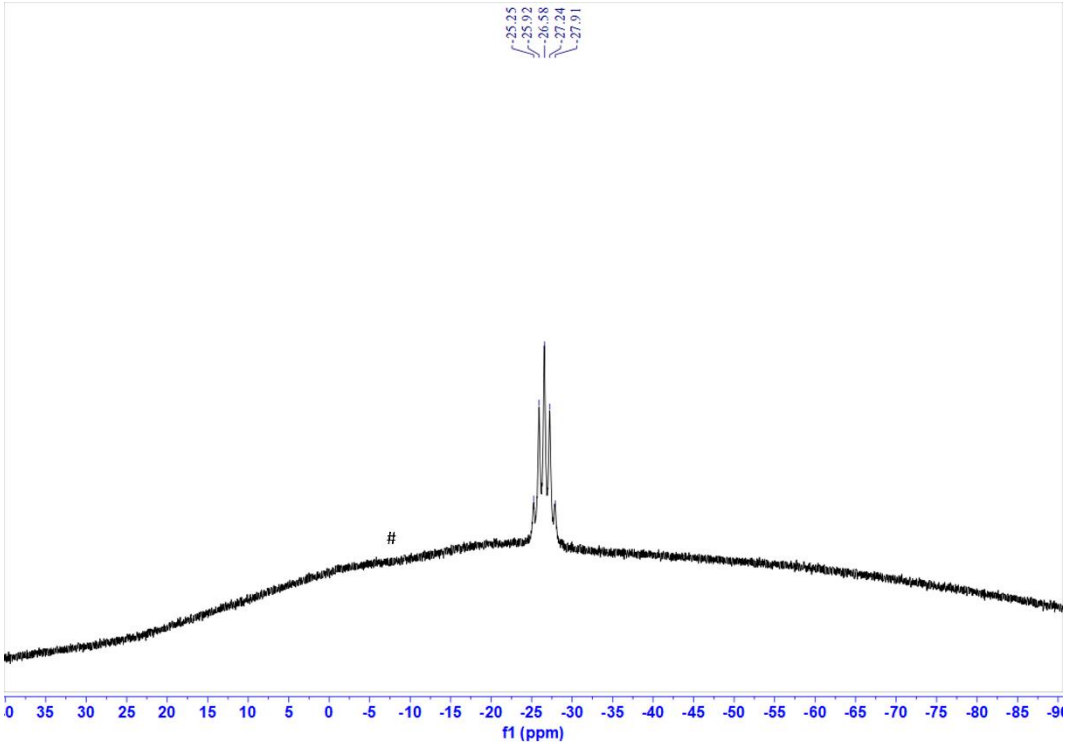

Figure S2. ^{11}B NMR spectrum of [La(η^{8}-COT^{TIPS})BH$_4$] (**1**) in THF-d_8: #, background signal from NMR tube (made of borosilicate glass).

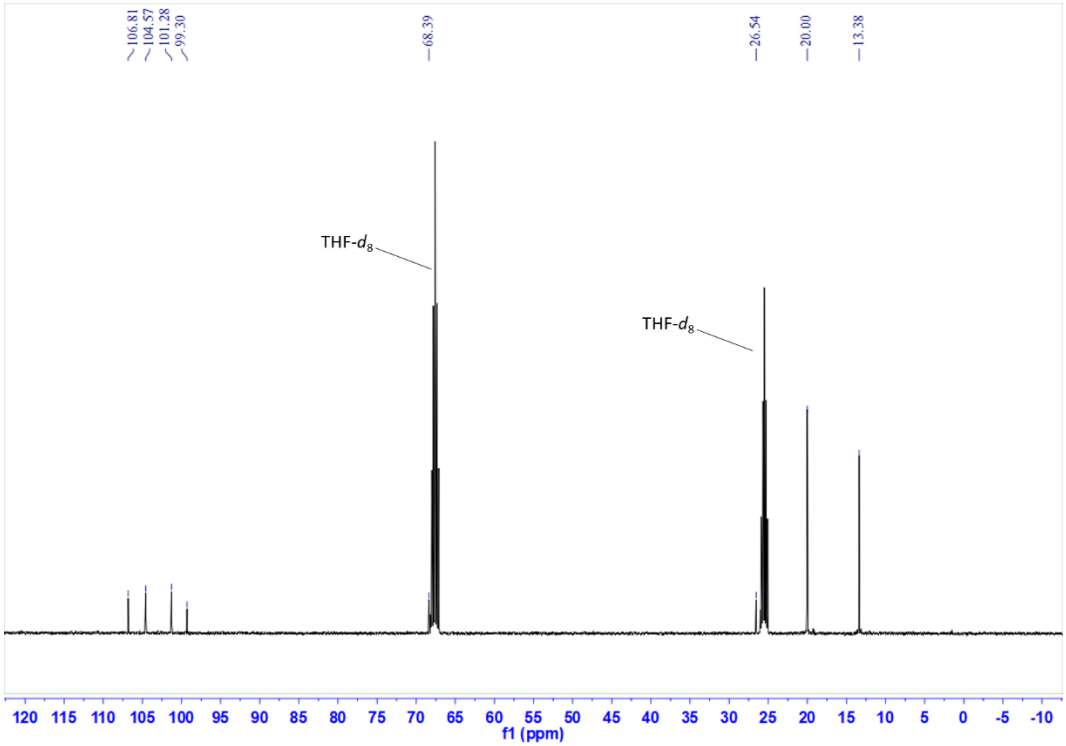

Figure S3. $^{13}C\{^1H\}$ NMR spectrum of [La(η^8-COT^{TIPS})BH_4] (**1**) in THF-d_8.

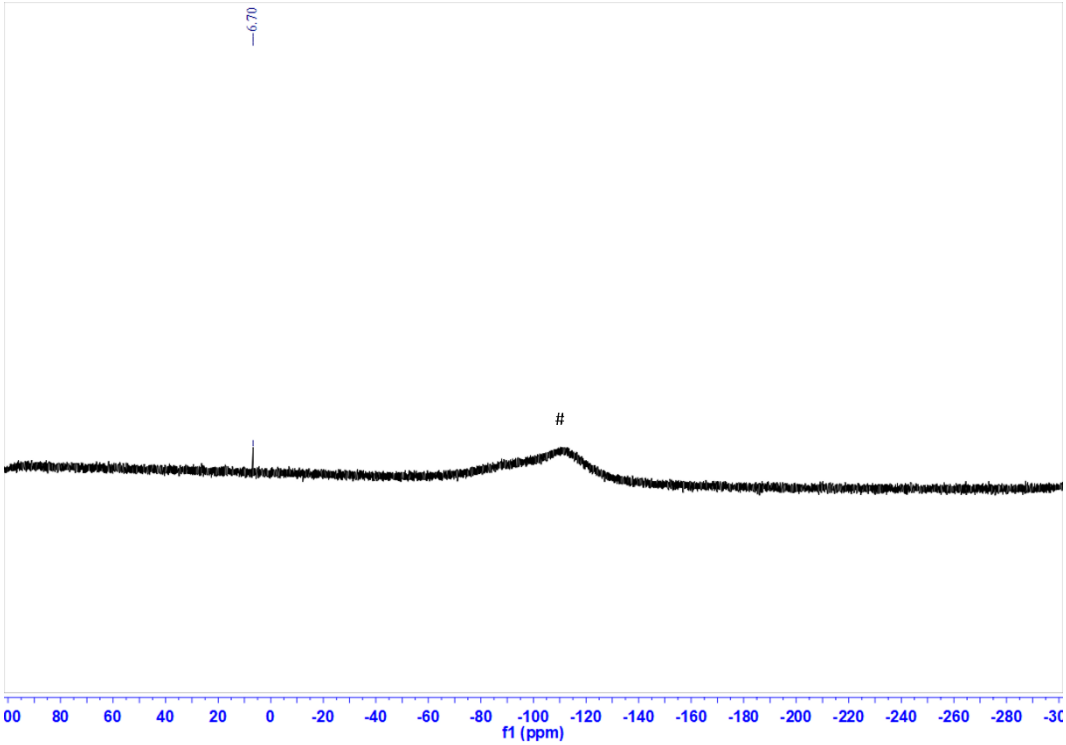

Figure S4. $^{29}Si\{^1H\}$ NMR spectrum of [La(η^8-COT^{TIPS})BH_4] (**1**) in THF-d_8: #, background signal from NMR tube (made of borosilicate glass).

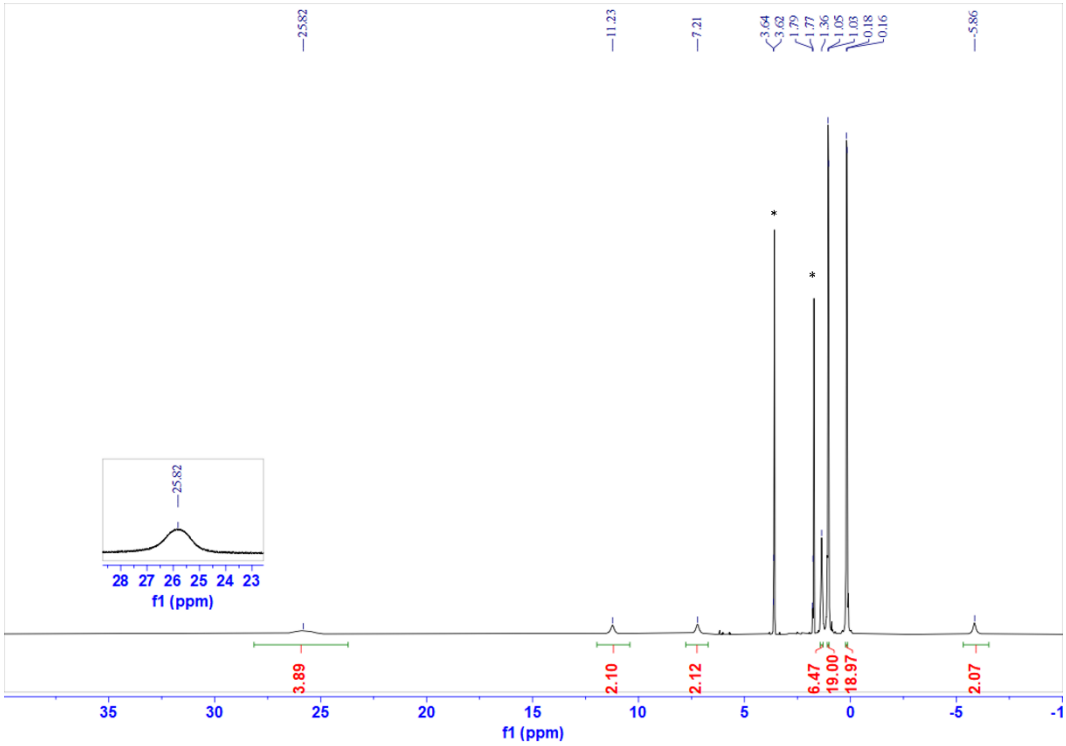

Figure S5. ^{1}H NMR spectrum of [Ce(η^{8}-COT^{TIPS})BH$_4$] (**2**) in THF-d_8: *, residual protio solvent signal.

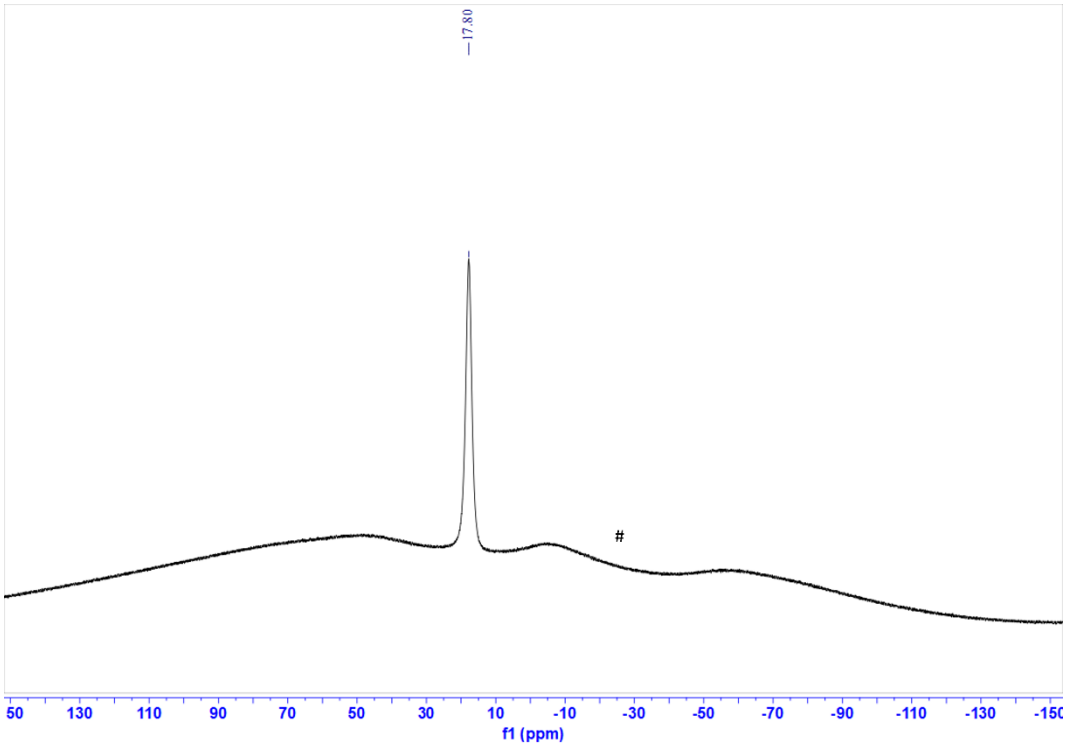

Figure S6. ^{11}B NMR spectrum of [Ce(η^{8}-COT^{TIPS})BH$_4$] (**2**) in THF-d_8: #, background signal from NMR tube (made of borosilicate glass).

.

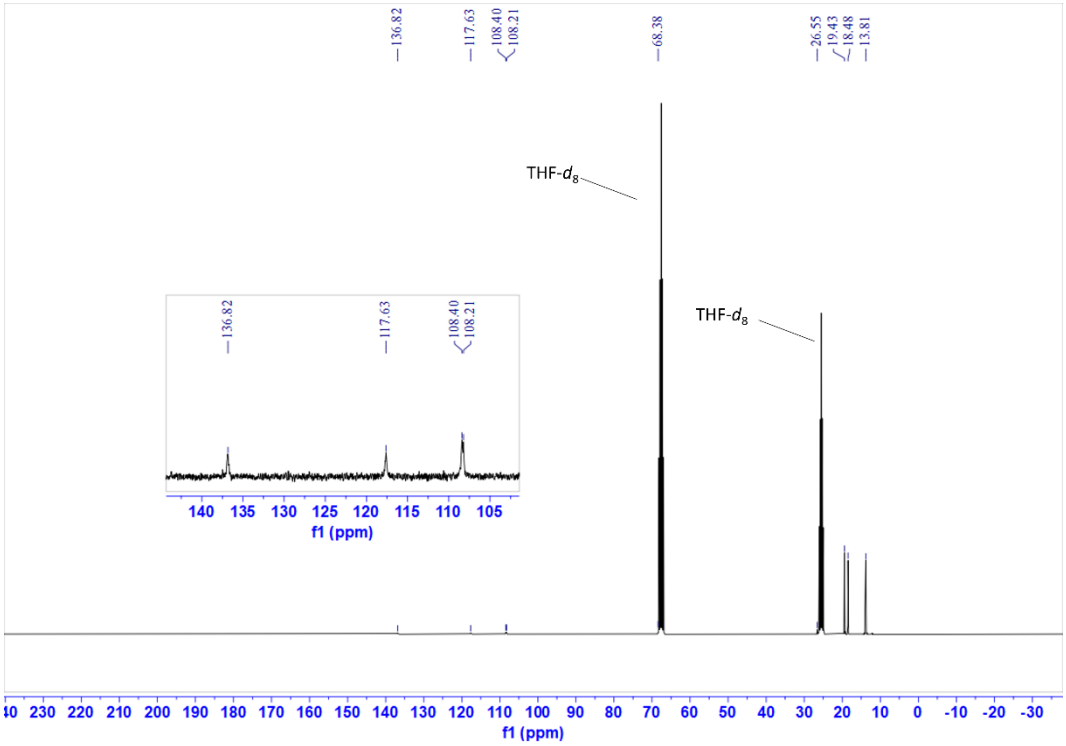

Figure S7. $^{13}C\{^{1}H\}$ NMR spectrum of [Ce(η^8-COT^{TIPS})BH_4] (**2**) in THF-d_8.

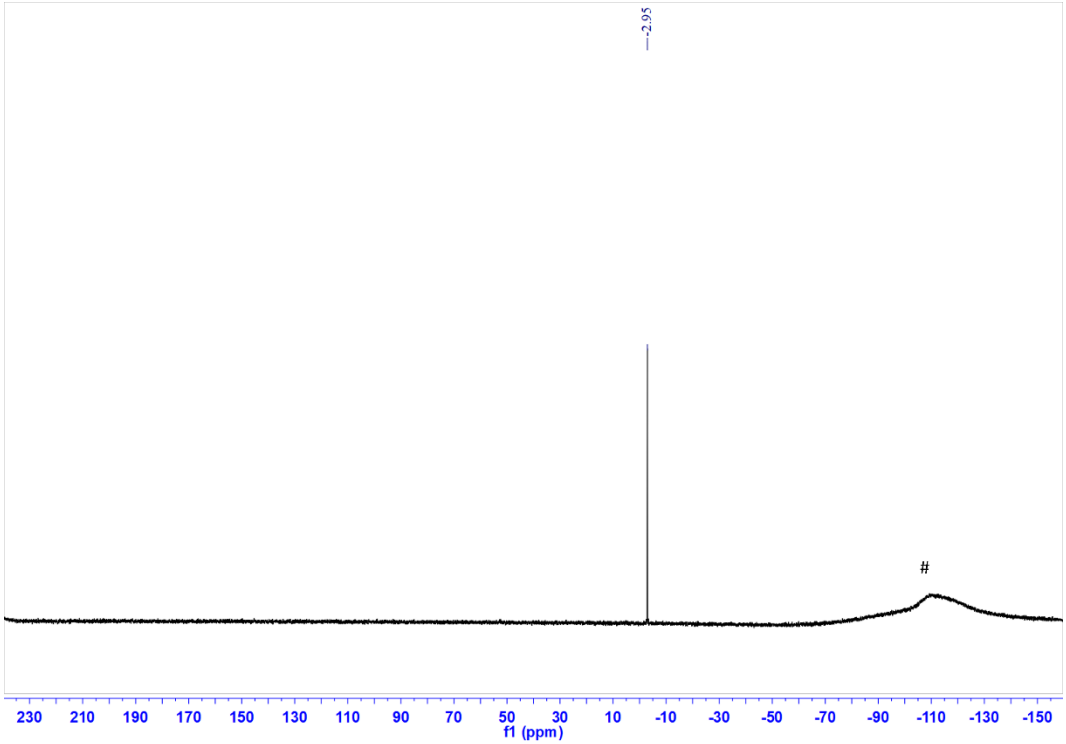

Figure S8. $^{29}Si\{^{1}H\}$ NMR spectrum of [Ce(η^8-COT^{TIPS})BH_4] (**2**) in THF-d_8: #, background signal from NMR tube (made of borosilicate glass).

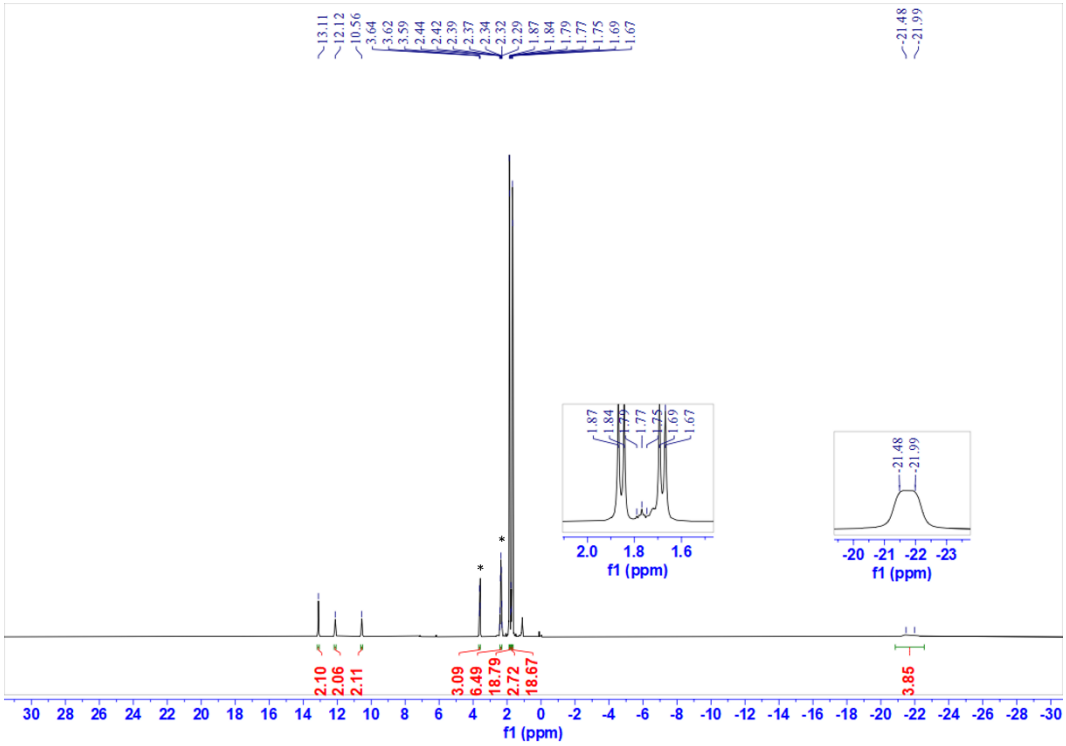

Figure S9. ^{1}H NMR spectrum of [Sm(η^{8}-COT^{TIPS})BH$_4$] (**3**) in THF-d_8: *, residual protio solvent signal.

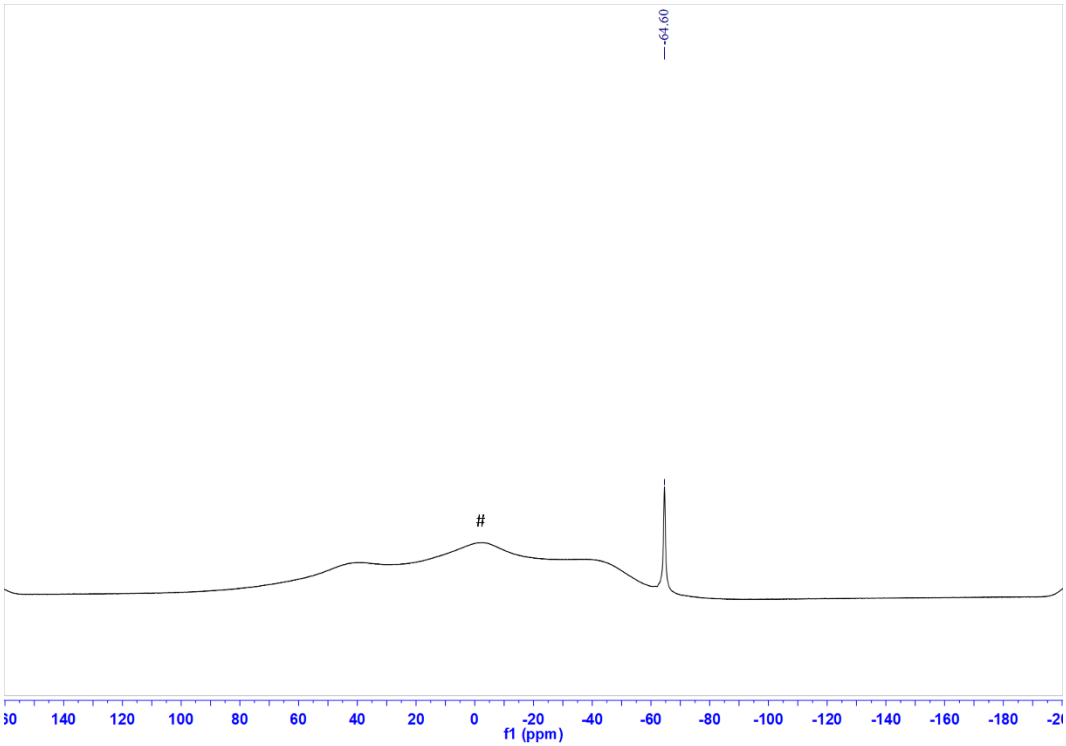

Figure S10. ^{11}B NMR spectrum of [Sm(η^{8}-COT^{TIPS})BH$_4$] (**3**) in THF-d_8: #, background signal from NMR tube (made of borosilicate glass).

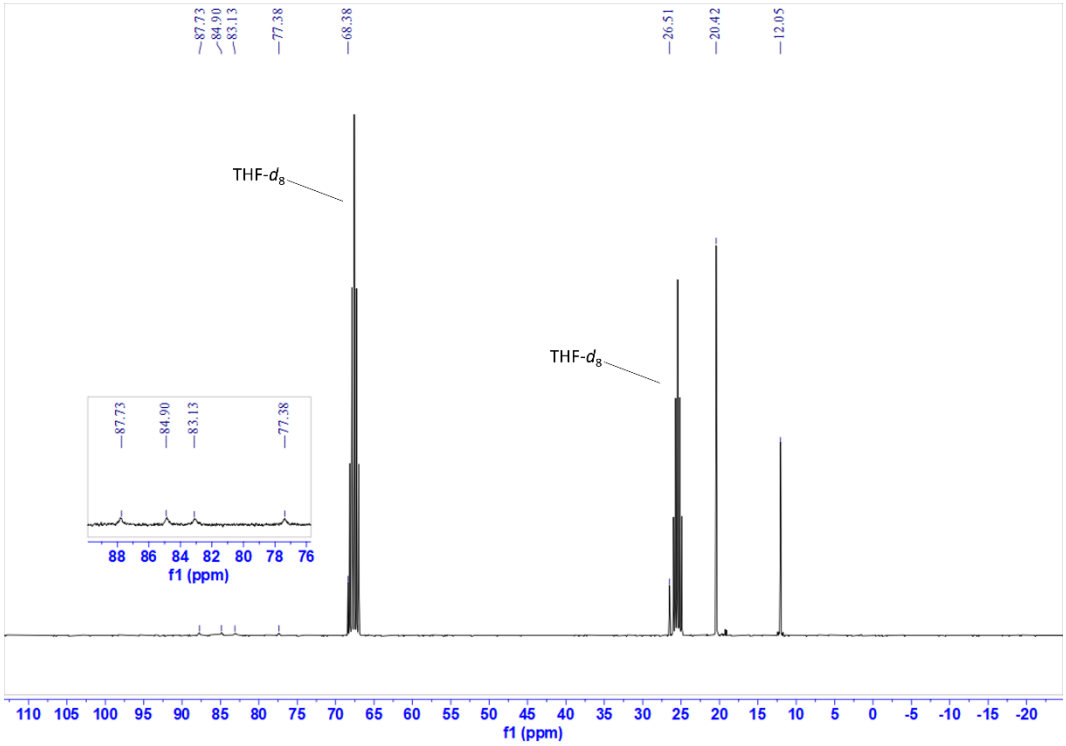

Figure S11. $^{13}C\{^1H\}$ NMR spectrum of [Sm(η^8-COT^{TIPS})BH_4] (**3**) in THF-d_8.

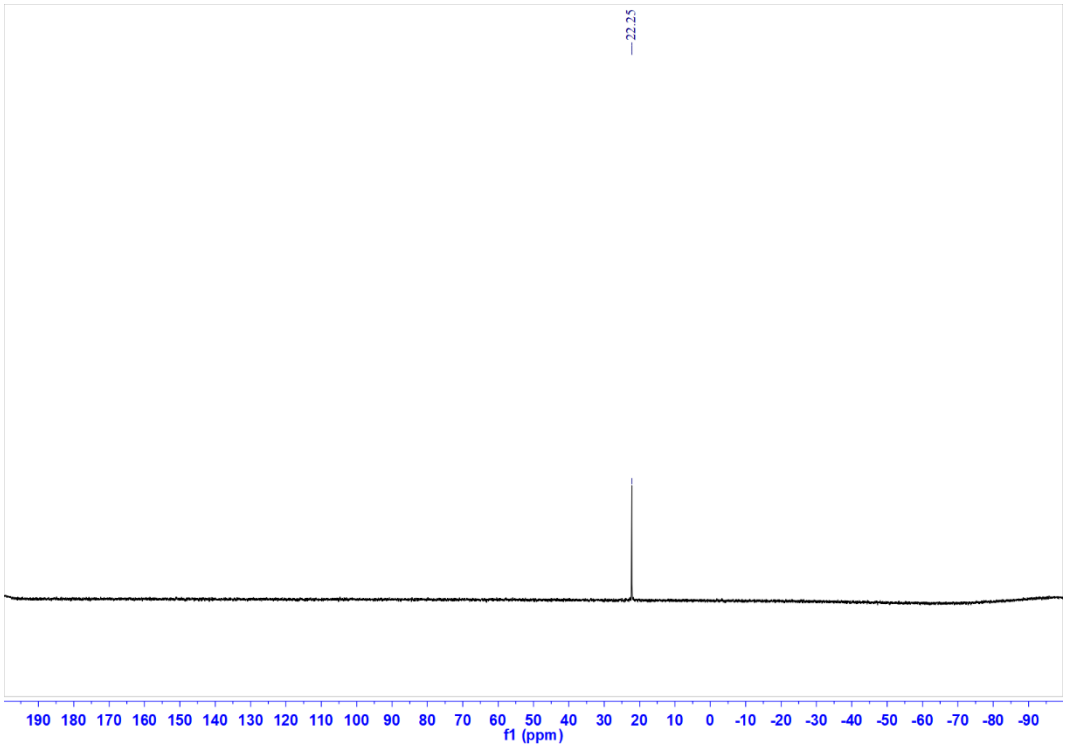

Figure S12. $^{29}Si\{^1H\}$ NMR spectrum of [Sm(η^8-COT^{TIPS})BH_4] (**3**) in THF-d_8.

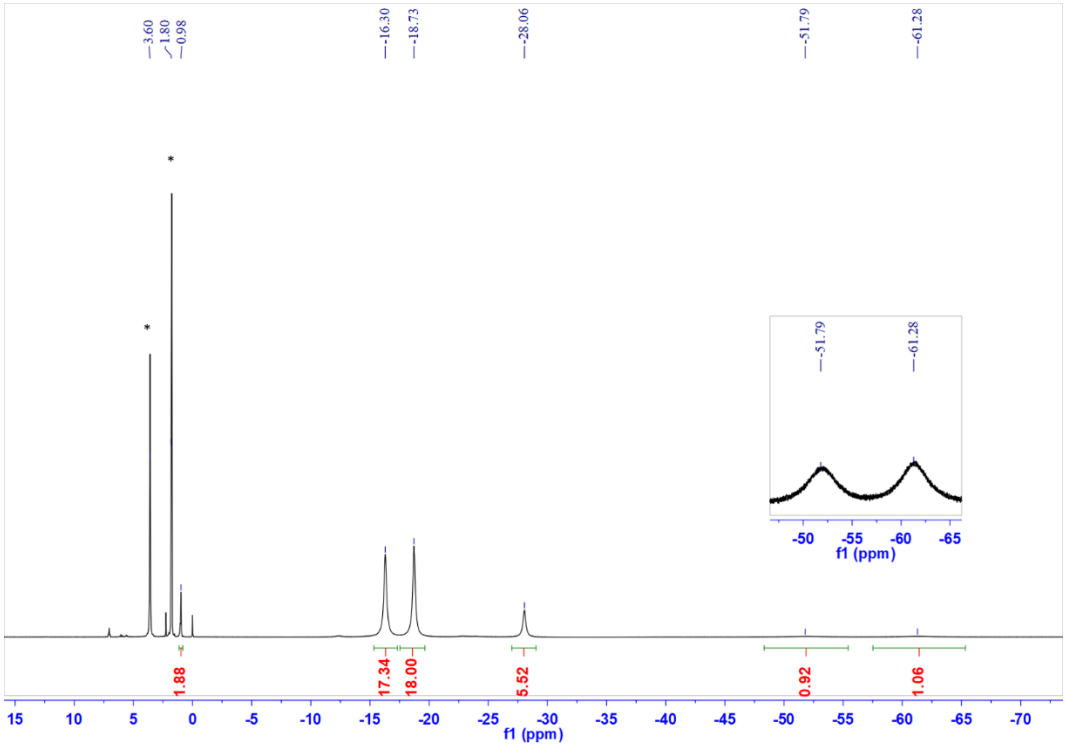

Figure S13. ^{1}H NMR spectrum of [Er(η^{8}-COT^{TIPS})BH$_4$] (**4**) in THF-d_8: *, residual protio solvent signal.

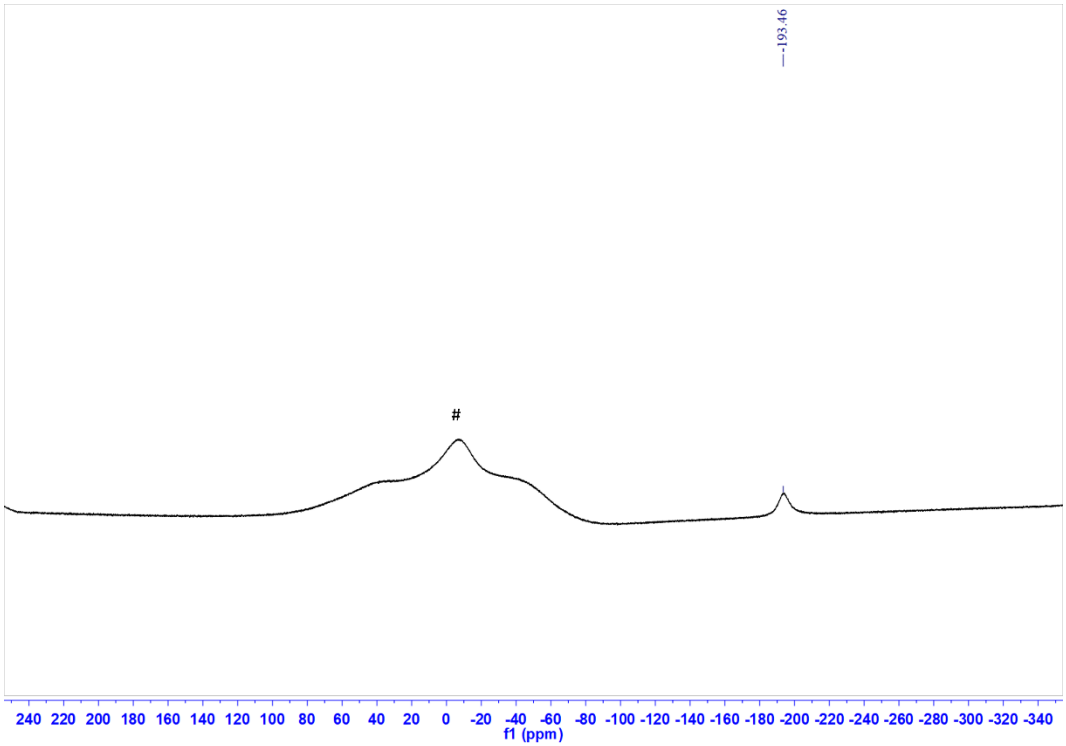

Figure S14. ^{11}B NMR spectrum of [Er(η^{8}-COT^{TIPS})BH$_4$] (**4**) in THF-d_8: #, background signal from NMR tube (made of borosilicate glass).

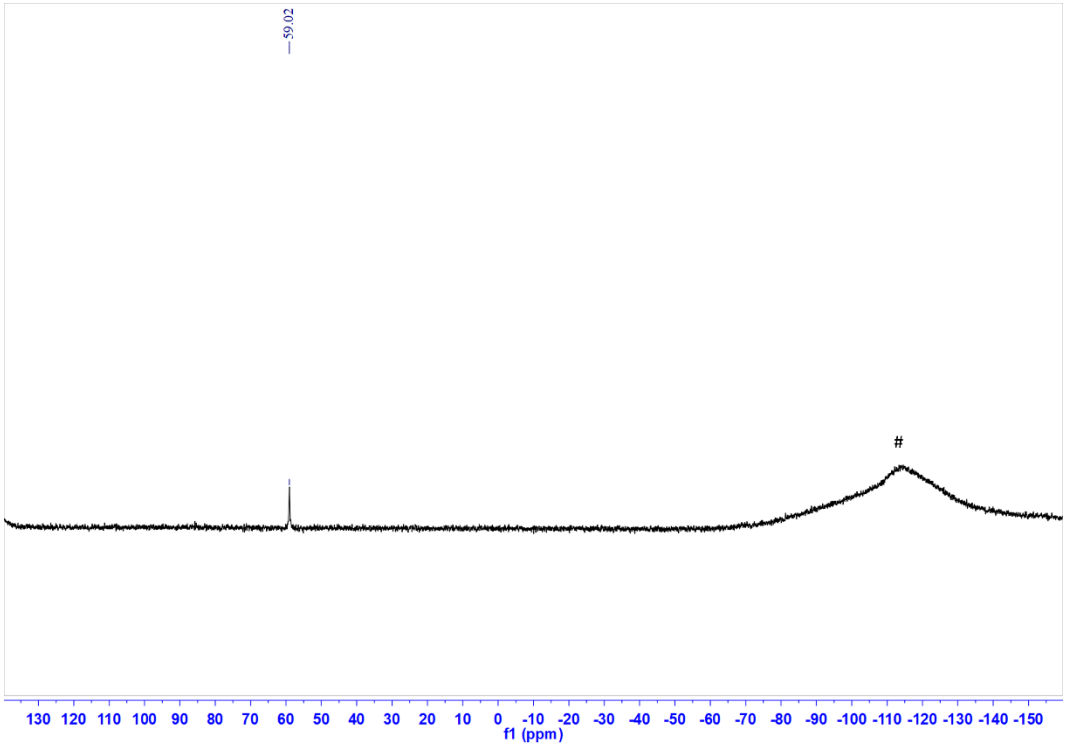

Figure S15. $^{29}Si\{^{1}H\}$ NMR spectrum of [Er(η^8-COT^{TIPS})BH_4] (**4**) in THF-d_8: #, background signal from NMR tube (made of borosilicate glass).

NMR Spectra of 5-10

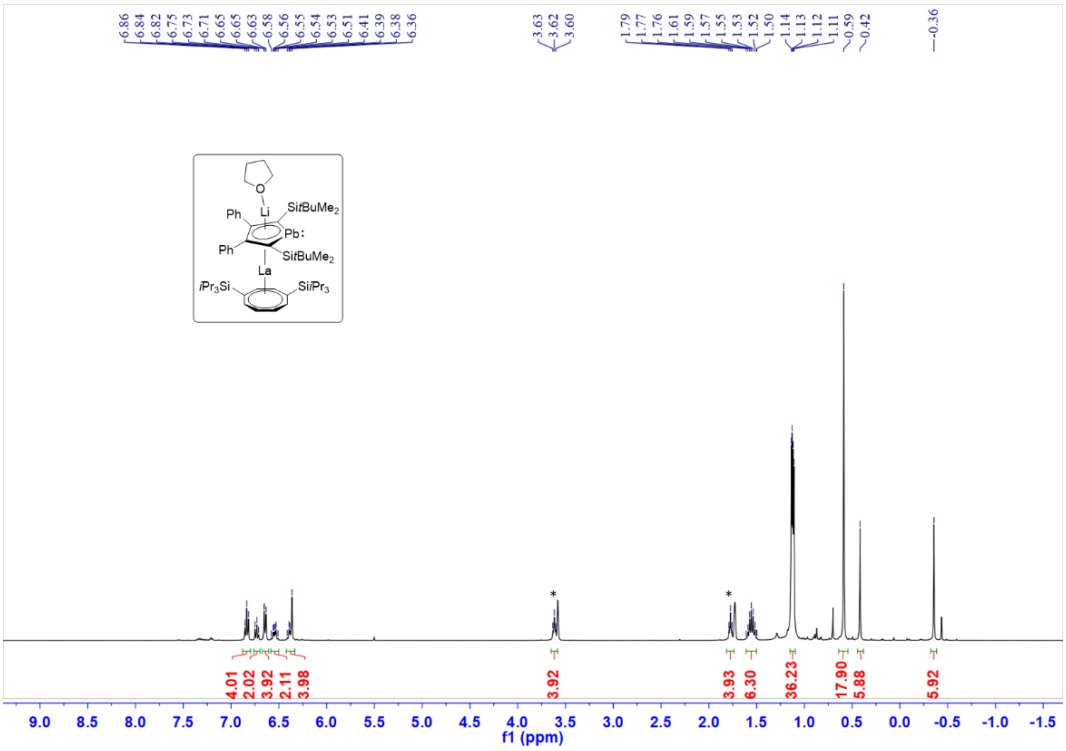

Figure S16. ^{1}H NMR spectrum of [Li(thf)(η^5-L^{Pb})La(η^8-COT^{TIPS})] (**5**) in THF-d_8: *, residual protio solvent signal.

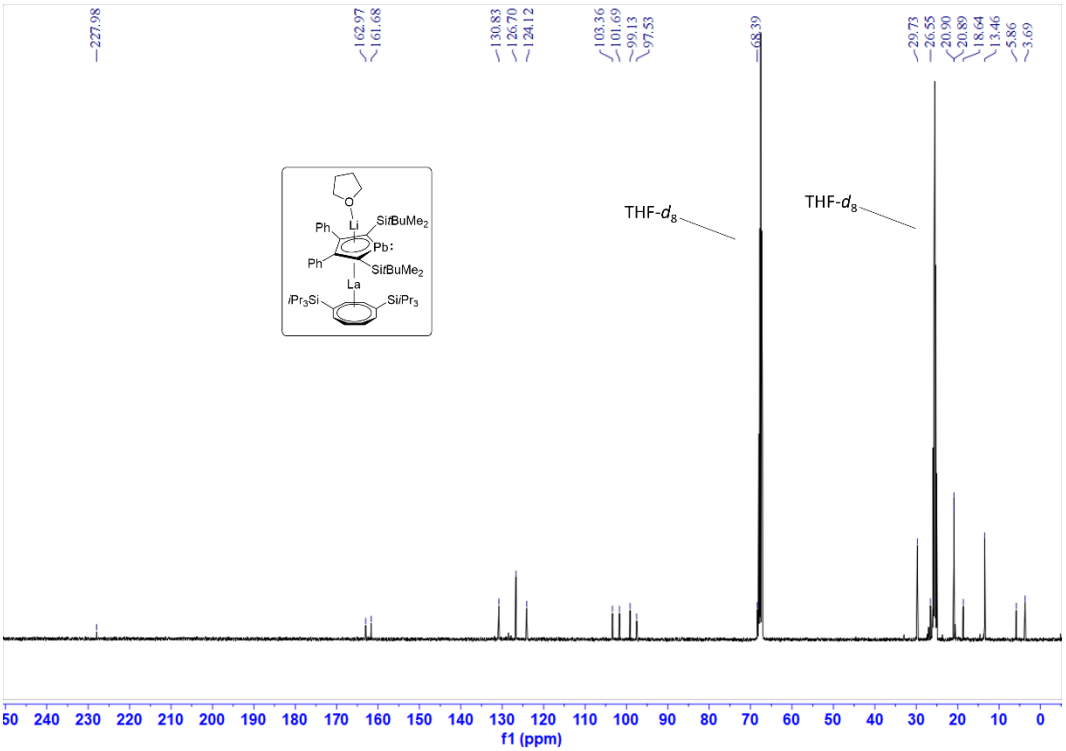

Figure S17. ^{13}C{^{1}H} NMR spectrum of [Li(thf)(η^5-L^{Pb})La(η^8-COT^{TIPS})] (**5**) in THF-d_8.

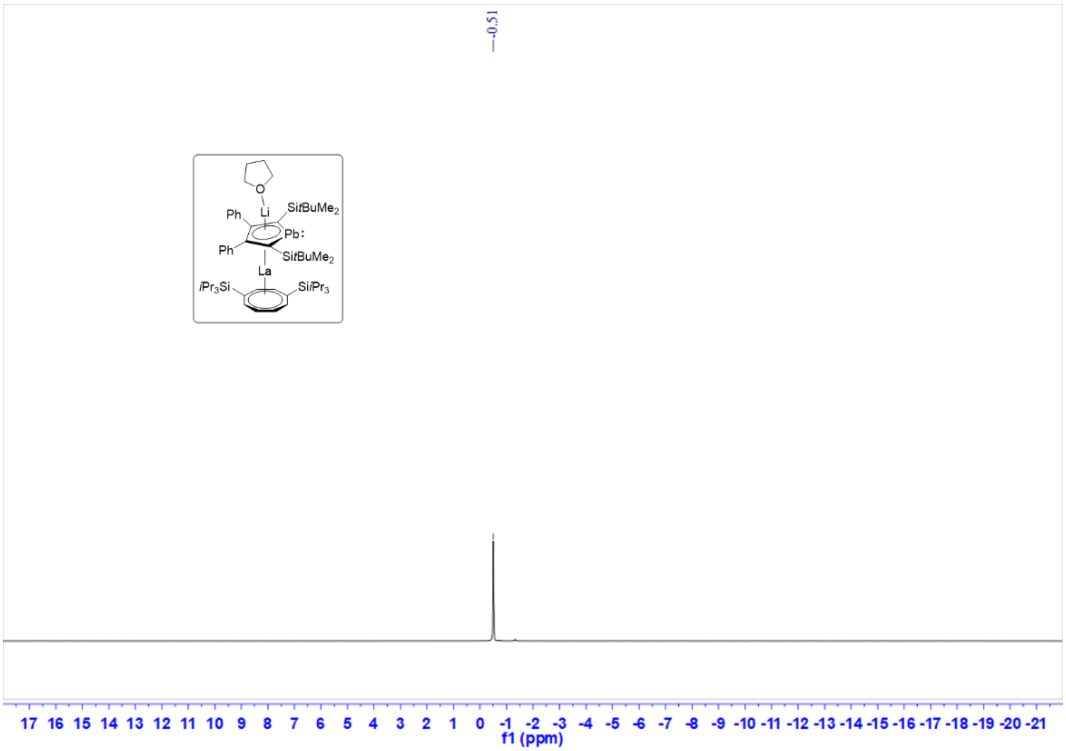

Figure S18. ^{7}Li{^{1}H} NMR spectrum of [Li(thf)(η^5-L^{Pb})La(η^8-COT^{TIPS})] (**5**) in THF-d_8.

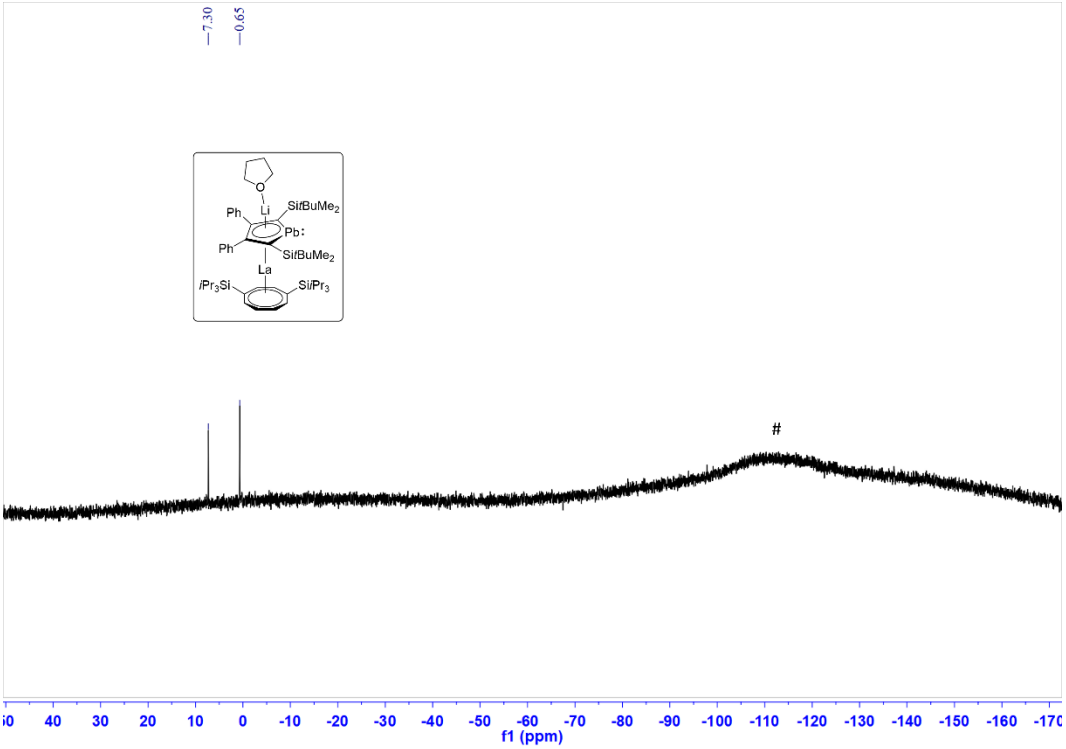

Figure S19. ^{29}Si{^{1}H} NMR spectrum of [Li(thf)(η^5-L^{Pb})La(η^8-COT^{TIPS})] (**5**) in THF-d_8: #, background signal from NMR tube (made of borosilicate glass).

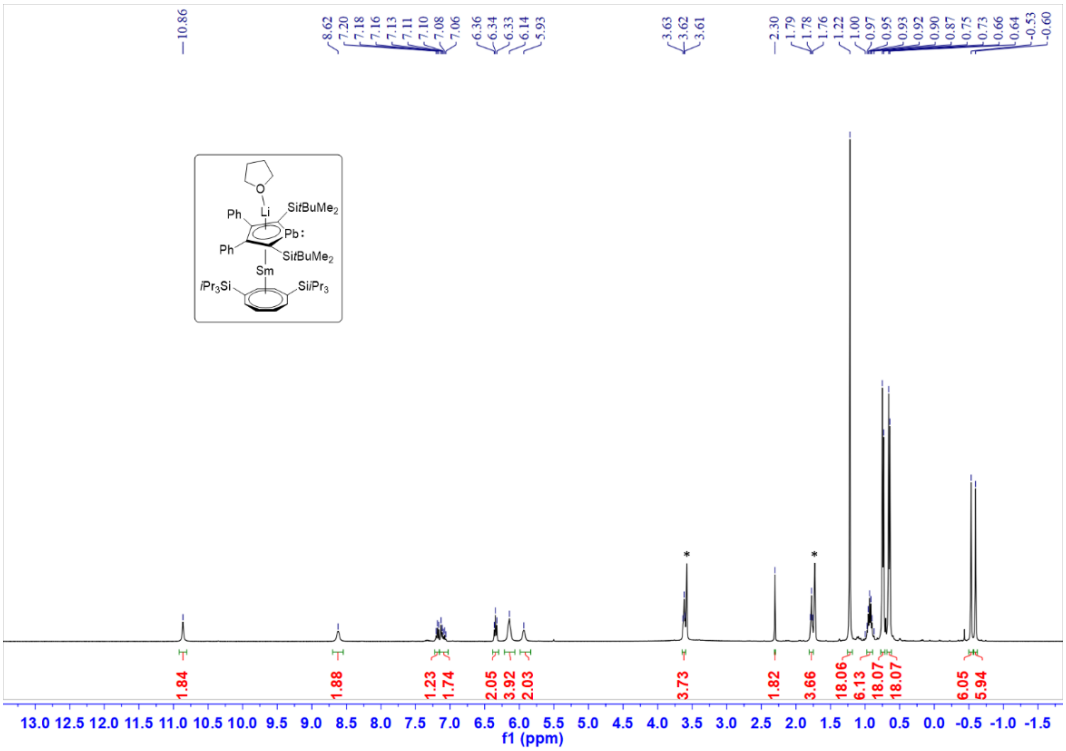

Figure S20. ^{1}H NMR spectrum of [Li(thf)(η^5-L^{Pb})Sm(η^8-COT^{TIPS})] (**6**) in THF-d_8: *, residual protio solvent signal.

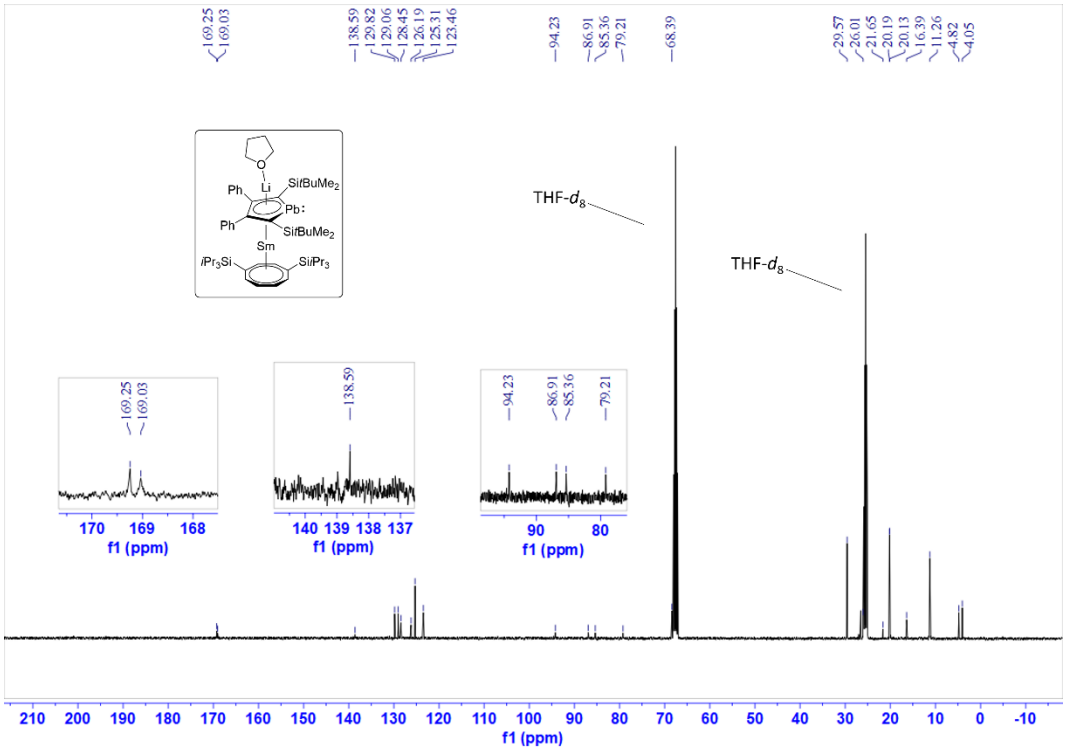

Figure S21. ^{13}C{^{1}H} NMR spectrum of [Li(thf)(η^5-L^{Pb})Sm(η^8-COT^{TIPS})] (**6**) in THF-d_8.

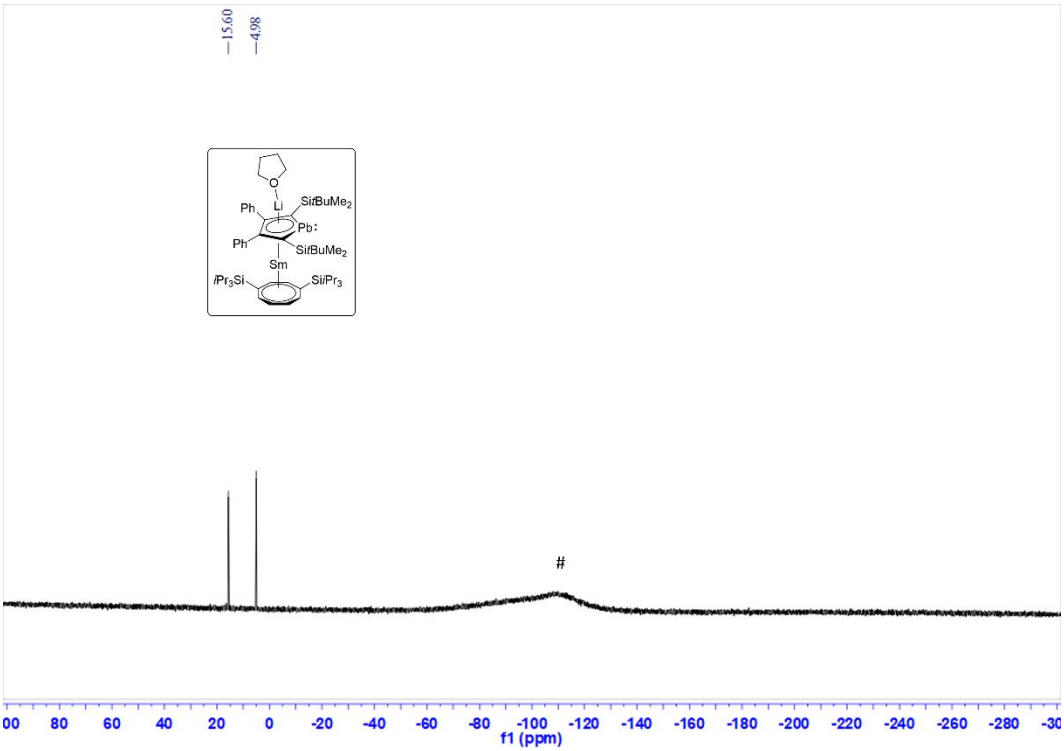

Figure S22. $^{29}Si\{^{1}H\}$ NMR spectrum of [Li(thf)(η^5-L^{Pb})Sm(η^8-COT^{TIPS})] (**6**) in THF-d_8: #, background signal from NMR tube (made of borosilicate glass).

FT-Raman Spectra

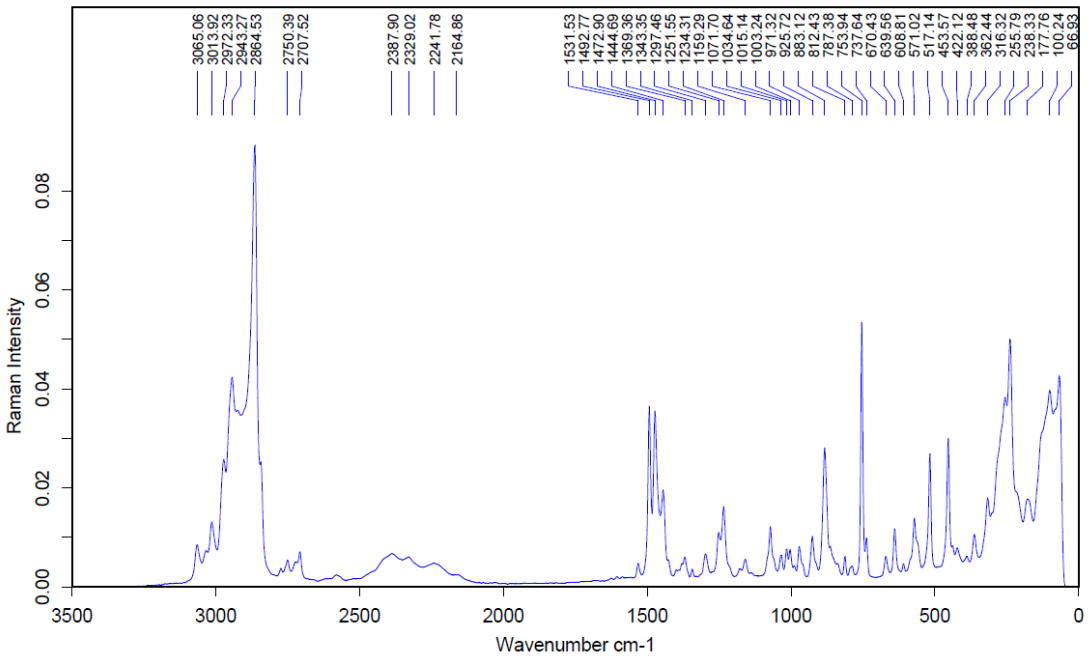

Figure S23. FT-Raman spectrum of [La(η^8-COT^{TIPS})BH$_4$] (**1**).

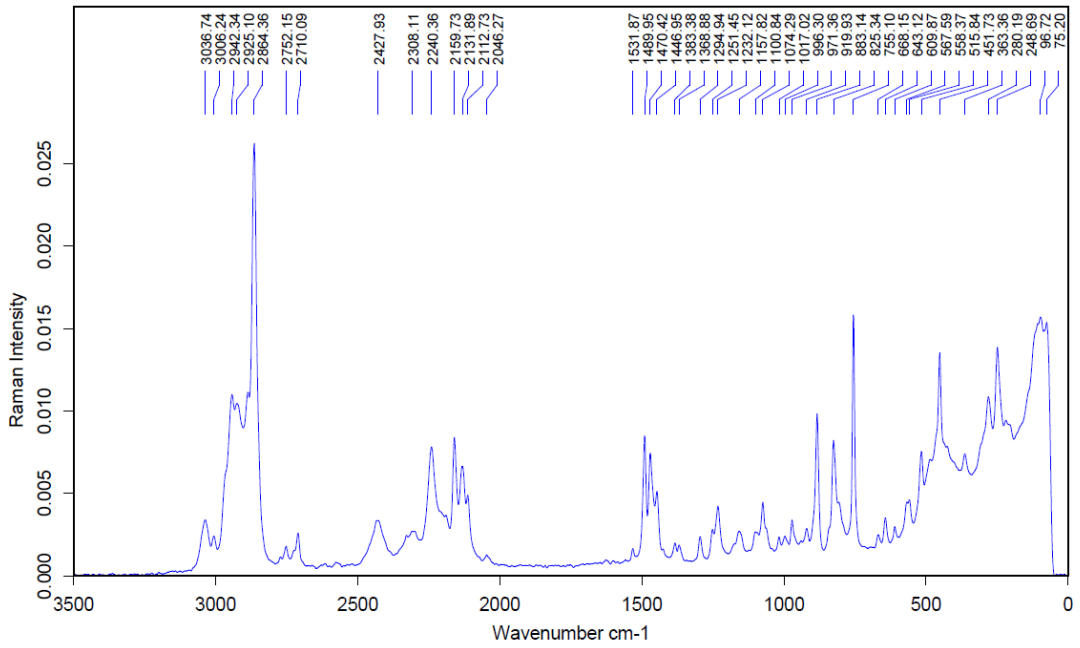

Figure S24. FT-Raman spectrum of [Ce(η^8-COT^{TIPS})BH$_4$] (**2**).

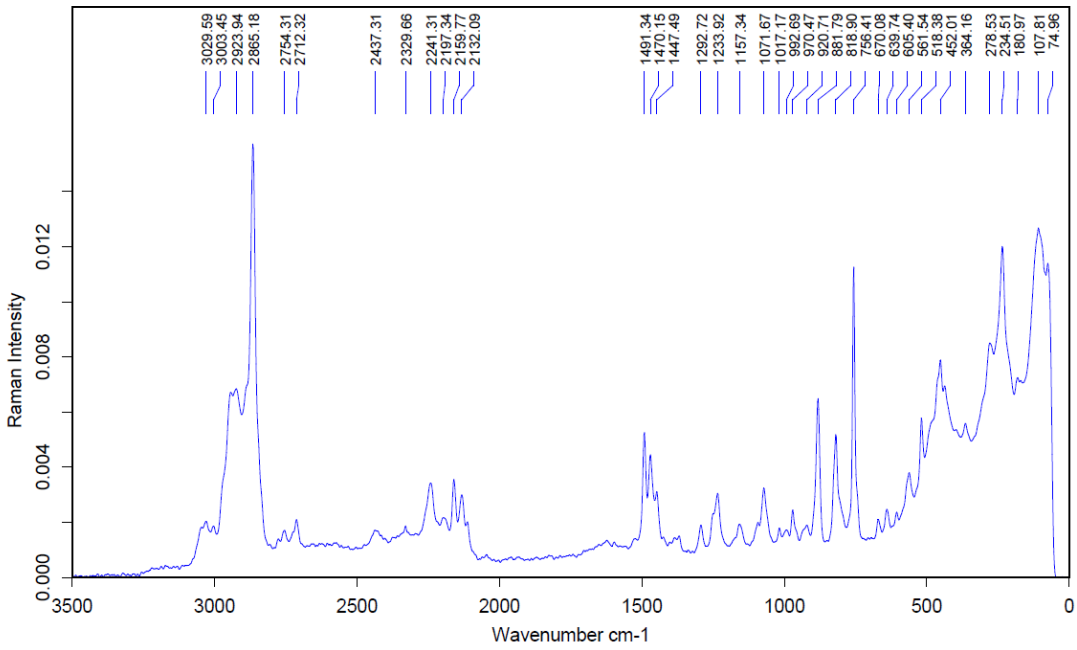

Figure S25. FT-Raman spectrum of [Sm(η^8-COT^{TIPS})BH$_4$] (**3**).

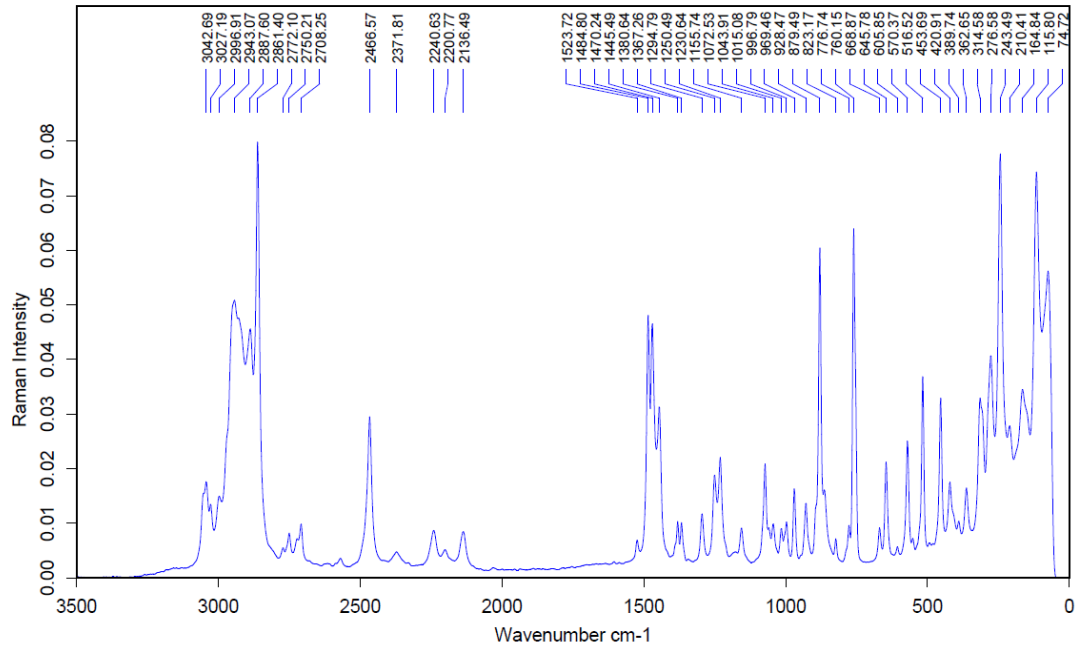

Figure S26. FT-Raman spectrum of [Er(η^8-COT^{TIPS})BH$_4$] (**4**).

FT-IR Spectra

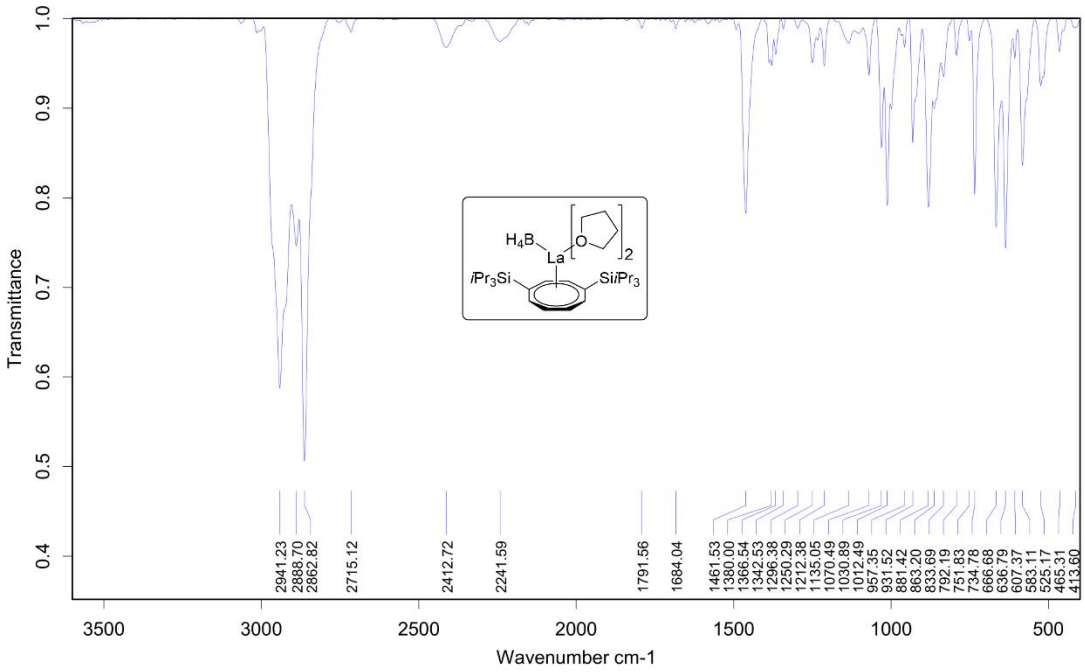

Figure S27. IR spectrum of [La(η^8-COT^{TIPS})BH$_4$] (**1**).

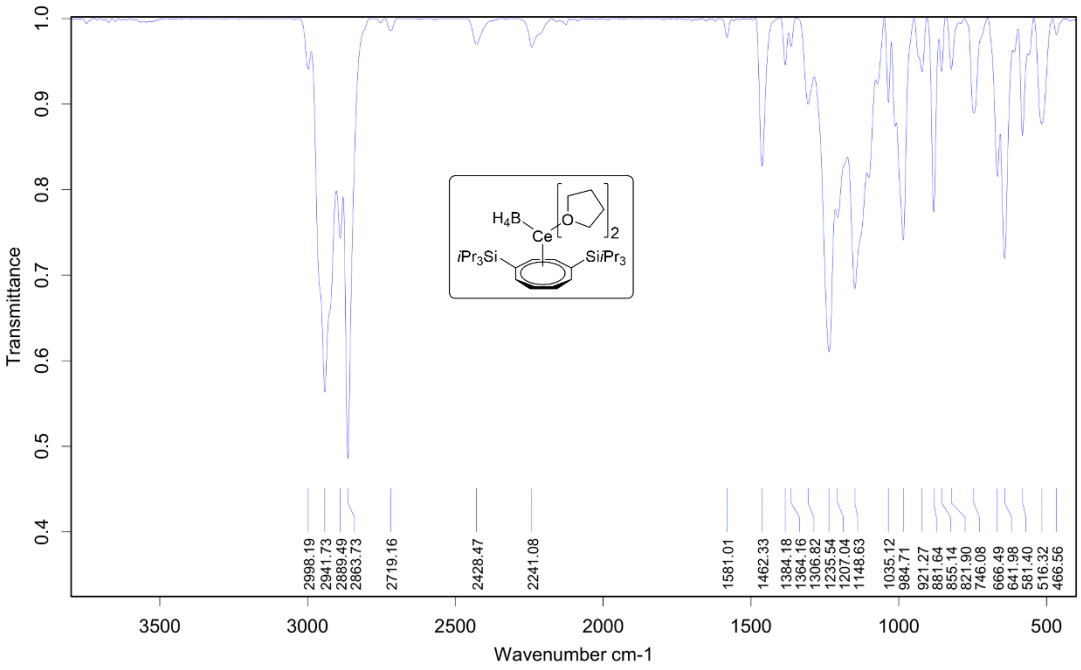

Figure S28. IR spectrum of [Ce(η^8-COT^{TIPS})BH$_4$] (**2**).

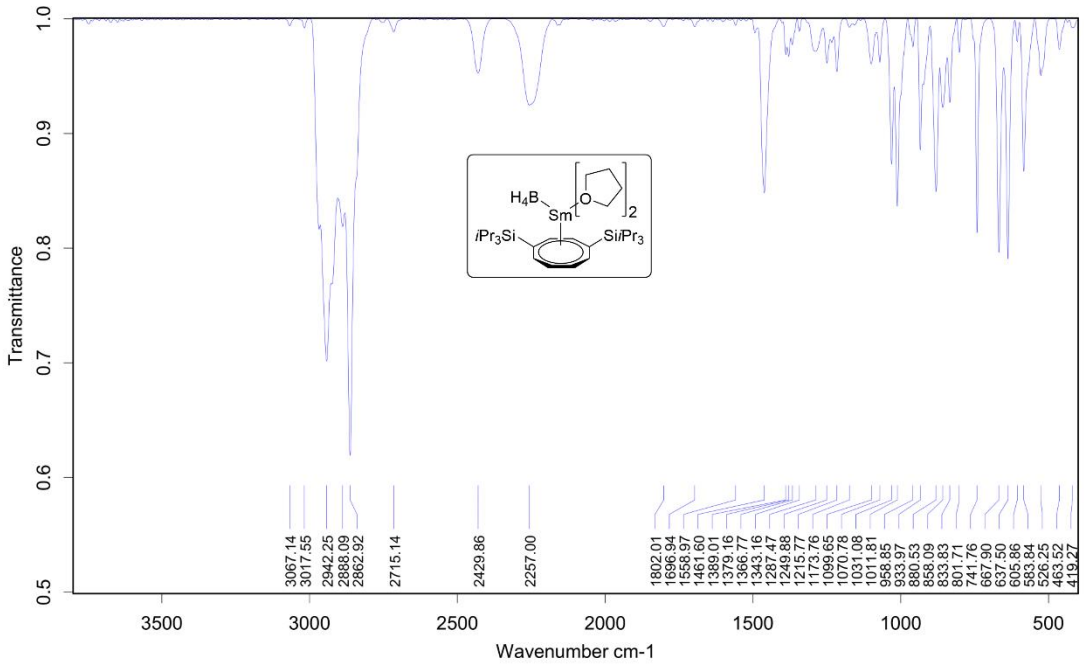

Figure S29. IR spectrum of [Sm(η^8-COT^{TIPS})BH_4] (**3**).

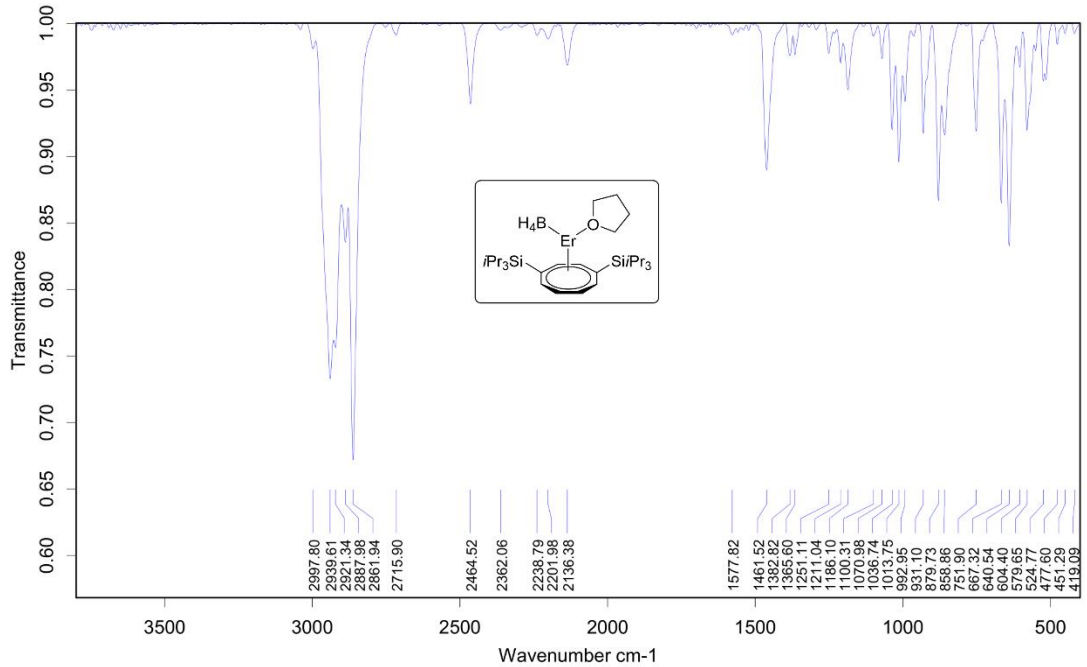

Figure S30. IR spectrum of [Er(η^8-COT^{TIPS})BH_4] (**4**).

The binding mode of borohydride ligands can readily be examined by vibrational spectroscopy. To support the end on η^3-binding mode elucidated by X-ray diffraction studies (*vide infra*), two distinct bands at approximately 2200 cm^{-1} and 2400 cm^{-1} are expected for the bridging and terminal hydrogen-boron bonds, respectively. The expected bands can be observed in Raman spectra of compounds **1**-**4** (Figure S23 - Figure S26). However, these signals overlap with other resonances, that cannot be unambiguously assigned without further support by calculations. These possibly arise from vibrational modes that are IR forbidden and not well described in in literature. As expected, IR spectra of **1**-**4** solely feature above mentioned characteristic bands (Figure S27 - Figure S30). These are rather intense, do not overlap with further signals, and are found in a similar position compared to those observed in the Raman spectra (Table S1). Thus, the proposed η^3-binding mode of the borohydride ligands is validated by these findings.

Table S1. Comparison of IR and Raman resonances that are unambiguously assignable to vibrational modes of the borohydride ligands in compounds **1**-**4**.

Compound	Wavenumber Raman [cm^{-1}]		Wavenumber IR [cm^{-1}]	
1	2388	2242	2413	2242
2	2428	2240	2428	2241
3	2437	2241	2430	2257
4	2467	2136	2465	2136

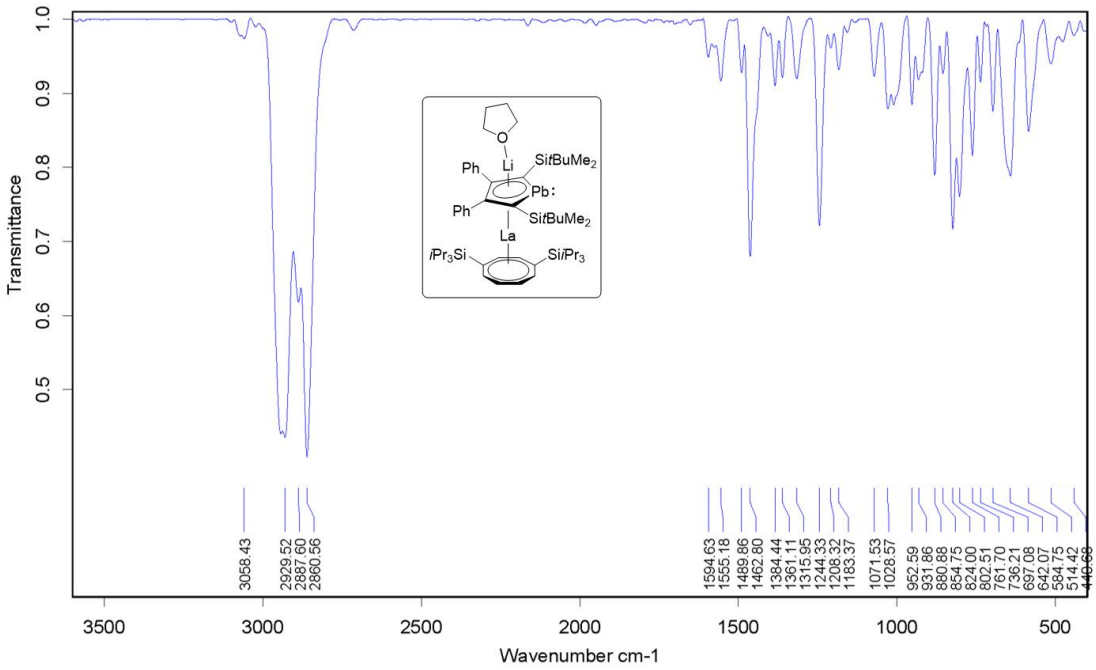

Figure S31. IR spectrum of [Li(thf)(η^5-L^{Pb})La(η^8-COT^{TIPS})] (**5**).

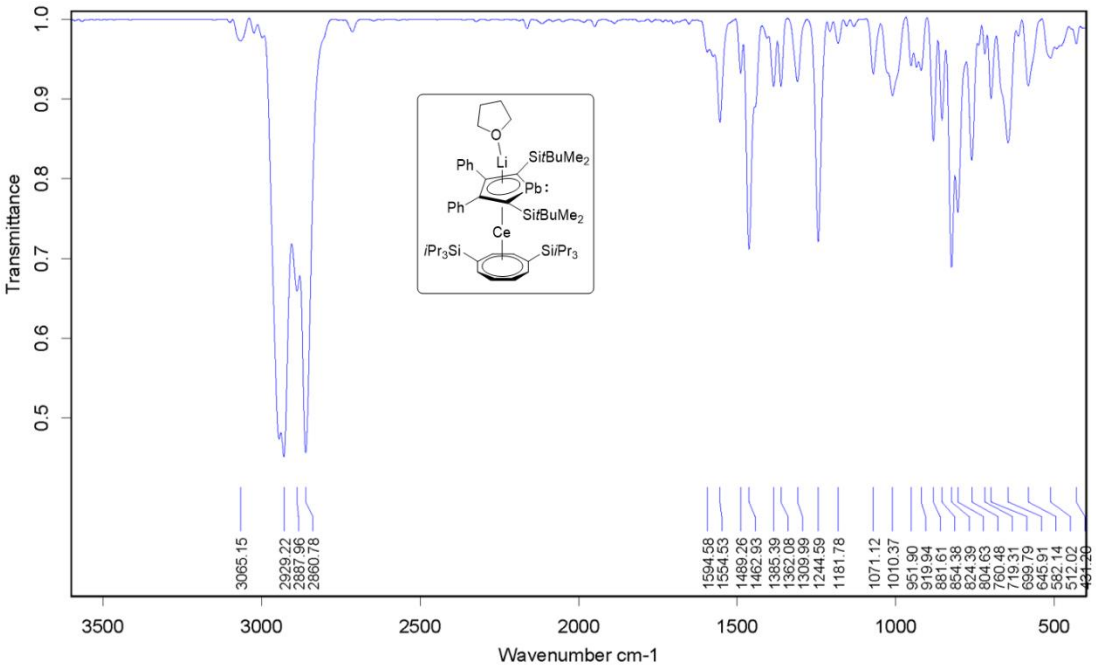

Figure S32. IR spectrum of [Li(thf)(η^5-L^{Pb})Ce(η^8-COT^{TIPS})] (**6**).

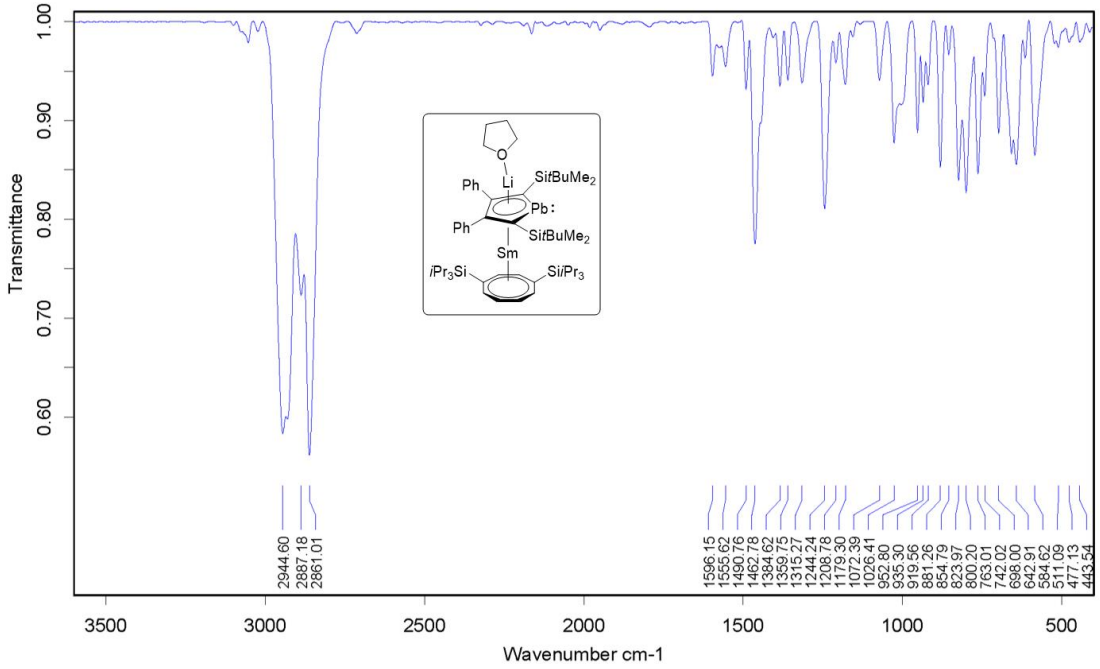

Figure S33. IR spectrum of [Li(thf)(η^5-L^{Pb})Sm(η^8-COT^{TIPS})] (**7**).

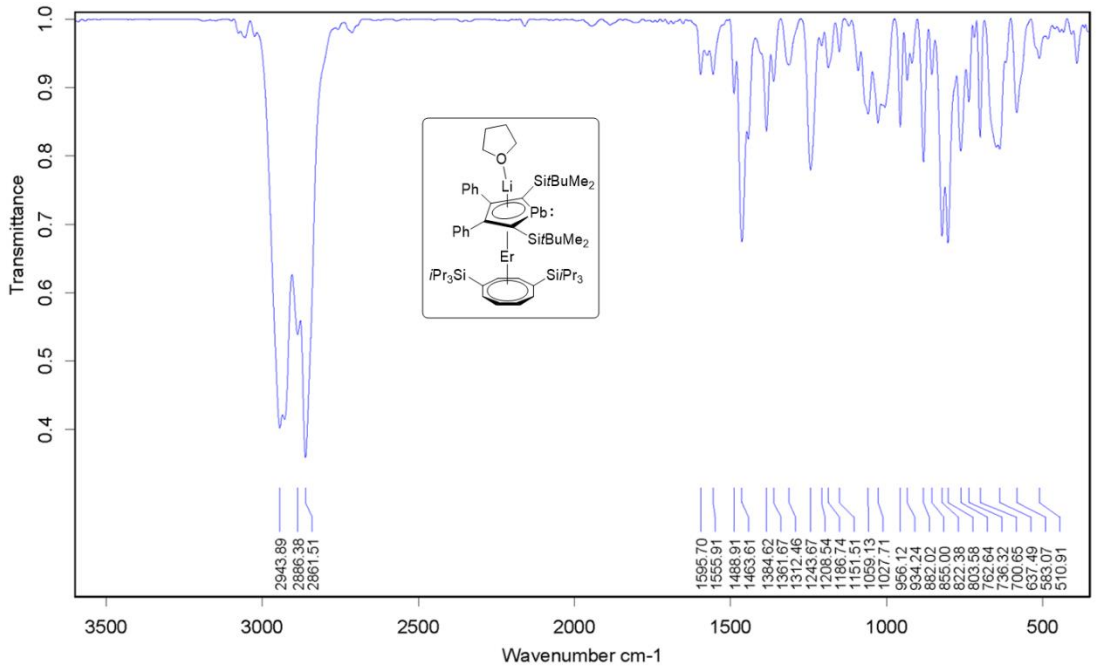

Figure S34. IR spectrum of [Li(thf)(η^5-L^{Pb})Er(η^8-COT^{TIPS})] (**8**).

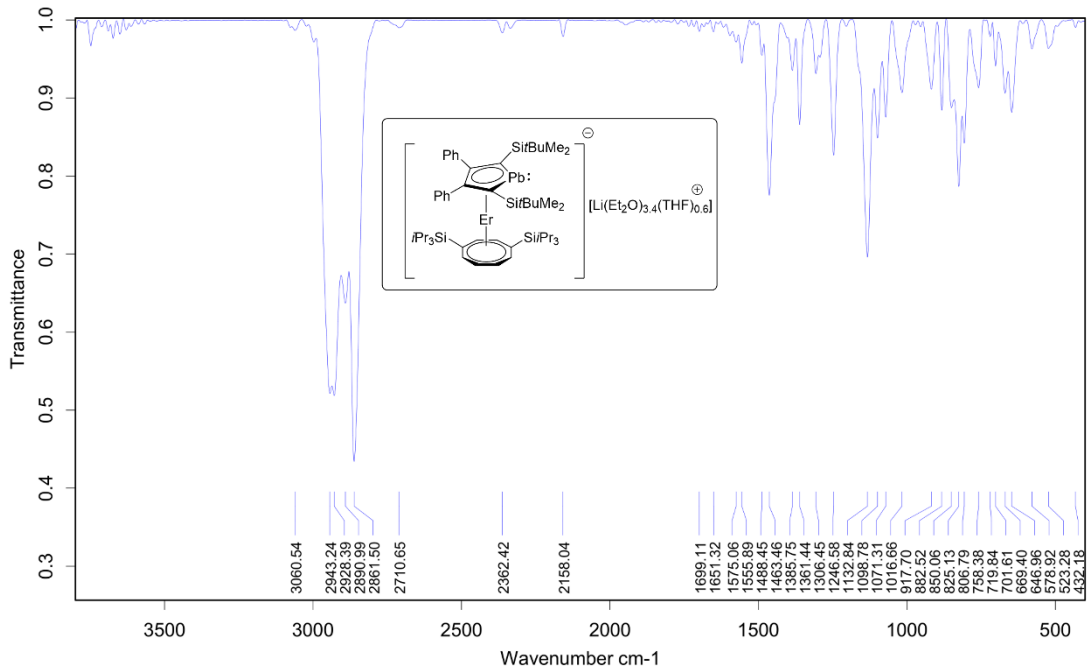

Figure S35. IR spectrum of $[Li(Et_2O)_{3.4}(thf)_{0.6}][(\eta^5\text{-}L^{Pb})Er(\eta^8\text{-}COT^{TIPS})]$ (**9**).

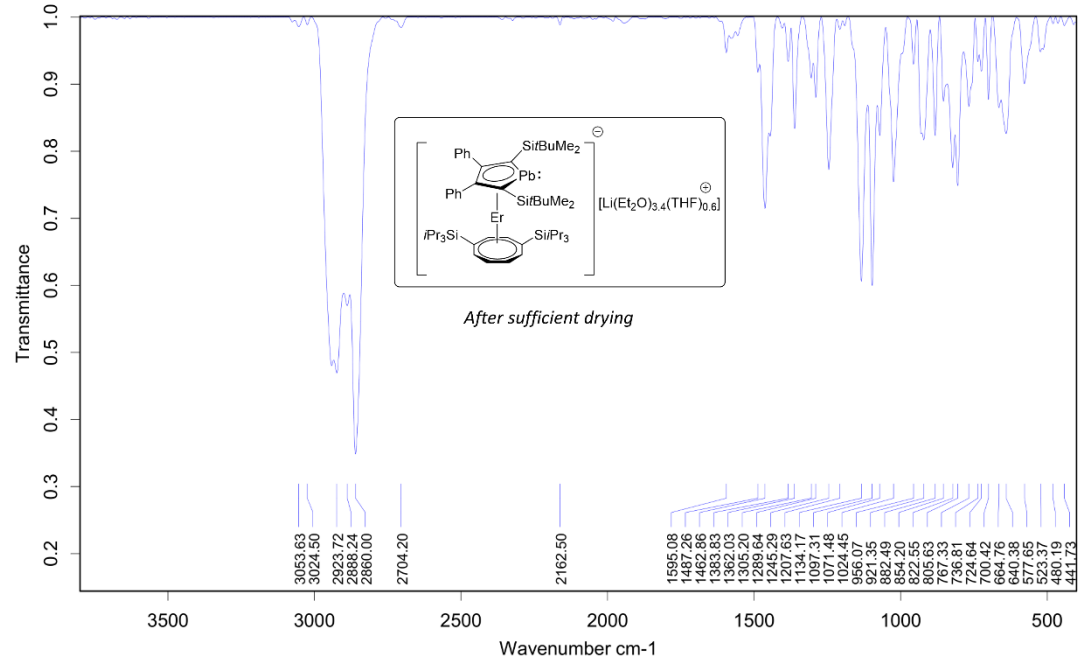

Figure S36. IR spectrum of $[Li(Et_2O)_{3.4}(thf)_{0.6}][(\eta^5\text{-}L^{Pb})Er(\eta^8\text{-}COT^{TIPS})]$ (**9**) after sufficient drying under vacuum.

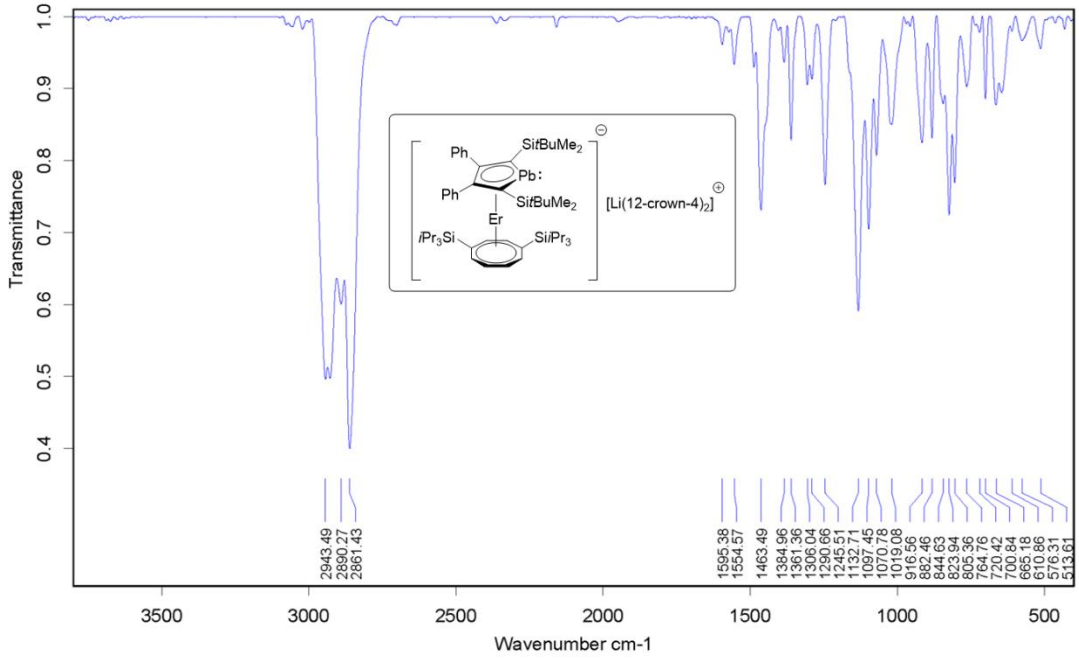

Figure S37. IR spectrum of [Li(12-c-4)$_2$][(η^5-L^{Pb})Er(η^8-COT^{TIPS})] (**10**).

X-ray Crystallographic Studies

Suitable crystals were selected under an optic microscope equipped with polarizing filters, covered in mineral oil (Aldrich) and mounted on a *MiTeGen* holder. The crystals were transferred directly to the cold stream of a STOE IPDS 2 (150 K) or STOE StadiVari (100 K) diffractometer, equipped with a Mo-sealed tube, MoGenix 3D HF or a Ga-MetalJet X-ray source. All structures were solved using the programs SHELXS/T and Olex2 1.2.[4,5,6] The remaining non-hydrogen atoms were located from successive difference Fourier map calculations. The refinements were carried out by using full-matrix least-squares techniques on F^2 by using the program SHELXL. In each case, the locations of the largest peaks in the final difference Fourier map calculations, as well as the magnitude of the residual electron densities, were of no chemical significance.
Specific comments on the structures discussed here are given below.

[La(η^8-COT^{TIPS})BH_4] (**1**): Crystals of **1** showed severe structural defects upon cooling to 100 K, most likely caused by a temperature induced phase transition. We attempted to omit this problem by elevating the cryostream temperature. However, cracks in the crystal were observed up to 273.15 K. A stable measurement could only be achieved at room temperature, where exceedingly large ADPs were observed. As a result, the obtained data will not be discussed here.
Cell found by SCXRD:
a = 8.016 Å
b = 24.547 Å
c = 22.298 Å
α = γ = 90°
β = 89.728°
Ball and stick model to proof connectivity:

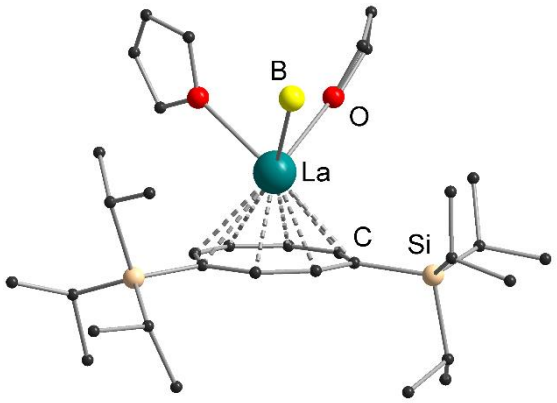

Figure S38: Ball and stick model of compound **1** as obtained by SCXRD measurement at room temperature. Due to very large ADPs under these conditions, no bond metrics and detials will be given here.

[Er(η^8-COT^{TIPS})BH$_4$] (**4**): Compound **4** was solved and refined in the orthorhombic space group *Pnma*. The mirror plane, which goes through the center of the molecule, generates a positionally disordered THF ligand. To model the disordered moiety, SIMU, RIGU and SADI constraints were applied.

[Li(thf)(η^5-L^{Pb})La(η^8-COT^{TIPS})] (**5**): The crystal structure of **5** showed severe positional disorders of the Li-coordinated THF ligand, both phenyl rings, both TIPS groups and on TBDMS group. These were split in two parts with an approximate occupancy of 50% for both. Modelling of the disordered substituents was achieved with RIGU, SIMU, DELU and SADI restraints where appropriate. One disordered phenyl-carbon atom (C14a) was additionally restrained using ISOR. Interestingly, compounds **5**, **6** and **8** were best solved and refined in the acentric space group $P2_1$, although no implications of chirality were observed. In contrast, **7** crystallized in the centric space group $P2_1/n$. Here the possible reason might be the solvent choice. Complexes **5**, **6** and **8** were crystallized from *n*-heptane, while **7** was crystallized from toluene.

[Li(thf)(η^5-L^{Pb})Ce(η^8-COT^{TIPS})] (**6**): As described above, the crystal structure of **6** was solved and refined in the acentric space group $P2_1$. Crystals of **6** were measured using a Gallium-jet X-ray source. Due to the experimental setup, reflections at high angles could not be measured, leading to a lower-than-expected Friedel-pair coverage and completeness. No measuring strategy that circumvents this problem could be found., despite several attempts.

[Li(thf)(η^5-L^{Pb})Sm(η^8-COT^{TIPS})] (**7**): As described above, the crystal structure of **7** was, in contrast to the structures of **5**, **6** and **8**, solved and refined in the centric space group $P2_1/n$. The reason for this discrepancy most likely is the different solvent used for crystallization. The crystal structure of **7** contains one molecule of toluene per asymmetric unit.

[Li(thf)(η^5-L^{Pb})Er(η^8-COT^{TIPS})] (**8**): As described above, the crystal structure of **8** was solved and refined in the acentric space group $P2_1$. Compare [Li(thf)(η^5-L^{Pb})La(η^8-COT^{TIPS})] (**5**).

[Li(Et$_2$O)$_{3.4}$(thf)$_{0.6}$][(η^5-L^{Pb})Er(η^8-COT^{TIPS})] (**9**): The crystal structure of **9** shows a charge separated species comprising a Et$_2$O solvated Li-cation. However, careful consideration of the residual electron density in the coordination sphere of the cation led to the assumption that one Et$_2$O position is mixed with a molecule of THF in a ratio of 40:60. The half-occupied ligand moieties were modelled with SIMU, RIGU and DELU restraints.
Alert level B:
PROBLEM: Check Calcd Resid. Dens. 0.80A From Pb1 -2.85 eA-3
RESPONSE: truncation error

[Li(12-c-4)$_2$][(η^5-L^{Pb})Er(η^8-COT^{TIPS})] (**10**): In the crystal structure of **10** the Li-cation is located on two special positions on two opposing sides of the central [(η^5-L^{Pb})Er(η^8-COT^{TIPS})]-anion. Both positions are half-occupied. Accordingly, the 12-c-4 ligands coordinating to the Li-cation show a positional disorder with a ratio of 50:50. The asymmetric unit also contains a half molecule of toluene, which could not be modelled satisfactorily. Therefore, the correlated electron density was removed from the electron density map using the solvent mask of Olex2.[6]

Crystallographic data for the structures reported in this paper have been deposited with the Cambridge Crystallographic Data Centre as a supplementary publication no. 2067569-2067577. Copies of the data can be obtained free of charge on application to CCDC, 12 Union Road, Cambridge CB21EZ, UK (fax: (+(44)1223-336-033; email: deposit@ccdc.cam.ac.uk).

Table S2. Crystal data and structure refinement for compounds **2-5**.

Compound	**2**	**3**	**4**	**5**
Formula	$C_{34}H_{68}BCeO_2Si_2$	$C_{34}H_{68}BO_2Si_2Sm$	$C_{30}H_{60}BErOSi_2$	$C_{58}H_{97}LaLiOPbSi_4$
$D_{calc.}$/ g cm^{-3}	1.247	1.268	1.325	1.384
m/mm^{-1}	1.283	1.633	2.586	3.547
Formula Weight	715.99	726.22	671.03	1275.75
Color	clear yellow	clear violet	clear pink	clear orange
Shape	block	block	irregular	rod
Size/mm^3	0.63×0.38×0.23	0.35×0.28×0.17	0.48×0.34×0.09	0.67×0.34×0.09
T/K	100	150	150	100
Crystal System	monoclinic	monoclinic	orthorhombic	monoclinic
Space Group	$P2_1/c$	$P2_1/c$	*Pnma*	$P2_1$
a/Å	7.4686(5)	7.5051(3)	15.8956(3)	13.4752(3)
b/Å	26.405(2)	26.3267(9)	24.9080(5)	13.6204(2)
c/Å	19.5200(11)	19.4417(8)	8.4943(7)	16.9090(4)
α/°				
β/°	97.925(5)	98.004(3)		99.420(2)
γ/°				
V/Å^3	3812.7(5)	3804.0(3)	3363.1(3)	3061.59(11)
Z	4	4	4	2
Z'	1	1	0.5	1
Wavelength/Å	0.71073	0.71073	0.71073	0.71073
Radiation type	MoK$_\alpha$	MoK$_\alpha$	MoK$_\alpha$	MoK$_\alpha$
Q_{min}/	2.860	1.310	2.533	1.532
Q_{max}/°	29.596	26.701	26.371	30.073
Measured Refl.	20247	17774	18104	52341
Independent Refl.	9388	7993	3514	15998
Reflections with I > 2(I)	7658	6251	2931	14247
R_{int}	0.0370	0.0399	0.0239	0.0450
Parameters	389	389	212	939
Restraints	0	0	66	357
Largest Peak	0.842	0.987	0.777	1.791
Deepest Hole	-0.867	-3.387	-0.313	-1.624
GooF	0.977	1.021	0.991	1.035
wR_2 (all data)	0.0898	0.1380	0.0599	0.1242
wR_2	0.0866	0.1335	0.0591	0.1169
R_1 (all data)	0.0441	0.0622	0.0279	0.0591
R_1	0.0346	0.0510	0.0232	0.0490
Flack Parameter	-	-	-	-0.004(4)
Hooft Parameter	-	-	-	-0.0274(14)

Table S3. Crystal data and structure refinement for compounds **6-10**.

Compound	**6**	**7**	**8**	**9**	**10**
Formula	$C_{58}H_{96}CeLiOPbSi_4$	$C_{65}H_{104}LiOPbSi_4Sm$	$C_{58}H_{96}ErLiOPbSi_4$	$C_{70}H_{126.8}ErLiO_4PbSi_4$	$C_{73.5}ErH_{124}LiO_8PbSi_4$
$D_{calc.}$/ g cm^{-3}	1.391	1.372	1.466	1.353	1.379
m/mm^{-1}	8.124	3.499	4.378	3.462	3.315
Formula Weight	1275.95	1378.32	1303.09	1526.26	1629.47
Color	clear orange	clear orange	clear orange	clear red	clear red
Shape	needle	plate	rod	block	plate
Size/mm^3	0.87×0.55×0.32	0.69×0.40×0.10	0.38×0.19×0.08	0.78×0.60×0.40	0.20×0.15×0.05
T/K	150	150	100	100	100
Crystal System	monoclinic	monoclinic	monoclinic	monoclinic	triclinic
Space Group	$P2_1$	$P2_1/n$	$P2_1$	$P2_1/n$	$P\bar{1}$
a/Å	13.4211(2)	13.5678(8)	13.3164(4)	22.0069(7)	13.1318(10)
b/Å	13.6559(2)	13.7727(5)	13.3190(3)	16.3287(4)	13.3996(16)
c/Å	16.7671(3)	35.796(2)	16.7792(6)	22.8084(7)	24.0543(14)
α/°					90.114(7)
β/°	97.5760(10)	93.725(5)	97.425(3)	113.880(2)	99.276(5)
γ/°					109.783(8)
V/Å^3	3046.20(8)	6674.8(6)	2951.02(15)	7494.4(4)	3923.4(6)
Z	2	4	2	4	2
Z'	1	1	1	1	1
Wavelength/Å	1.34143	0.71073	0.71073	0.71073	0.71073
Radiation type	GaK_α	MoK_α	MoK_α	MoK_α	MoK_α
Q_{min}/°	2.313	1.140	1.959	1.584	1.878
Q_{max}/°	64.042	25.061	31.506	30.184	30.336
Measured Refl.	36517	26635	48486	41204	46121
Independent Refl.	10731	11719	16698	18594	19762
Reflections with I > 2(I)	10291	9865	13996	14645	16136
R_{int}	0.0208	0.0285	0.0381	0.0557	0.0208
Parameters	646	681	617	796	935
Restraints	73	0	1	54	0
Largest Peak	0.910	1.498	0.968	2.076	0.951
Deepest Hole	-1.654	-0.791	-0.944	-2.910	-0.701
GooF	1.116	0.997	0.949	1.015	1.043
wR_2 (all data)	0.0797	0.0746	0.0677	0.1214	0.0608
wR_2	0.0780	0.0728	0.0642	0.1128	0.0576
R_1 (all data)	0.0324	0.0362	0.0495	0.0636	0.0397
R_1	0.0307	0.0296	0.0358	0.0456	0.0269
Flack Parameter	0.018(3)	-	-0.019(3)	-	-
Hooft Parameter	0.0133(10)	-	-0.026(2)	-	-

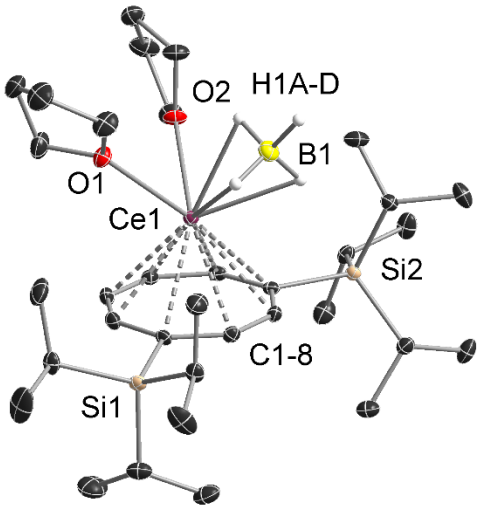

Figure S39. Molecular structure of **2** in the solid state. Thermal ellipsoids are represented at 50% probability. Hydrogen atoms except the freely refined hydridic ones are omitted for clarity. For selected bond lengths and angles see Table S4.

Table S4. Selected bond lengths and angles for [Ce(η^8-COT^{TIPS})BH_4] (**2**); Ct = Centroid of the subscript ring moiety.

Length/Å		**Angle/°**	
Ce1-$Ct_{COTTIPS}$	1.973(4)	$Ct_{COTTIPS}$-Ce1-B1	135.29(7)
Ce1-$C_{COTTIPS}$	2.673(2)-2.728(2)	$Ct_{COTTIPS}$-Ce1-O1	130.04(4)
Ce1-B1	2.720(3)	$Ct_{COTTIPS}$-Ce1-O2	122.52(4)
Ce1-O1	2.551(2)		
Ce1-O2	2.590(2)		

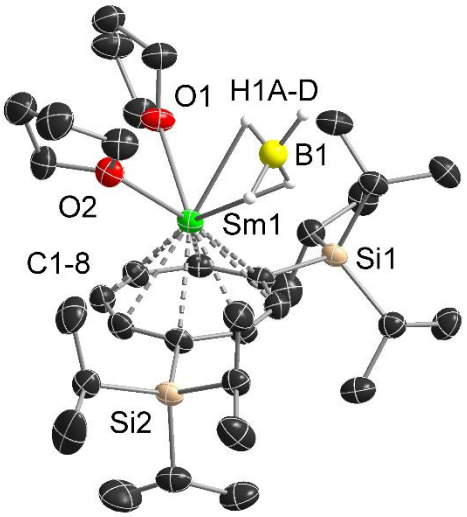

Figure S40. Molecular structure of **3** in the solid state. Thermal ellipsoids are represented at 50% probability. Hydrogen atoms except the freely refined hydridic ones are omitted for clarity. For selected bond lengths and angles see Table S5.

Table S5. Selected bond lengths and angles for [Sm(η^8-COT^{TIPS})BH$_4$] (**3**); Ct = Centroid of the subscript ring moiety

Length/Å		**Angle/°**	
Sm1-Ct$_{COTTIPS}$	1.887(4)	Ct$_{COTTIPS}$- Sm1-B1	135.57(13)
Sm1-C$_{COTTIPS}$	2.637(4)-2.667(4)	Ct$_{COTTIPS}$- Sm1-O1	123.05(7)
Sm1-B1	2.606(5)	Ct$_{COTTIPS}$- Sm1-O2	129.03(7)
Sm1-O1	2.536(3)		
Sm1-O2	2.487(3)		

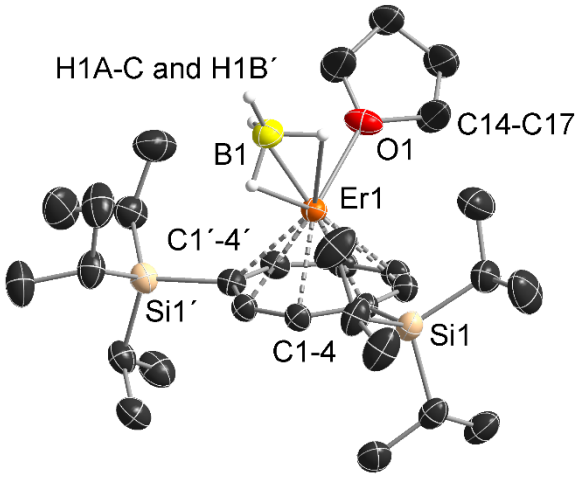

Figure S41. Molecular structure of **4** in the solid state. Thermal ellipsoids are represented at 50% probability. Hydrogen atoms except the freely refined hydridic ones are omitted for clarity. Only one part of the symmetry generated, disordered THF ligand is depicted. For selected bond lengths and angles see Table S6.

Table S6. Selected bond lengths and angles for [Er(η^8-COT^{TIPS})BH_4] (**4**); Ct = Centroid of the subscript ring moiety

Length/Å		Angle/°	
Er1-$Ct_{COTTIPS}$	1.725(1)	$Ct_{COTTIPS}$- Er1-B1	147.41(10)
Er1-$C_{COTTIPS}$	2.503(3)-2.564(3)	$Ct_{COTTIPS}$- Er1-O1	124.97(6)
Er1-B1	2.489(4)		
Er1-O1	2.347(3)		

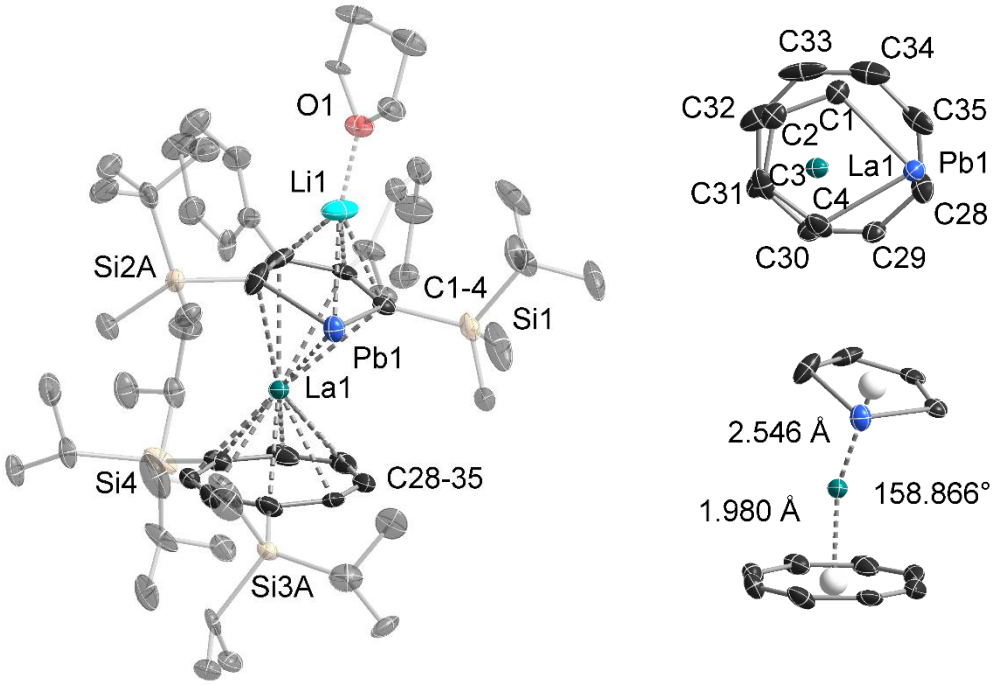

Figure S42. Left: Molecular structure of **5** in the solid state. Thermal ellipsoids are represented at 50% probability. Hydrogen atoms are omitted for clarity. Only one part of the disordered TIPS-, TBDMS- and Phenyl-groups and THF ligand is depicted. For selected bond lengths and angles see Table S7. Top right: Top view of the central complex fragment. Bottom right: Front view of the central complex fragment with La1-Ct distances (left) and Ct-La1-Ct angle (right).

Table S7. Selected bond lengths and angles for [Li(thf)(η^5-L^{Pb})La(η^8-COT^{TIPS})] (**5**); Ct = Centroid of the subscript ring moiety

Length/Å		**Angle/°**	
La1-$Ct_{COTTIPS}$	1.9804(4)	$Ct_{COTTIPS}$-La1-Ct_{LPb}	147.41(10)
La1-Ct_{LPb}	2.5464(4)	La1-Ct_{LPb}-Li1	158.87(6)
Li1-Ct_{LPb}	1.80(2)	Angle sum COT^{TIPS}	1079.0
La1-Pb1	3.3530(6)	Angle sum L^{Pb}	539.8
La1-$C_{COTTIPS}$	2.668(11)-2.783(10)		
La1-C_{LPb}	2.762(9)-2.953(8)		
Li1-O1	1.87(2)		

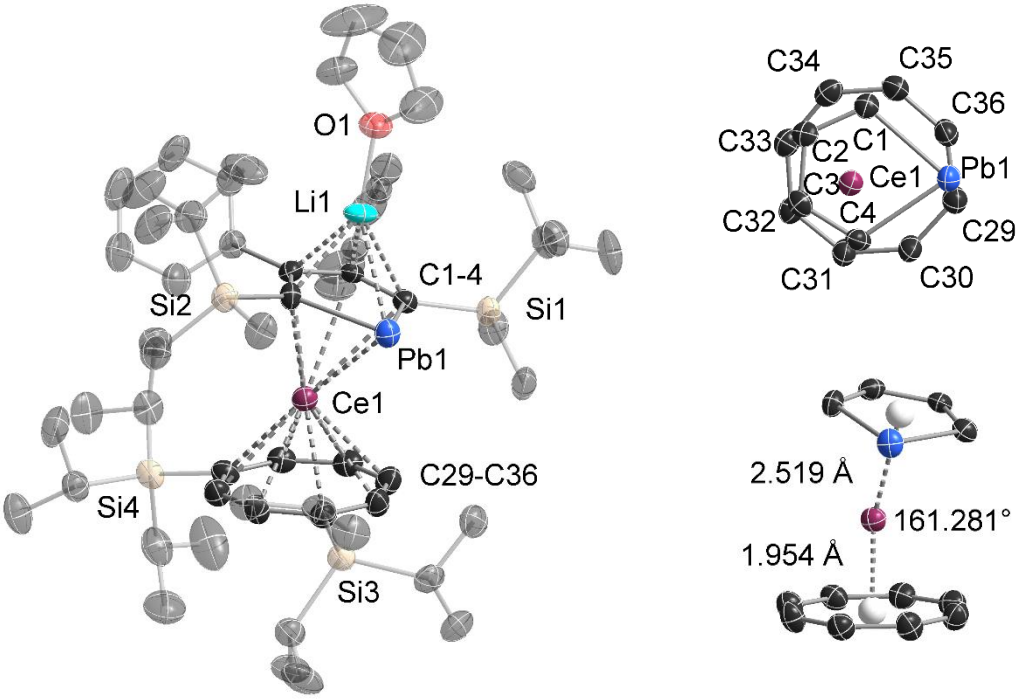

Figure S43. Left: Molecular structure of **6** in the solid state. Thermal ellipsoids are represented at 50% probability. Hydrogen atoms are omitted for clarity. Only one part of the disordered TIPS-group at Si4 is depicted. For selected bond lengths and angles see Table S8. Top right: Top view of the central complex fragment. Bottom right: Front view of the central complex fragment with Ce1-Ct distances (left) and Ct-Ce1-Ct angle (right).

Table S8. Selected bond lengths and angles for [Li(thf)(η^5-L^{Pb})Ce(η^8-COT^{TIPS})] (**6**); Ct = Centroid of the subscript ring moiety

Length/Å		**Angle/°**	
Ce1-$Ct_{COTTIPS}$	1.9540(4)	$Ct_{COTTIPS}$-Ce1-Ct_{LPb}	161.28(2)
Ce1-Ct_{LPb}	2.5186(4)	Ce1-Ct_{LPb}-Li1	168.3(4)
Li1-Ct_{LPb}	1.82(1)	Angle sum COT^{TIPS}	1079.9
Ce1-Pb1	3.3452(4)	Angle sum L^{Pb}	539.9
Ce1-$C_{COTTIPS}$	2.655(8)-2.771(7)		
Ce1-C_{LPb}	2.762(9)-2.953(8)		
Li1-O1	1.888(14)		

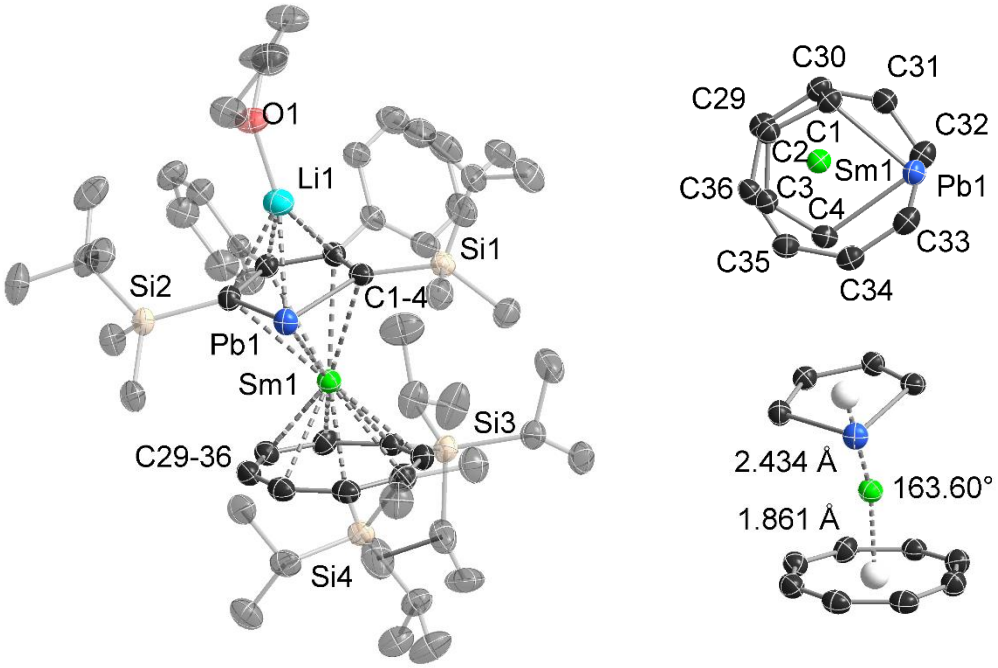

Figure S44. Left: Molecular structure of **7** in the solid state. Thermal ellipsoids are represented at 50% probability. Hydrogen atoms and one molecule of toluene are omitted for clarity. For selected bond lengths and angles see Table S9. Top right: Top view of the central complex fragment. Bottom right: Front view of the central complex fragment with Ce1-Ct distances (left) and Ct-Ce1-Ct angle (right).

Table S9. Selected bond lengths and angles for [Li(thf)(η^5-L^{Pb})Sm(η^8-COT^{TIPS})] (**7**); Ct = Centroid of the subscript ring moiety

Length/Å		**Angle/°**	
Sm1-Ct$_{COTTIPS}$	1.8614(3)	Ct$_{COTTIPS}$-Sm1-Ct$_{LPb}$	163.60(2)
Sm1-Ct$_{LPb}$	2.4344(3)	Sm1-Ct$_{LPb}$-Li1	169.9(2)
Li1-Ct$_{LPb}$	1.824(6)	Angle sum COT^{TIPS}	1079.9
Sm1-Pb1	3.2646(2)	Angle sum L^{Pb}	539.9
Sm1-C$_{COTTIPS}$	2.577(3)-2.715(3)		
Sm1-C$_{LPb}$	2.662(3)-2.870(3)		
Li1-O1	1.867(6)		

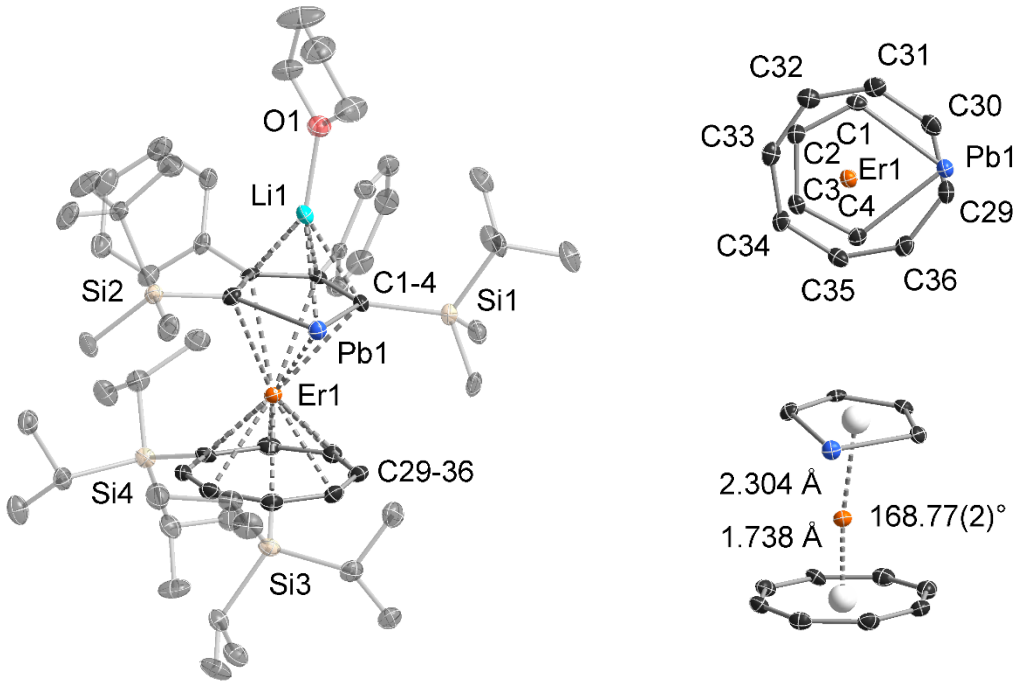

Figure S45. Left: Molecular structure of **8** in the solid state. Thermal ellipsoids are represented at 50% probability. Hydrogen atoms are omitted for clarity. For selected bond lengths and angles see Table S10. Top right: Top view of the central complex fragment. Bottom right: Front view of the central complex fragment with Er1-Ct distances (left) and Ct-Er1-Ct angle (right).

Table S10. Selected bond lengths and angles for [Li(thf)(η^5-L^{Pb})Er(η^8-COT^{TIPS})] (**8**); Ct = Centroid of the subscript ring moiety

Length/Å		**Angle/°**	
Er1-$Ct_{COTTIPS}$	1.7385(3)	$Ct_{COTTIPS}$-Er1-Ct_{LPb}	168.77(2)
Er1-Ct_{LPb}	2.3041(3)	Er1-Ct_{LPb}-Li1	171.3(3)
Li1-Ct_{LPb}	1.798(11)	Angle sum COT^{TIPS}	1079.8
Er1-Pb1	3.1492(4)	Angle sum L^{Pb}	539.7
Er1-$C_{COTTIPS}$	2.498(6)- 2.633(6)		
Er1-C_{LPb}	2.575(5)- 2.742(6)		
Li1-O1	1.894(12)		

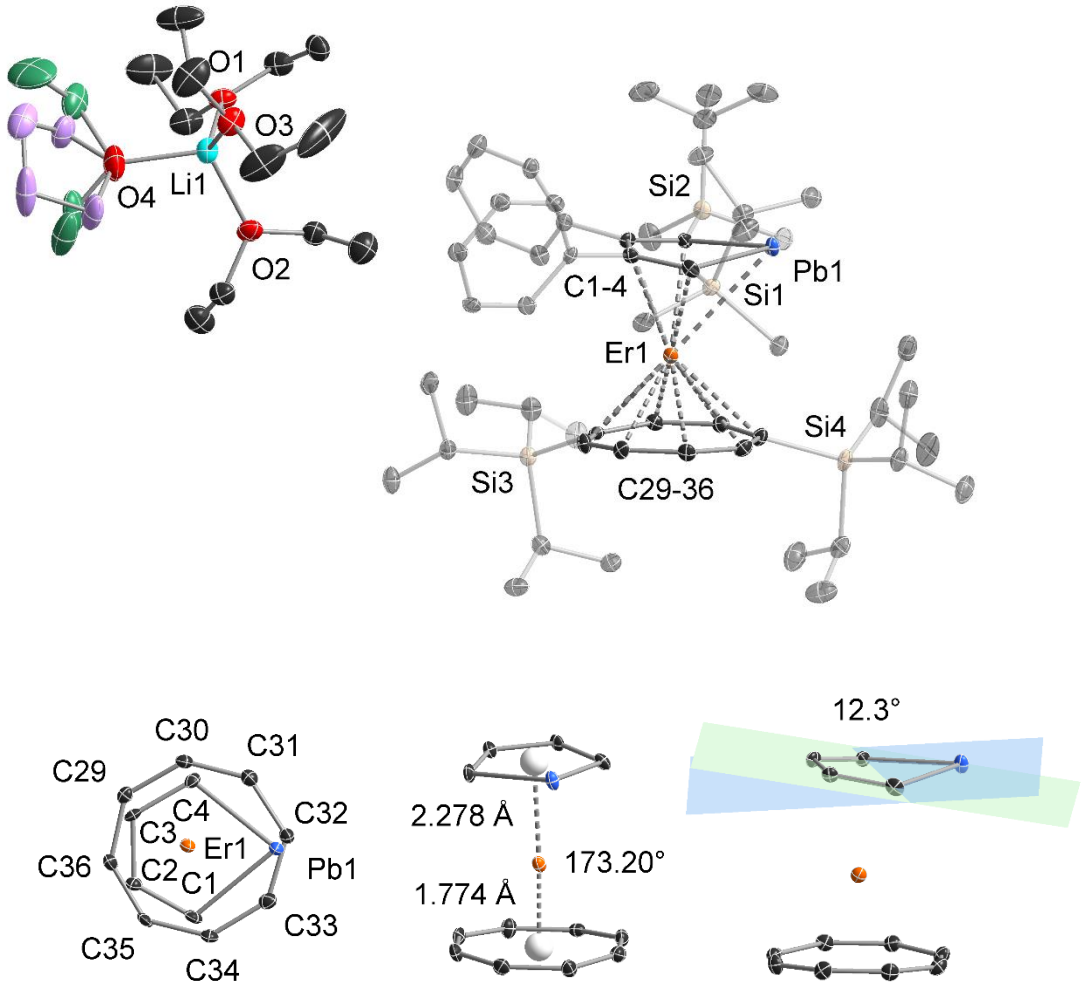

Figure S46. Left: Molecular structure of **9** in the solid state. Thermal ellipsoids are represented at 50% probability. Hydrogen atoms are omitted for clarity. The disordered THF and Et_2O ligands are depicted in pink and green, respectively. For selected bond lengths and angles see Table S11. Bottom left: Top view of the central complex fragment. Bottom middle: Front view of the central complex fragment with Er1-Ct distances (left) and Ct-Er1-Ct angle (right). Bottom right: Side view of the central complex fragment with the dihedral bending angle of the L^{Pb} ligand.

Table S11. Selected bond lengths and angles for $[Li(Et_2O)_{3.4}(thf)_{0.6}][(\eta^5\text{-}L^{Pb})Er(\eta^8\text{-}COT^{TIPS})]$ (**9**); Ct = Centroid of the subscript ring moiety

Length/Å		Angle/°	
Er1-$Ct_{COTTIPS}$	1.7737(4)	$Ct_{COTTIPS}$-Er1-Ct_{LPb}	173.20(2)
Er1-Ct_{LPb}	2.2777(4)	Angle sum COT^{TIPS}	1079.3
Li1-Ct_{LPb}	10.130(13)	Angle sum L^{Pb}	538.0
Er1-Pb1	3.1519(3)	Dihedral angle L^{Pb}	12.3(3)
Er1-$C_{COTTIPS}$	2.520(5)-2.634(4)		
Er1-C_{LPb}	2.583(4)-2.654(4)		
Li1-O1/2	1.981(10)/1.976(11)		
Li1-O2/3	1.948(10)/1.971(11)		

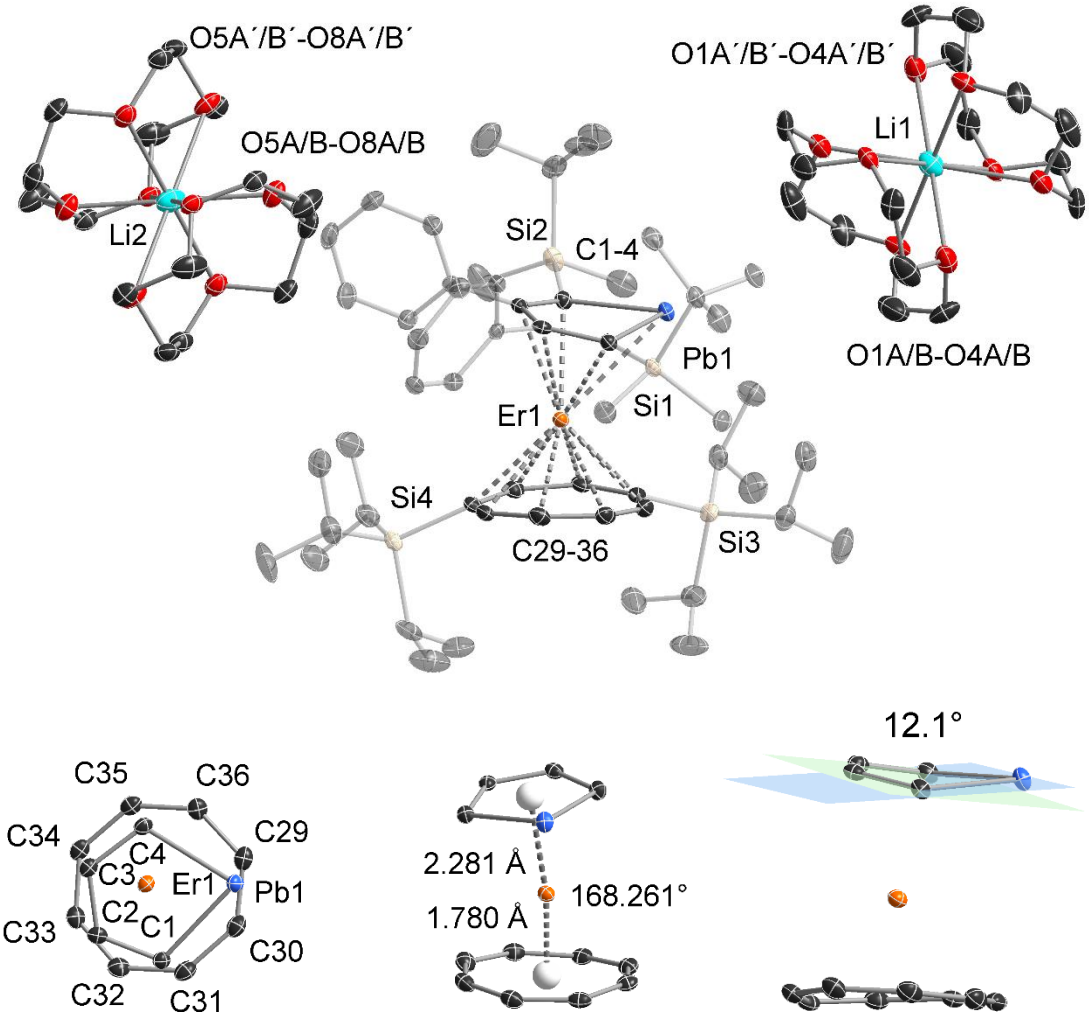

Figure S47. Top: Molecular structure of **10** in the solid state. Each $[Li(12\text{-c-}4)_2]^+$ cation is half-occupied. Thermal ellipsoids are represented at 50% probability. Hydrogen atoms are omitted for clarity. Only one part of the disordered parts of the Li-coordinated disordered 12-c-4 ligands are shown. For selected bond lengths and angles see Table S12. Bottom left: Top view of the central complex fragment. Bottom middle: Front view of the central complex fragment with Er1-Ct distances (left) and Ct-Er1-Ct angle (right). Bottom right: Side view of the central complex fragment with the dihedral bending angle of the L^{Pb} ligand.

Table S12. Selected bond lengths and angles for $[Li(12\text{-}c\text{-}4)_2][(\eta^5\text{-}L^{Pb})Er(\eta^8\text{-}COT^{TIPS})]$ (**10**); Ct = Centroid of the subscript ring moiety

Length/Å		**Angle/˚**	
$Er1\text{-}Ct_{COTTIPS}$	1.7800(3)	$Ct_{COTTIPS}\text{-}Er1\text{-}Ct_{LPb}$	168.26(2)
$Er1\text{-}Ct_{LPb}$	2.2807(4)	Angle sum COT^{TIPS}	1078.9
$Li1\text{-}Ct_{LPb}$	8.2603(7)	Angle sum L^{Pb}	541.2
$Li2\text{-}Ct_{LPb}$	9.4853(11)	Dihedral angle L^{Pb}	12.09(12)
Er1-Pb1	3.1576(3)		
$Er1\text{-}C_{COTTIPS}$	2.516(3)-2.669(2)		
$Er1\text{-}C_{LPb}$	2.576(3)-2.664(2)		
Li1-O (part 1)	2.396(5)-2.409(6)		
Li1-O (part 2)	2.284(6)-2.479(6)		
Li2-O (part 1)	2.200(4)-2.364(5)		
Li2-O (part 2)	2.196(4)-2.448(4)		

Magnetism and Calculations

Magnetism

DC and AC Susceptibility measurements were performed on a Quantum Design MPMS-XL SQUID-magnetometer. DC data was taken upon cooling from 300 K to 2 K in an applied field H_{DC} = 1000 Oe. AC susceptibility data was taken at various temperatures upon scanning the frequency of an alternating field H_{AC} = 3.5 Oe. Magnetization measurements were performed using a Quantum Design MPMS3 VSM SQUID-magnetometer. $M(H)$ curves were collected with a stable field at each point, while hysteresis loops were collected using a continuous field sweep of 50 Oe/s and 200 Oe/s. The powdered samples were sealed in a quartz glass tube with small amounts of eicosane to prevent sample movement. All data were corrected for the diamagnetic contributions of the sample, the quartz glass and the eicosane.

Calculations

Ab initio-CASSCF calculations were conducted using MOLCAS 8.2.[7] The input structures were taken from the crystal structure refinement. The applied basis sets were relativistic ANO basis sets taken from the Molcas-libraries. The size of the basis sets were VTZP for Er and Pb, VDZP for Li, O and coordinating C's, and VDZ for Si, H, and peripheral C's. 35 Quartets and 112 Doublets were employed during the orbital optimisation and subsequent spin-orbit coupling.

Table S13. Fitting parameters for [Li(thf)(η^5-L^{Pb})Er(η^8-COT^{TIPS})] (**8**). (H_{DC} = 0 Oe)

T/K	χ_T	χ_S	τ	α
2	3.92	1.81E-01	2.00E-02	3.01E-01
2.2	3.60	1.62E-01	1.97E-02	3.01E-01
2.4	3.27	1.38E-01	1.95E-02	3.04E-01
2.6	3.00	1.20E-01	1.93E-02	3.05E-01
2.8	2.78	1.05E-01	1.90E-02	3.06E-01
3	2.58	9.13E-02	1.88E-02	3.07E-01
3.2	2.41	7.96E-02	1.86E-02	3.08E-01
3.4	2.27	6.87E-02	1.83E-02	3.09E-01
3.6	2.14	5.86E-02	1.81E-02	3.10E-01
3.8	2.02	4.99E-02	1.79E-02	3.11E-01
4	1.91	4.28E-02	1.77E-02	3.11E-01
4.4	1.73	2.93E-02	1.73E-02	3.13E-01
4.8	1.58	1.80E-02	1.68E-02	3.14E-01
5.2	1.45	9.32E-03	1.63E-02	3.14E-01
5.6	1.34	2.67E-03	1.59E-02	3.15E-01
6	1.25	2.55E-18	1.54E-02	3.12E-01
6.4	1.17	2.19E-16	1.49E-02	3.07E-01
6.8	1.10	2.55E-16	1.44E-02	3.08E-01
7.2	1.17	1.24E-01	1.37E-02	3.06E-01
7.6	1.11	1.21E-01	1.30E-02	2.99E-01
8	1.05	1.18E-01	1.21E-02	2.90E-01
8.4	1.00	1.15E-01	1.10E-02	2.78E-01
8.8	9.51E-01	1.13E-01	9.77E-03	2.62E-01
9.2	9.05E-01	1.11E-01	8.31E-03	2.40E-01
9.6	8.62E-01	1.09E-01	6.74E-03	2.15E-01
10	8.22E-01	1.06E-01	5.21E-03	1.91E-01
11	7.39E-01	9.55E-02	2.29E-03	1.47E-01
12	6.73E-01	8.51E-02	8.79E-04	1.26E-01
13	6.23E-01	7.53E-02	3.39E-04	1.20E-01
14	5.80E-01	6.76E-02	1.34E-04	1.14E-01

Table S14. CASSCF states, axes, g-tensors for [Li(thf)(η^5-L^{Pb})Er(η^8-COT^{TIPS})] (**8**).

Doublet state	ΔE/cm^{-1}	ΔE/K	Angle between magnetic z-axes/°	g_x	g_y	g_z	Wavefunction composition
1	0	0	-	0.0025	0.0034	17.7831	∓ 98% |15/2›
2	95.61	137.55	65.74	0.7784	1.9254	13.8614	± 34% |5/2› ± 33% |3/2› ± 10% |13/2› ± 9% |7/2› ± 9% |1/2› ± 3% |9/2›
3	111.72	160.74	43.41	1.4517	3.5321	12.7676	∓ 25% |11/2› ∓ 24% |13/2› ∓ 17% |9/2› ∓ 12% |3/2› ∓ 8% |1/2› ∓ 7% |7/2› ± 6% |5/2›
4	130.57	187.86	25.81	7.2108	6.6231	0.6428	± 48% |1/2› ± 13% |7/2› ± 9% |5/2› ∓ 8% |13/2› ± 8% |9/2› ∓ 7% |3/2› ± 6% |11/2›
5	151.47	217.93	52.18	1.4248	1.7435	13.0270	± 42% |7/2› ± 20% |13/2› ± 16% |5/2› ± 11% |1/2› ± 8% |3/2›
6	173.97	250.30	56.55	1.3596	3.2096	11.3262	∓ 27% |3/2› ∓ 25% |9/2› ∓ 19% |1/2› ∓ 13% |13/2› ∓ 7% |11/2› ± 6% |5/2› ± 2% |7/2›
7	196.03	282.04	52.31	1.5352	3.1801	12.7121	∓ 28% |5/2› ∓ 27% |9/2› ∓ 18% |7/2› ∓ 12% |3/2› ∓ 10% |13/2› ∓ 3% |1/2› ± 2% |11/2›
8	223.84	322.06	38.28	0.2837	0.4327	15.6427	± 57% |11/2› ± 18% |9/2› ± 14% |13/2› ± 7% |7/2› ± 2% |3/2›

Table S15. Transition probabilities within the lowest three doublet states of [Li(thf)(η^5-L^{Pb})Er(η^8-COT^{TIPS})] (***8***).

	1	2	3	4	5	6
1		0.1466E-05	0.1183E-01	0.9824E+00	0.7444E+00	0.1361E+00
2	0.1466E-05		0.9824E+00	0.1183E-01	0.1361E+00	0.7444E+00
3	0.1183E-01	0.9824E+00		0.4446E+00	0.1158E+01	0.4076E+01
4	0.9824E+00	0.1183E-01	0.4446E+00		0.4076E+01	0.1158E+01
5	0.7444E+00	0.1361E+00	0.1158E+01	0.4076E+01		0.1239E+02
6	0.1361E+00	0.7444E+00	0.4076E+01	0.1158E+01	0.1239E+02	

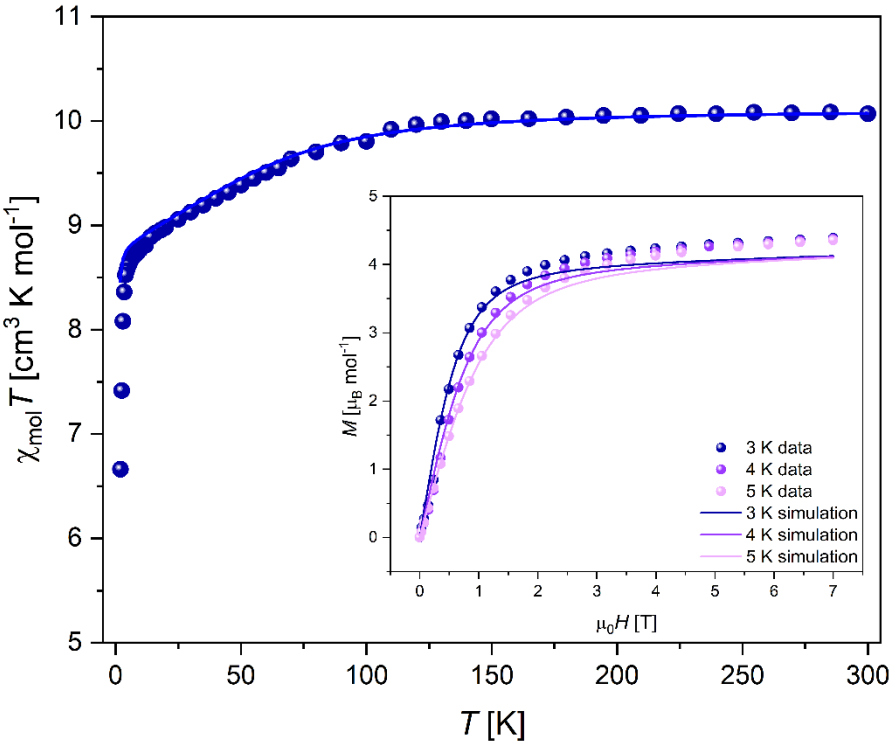

Figure S48. Susceptibility and Magnetization of [Li(thf)(η^5-L^{Pb})Er(η^8-COT^{TIPS})] (**8**).

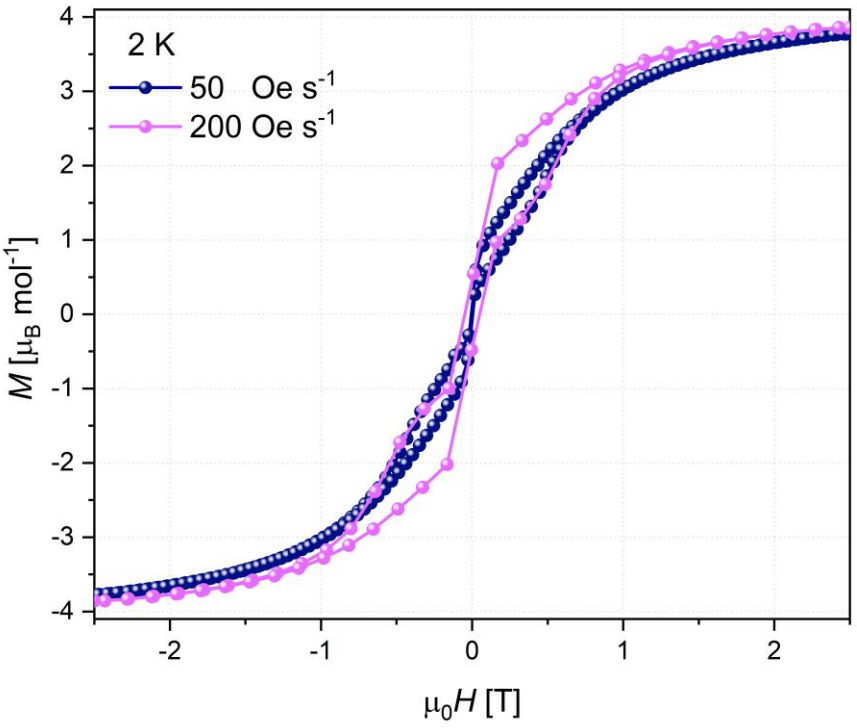

Figure S49. Hysteresis at 2 K of [Li(thf)(η^5-L^{Pb})Er(η^8-COT^{TIPS})] (**8**).

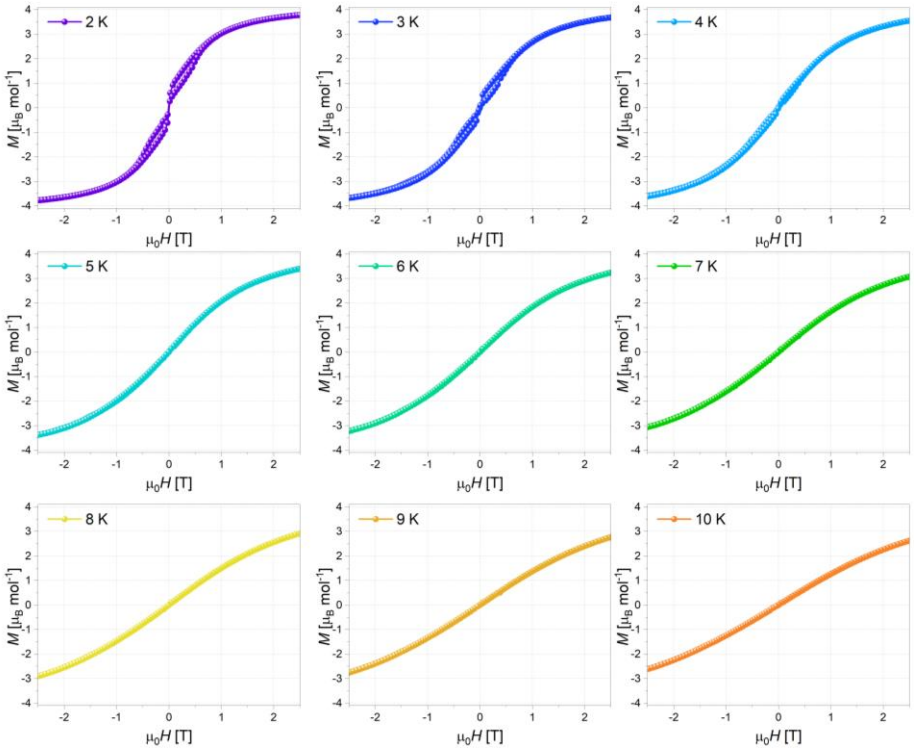

Figure S50. Hysteresis at different T (50 Oe/s) of [Li(thf)(η^5-L^{Pb})Er(η^8-COT^{TIPS})] (**8**).

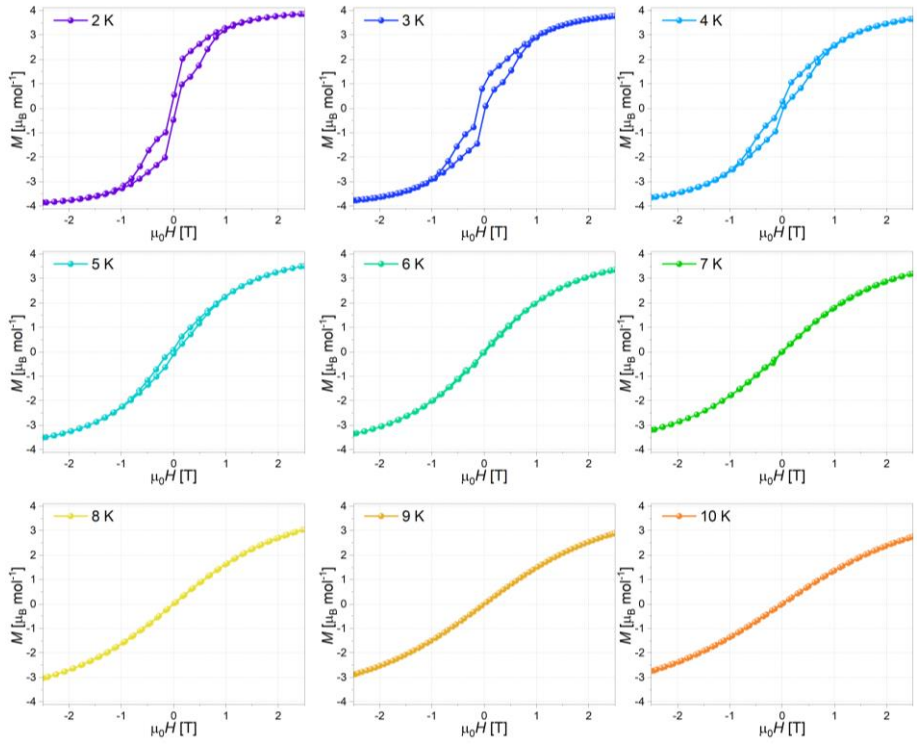

Figure S51. Hysteresis at different T (200 Oe/s) of [Li(thf)(η^5-L^{Pb})Er(η^8-COT^{TIPS})] (**8**).

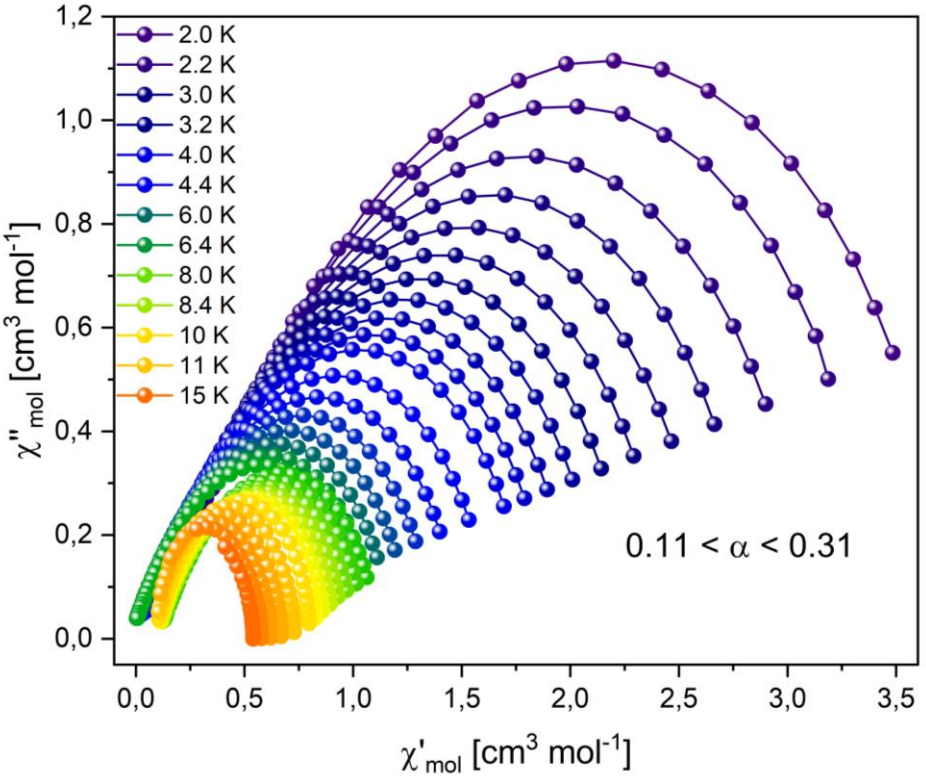

Figure S52. Cole-Cole plot of [Li(thf)(η^5-L^{Pb})Er(η^8-COT^{TIPS})] (**8**) (H_{DC} = 0 Oe).

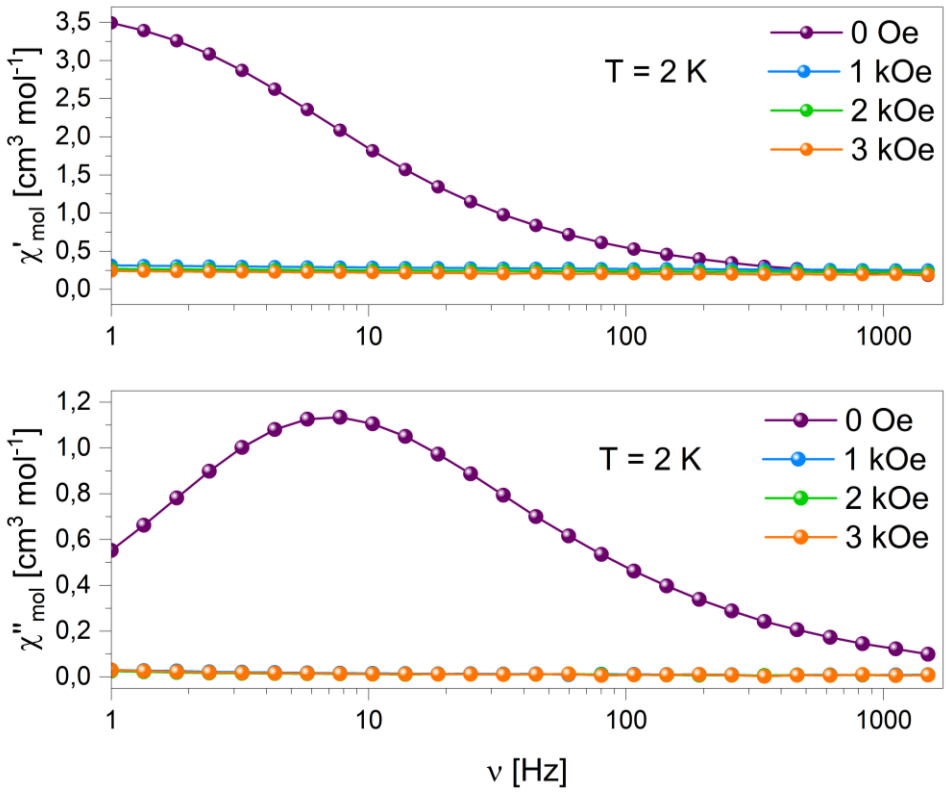

Figure S53. Field-dependent test measurement of [Li(thf)(η^5-L^{Pb})Er(η^8-COT^{TIPS})] (**8**).

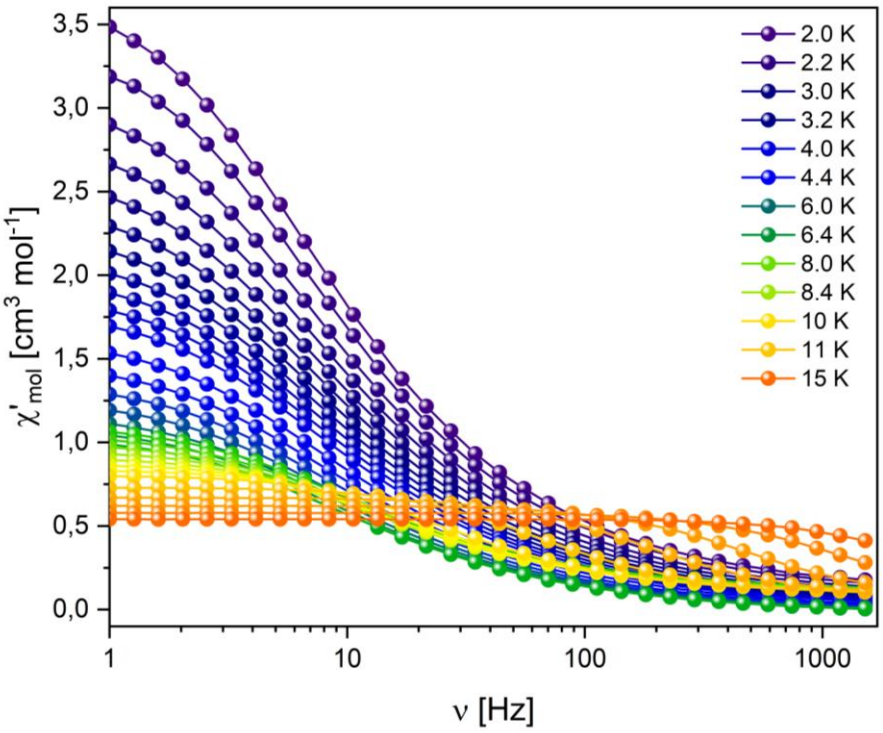

Figure S54. In-phase-component of the mag. susceptibility vs frequency of [Li(thf)(η^5-L^{Pb})Er(η^8-COT^{TIPS})] (**8**) (H_{DC} = 0 Oe).

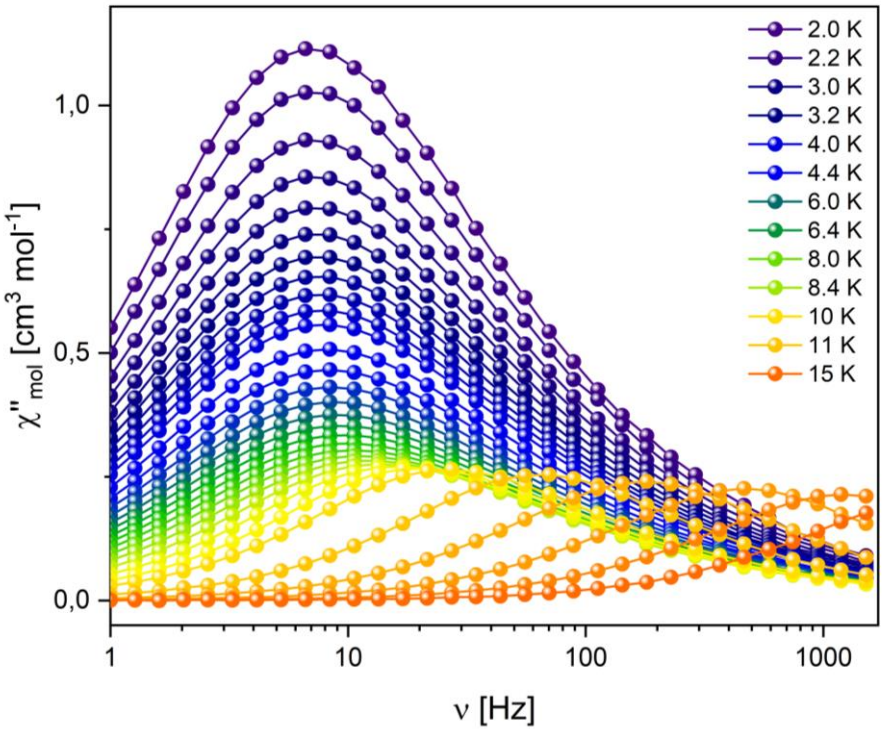

Figure S55. Out-of-phase-component of the mag. susceptibility vs frequency of [Li(thf)(η^5-L^{Pb})Er(η^8-COT^{TIPS})] (**8**) (H_{DC} = 0 Oe).

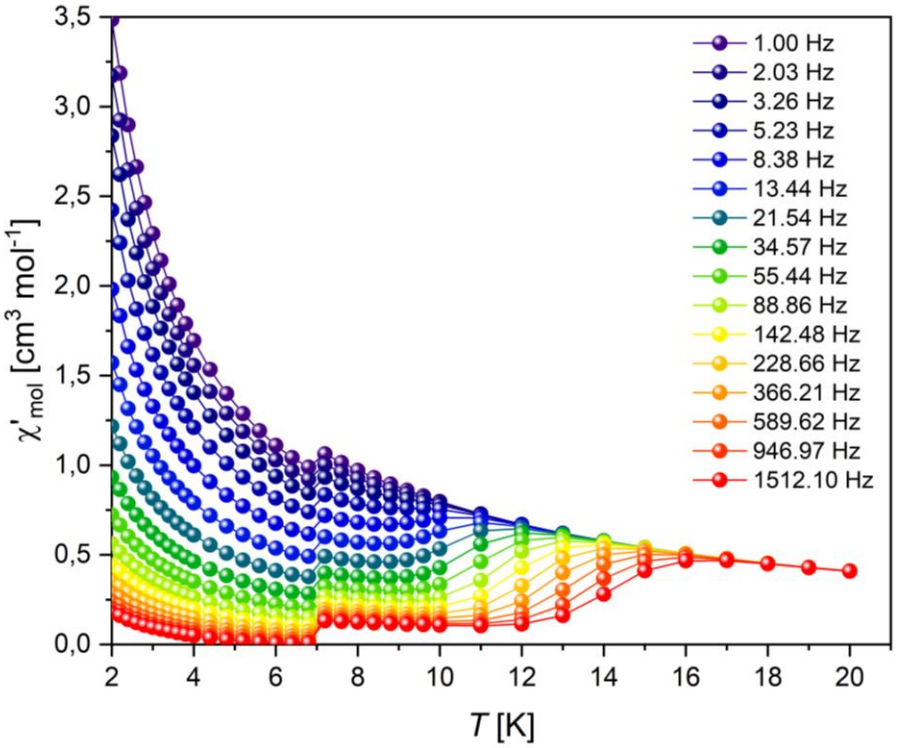

Figure S56. In-phase-component of the mag. susceptibility vs temperature of [Li(thf)(η^5-L^{Pb})Er(η^8-COT^{TIPS})] (**8**) (H_{DC} = 0 Oe).

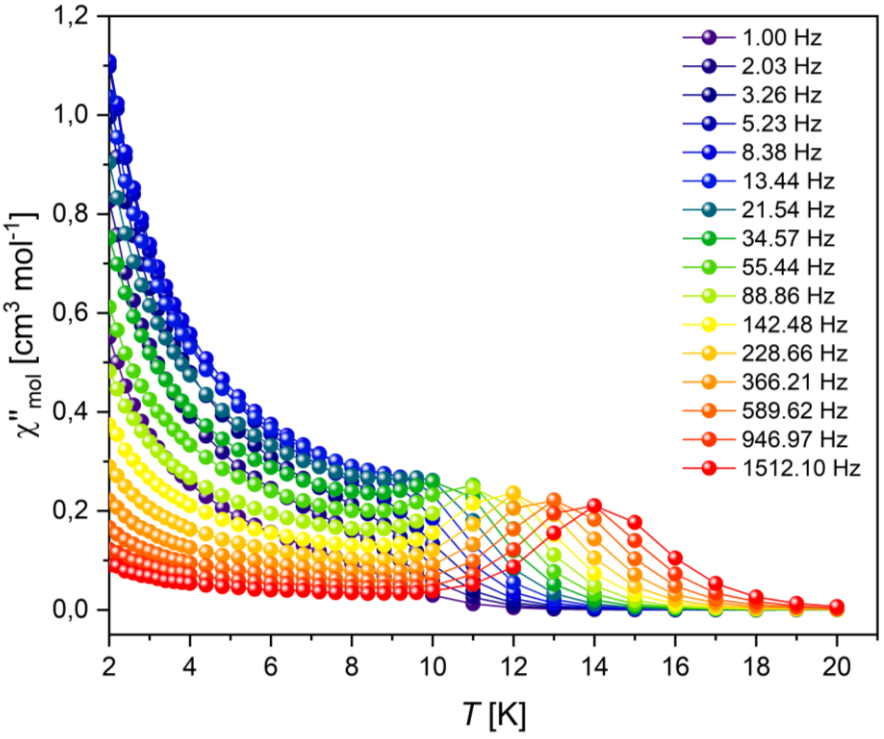

Figure S57. Out-of-phase-component of the mag. susceptibility vs Temperature of [Li(thf)(η^5-L^{Pb})Er(η^8-COT^{TIPS})] (**8**) (H_{DC} = 0 Oe).

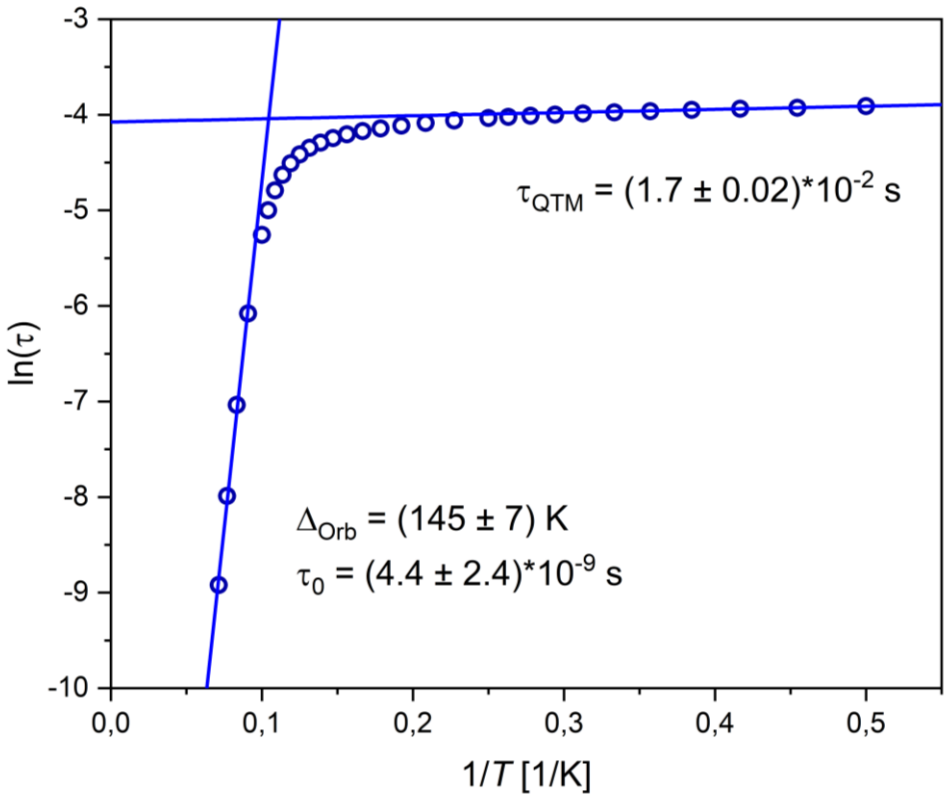

Figure S58. Arrhenius plot of [Li(thf)(η^5-L^{Pb})Er(η^8-COT^{TIPS})] (**8**).

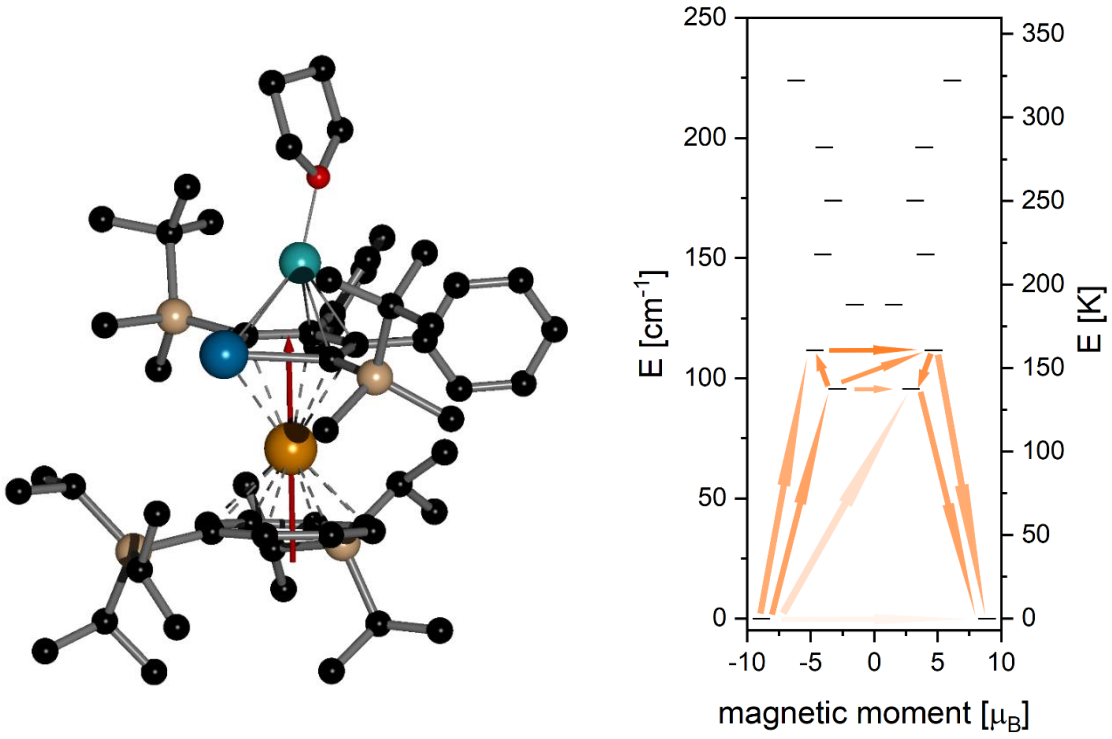

Figure S59. Left: Magnetic anisotropy axis of [Li(thf)(η^5-L^{Pb})Er(η^8-COT^{TIPS})] (**8**). Right: *Ab inito* states.

Table S16. Fitting parameters for [Li(12-c-4)$_2$][(η^5-L^{Pb})Er(η^8-COT^{TIPS})] (**10**). (H_{DC} = 0 Oe)

T/K	χ_T	χ_S	τ	α
2	4.26	6.96E-01	3.55E+01	3.06E-01
2.2	3.88	6.46E-01	3.45E+01	3.03E-01
2.4	3.60	6.44E-01	3.44E+01	2.90E-01
2.6	3.33	5.74E-01	3.31E+01	2.98E-01
2.8	3.10	5.17E-01	3.21E+01	3.07E-01
3	2.90	5.01E-01	3.17E+01	3.01E-01
3.2	2.72	4.69E-01	3.11E+01	3.03E-01
3.4	2.57	4.42E-01	3.04E+01	3.05E-01
3.6	2.43	4.39E-01	3.03E+01	2.97E-01
3.8	2.31	4.45E-01	3.04	2.85E-01
4	2.20	4.12E-01	2.96E+01	2.93E-01
4.4	2.01	3.85E-01	2.88E+01	2.92E-01
4.8	1.85	3.43E-01	2.75E+01	3.01E-01
5.2	1.72	3.32E-01	2.68E+01	2.91E-01
5.6	1.61	3.60E-01	2.58E+01	2.67E-01
6	1.51	3.62E-01	2.42E-01	2.46E-01
6.4	1.42	3.57E-01	2.14E+01	2.20E-01
6.8	1.35	3.29E-01	1.69E+01	2.05E-01
7.2	1.28	3.17E-01	1.30E+01	1.80E-01
7.6	1.22	2.30E-01	8.09E+00	1.93E-01
8	1.17	2.10E-01	5.47E+00	1.79E-01
8.4	1.12	7.45E-02	2.96E+00	2.00E-01

Table S17. CASSCF states, axes, g-tensors for [Li(12-c-4)$_2$][(η^5-L^{Pb})Er(η^8-COT^{TIPS})] (**10**).

Doublet state	ΔE/cm^{-1}	ΔE/K	Angle between magnetic z-axes/°	g_x	g_y	g_z	Wavefunction composition
1	0	0	-	0.0239	0.0690	17.0512	± 88% |15/2› ± 3% |9/2› ± 2% |11/2› ± 2% |5/2› ± 2% |7/2› ± 2% |13/2›
2	41.98	60.41	79.29	0.3563	0.7498	15.4643	± 33% |5/2› ± 24% |3/2› ± 21% |7/2› ± 6% |9/2› ± 5% |13/2› ± 5% |15/2› ± 5% |1/2›
3	73.42	105.64	83.27	0.1307	0.6712	13.7196	∓ 47% |1/2› ∓ 17% |3/2› ∓ 12% |7/2› ∓ 9% |9/2› ± 7% |5/2› ∓ 4% |11/2› ± 3% |13/2›
4	94.68	136.22	81.61	2.8407	5.8519	10.2572	∓ 32% |3/2› ∓ 24% |1/2› ∓ 13% |7/2› ∓ 12% |5/2› ∓ 8% |9/2› ∓ 6% |13/2› ∓ 3% |11/2›
5	126.30	181.72	41.76	0.6657	2.7365	10.6043	± 25% |9/2› ± 19% |7/2› ± 17% |5/2› ± 14% |13/2› ± 13% |11/2› ± 9% |1/2›
6	150.45	216.46	49.86	0.2878	3.0276	13.0358	∓ 32% |13/2› ∓ 19% |11/2› ∓ 18% |3/2› ∓ 15% |5/2› ∓ 11% |1/2› ∓ 2% |15/2›
7	175.14	251.99	51.55	0.9534	1.6034	15.4859	± 25% |9/2› ± 25% |7/2› ± 15% |11/2› ± 12% |13/2› ± 12% |5/2› ± 6% |3/2› ± 3% |1/2› ± 2% |15/2›
8	213.61	307.34	41.25	0.1262	0.1840	16.6757	∓ 42% |11/2› ∓ 25% |13/2› ∓ 22% |9/2› ∓ 7% |7/2› ∓ 2% |5/2›

Table S18. Transition probabilities within the lowest three doublet states for [Li(12-c-4)$_2$][(η^5-L^{Pb})Er(η^8-COT^{TIPS})] (**10**).

	1	2	3	4	5	6
1		0.4617E-03	0.2802E+01	0.2087E-01	0.1935E+00	0.2491E+00
2	0.4617E-03		0.2087E-01	0.2802E+01	0.2491E+00	0.1935E+00
3	0.2802E+01	0.2087E-01		0.1716E+00	0.1473E+01	0.3105E+01
4	0.2087E-01	0.2802E+01	0.1716E+00		0.3105E+01	0.1473E+01
5	0.1935E+00	0.2491E+00	0.1473E+01	0.3105E+01		0.1240E+02
6	0.2491E+00	0.1935E+00	0.3105E+01	0.1473E+01	0.1240E+02	

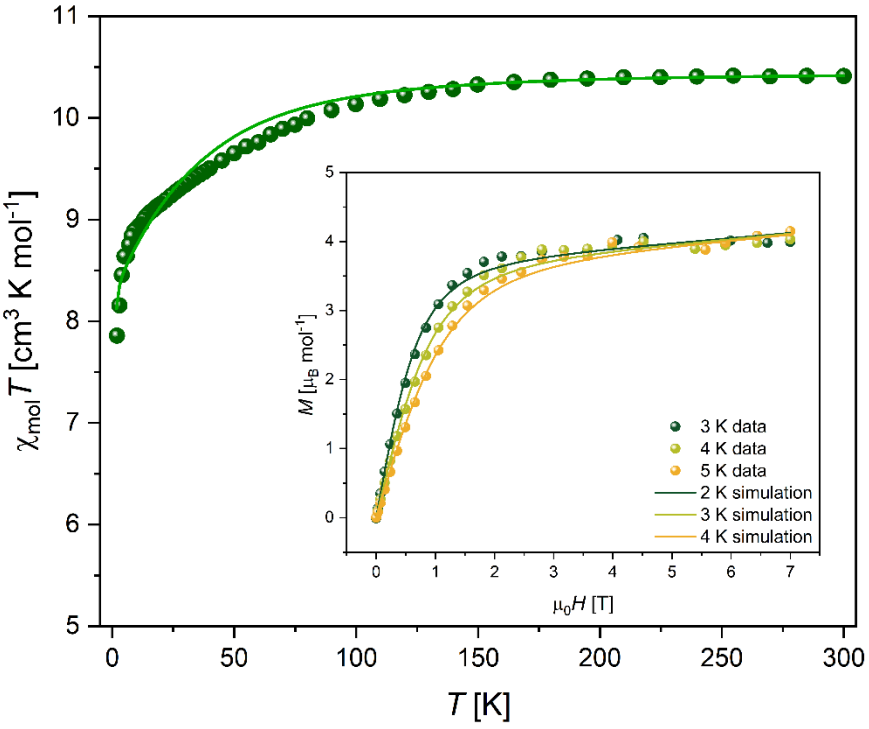

Figure S60. Susceptibility and Magnetization [Li(12-c-4)$_2$][(η^5-L^{Pb})Er(η^8-COT^{TIPS})] (**10**).

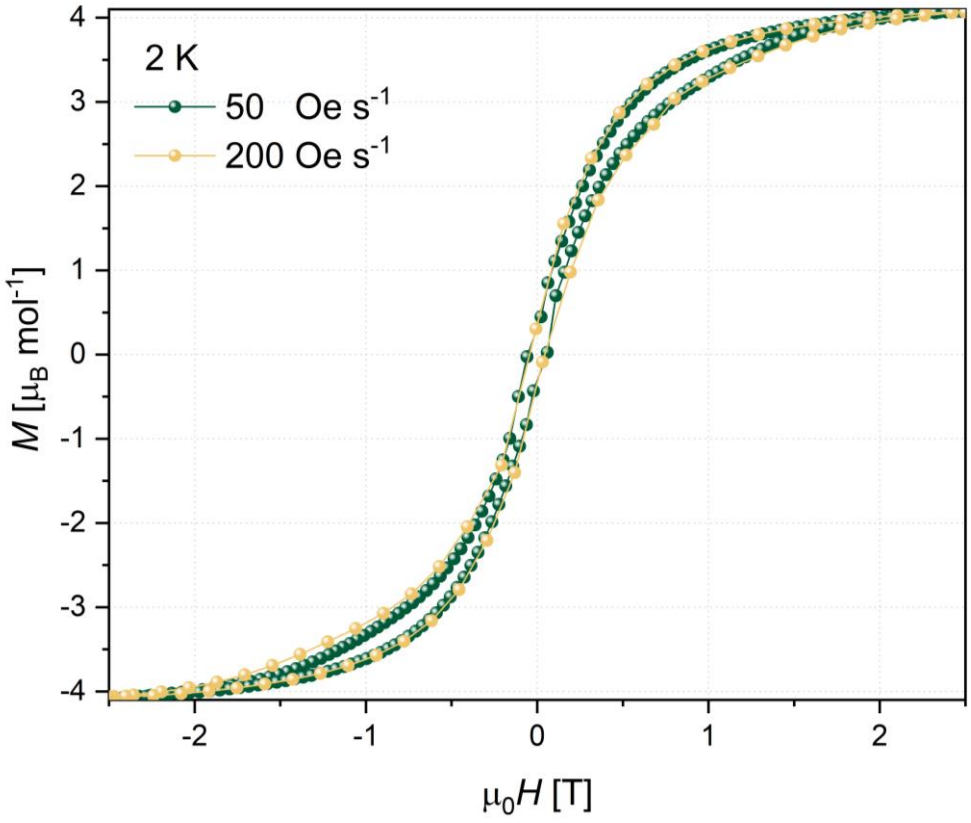

Figure S61. Hysteresis at 2 K for [Li(12-c-4)$_2$][(η^5-L^{Pb})Er(η^8-COT^{TIPS})] (**10**).

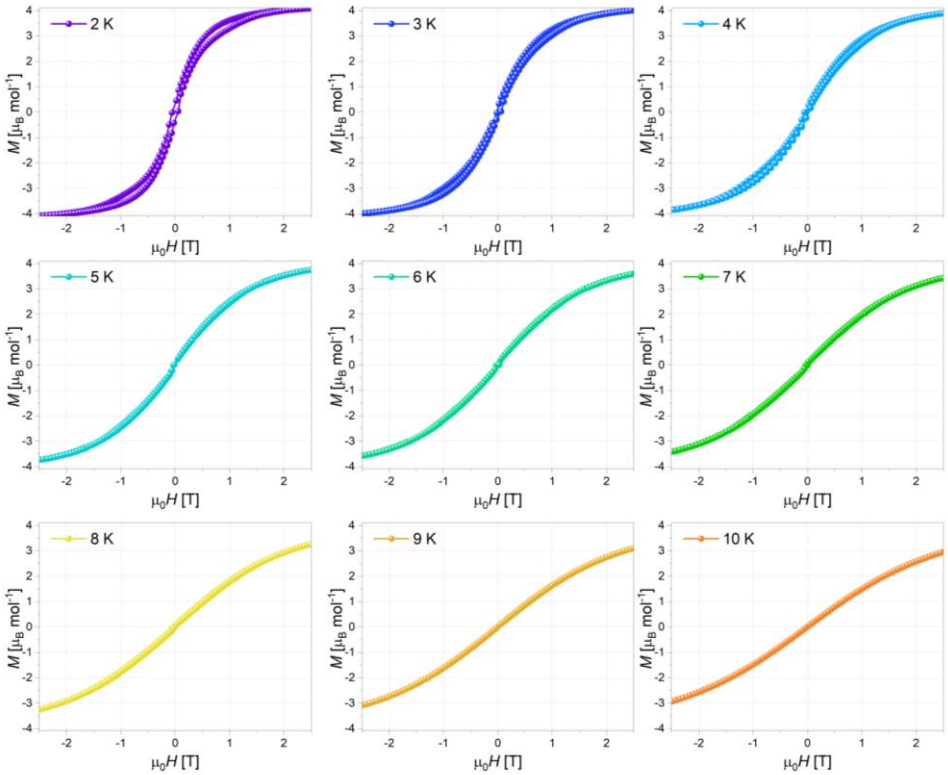

Figure S62. Hysteresis at different T (50 Oe/s) for [Li(12-c-4)$_2$][(η^5-L^{Pb})Er(η^8-COT^{TIPS})] (**10**).

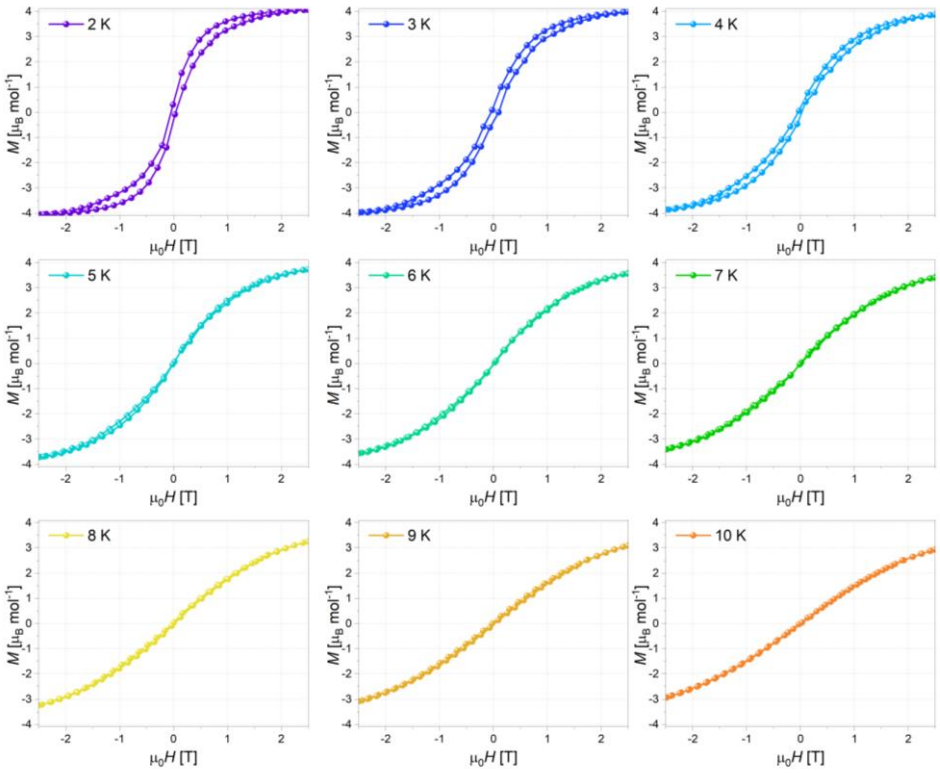

Figure S63. Hysteresis at different T (200 Oe/s) for [Li(12-c-4)$_2$][(η^5-L^{Pb})Er(η^8-COT^{TIPS})] (**10**).

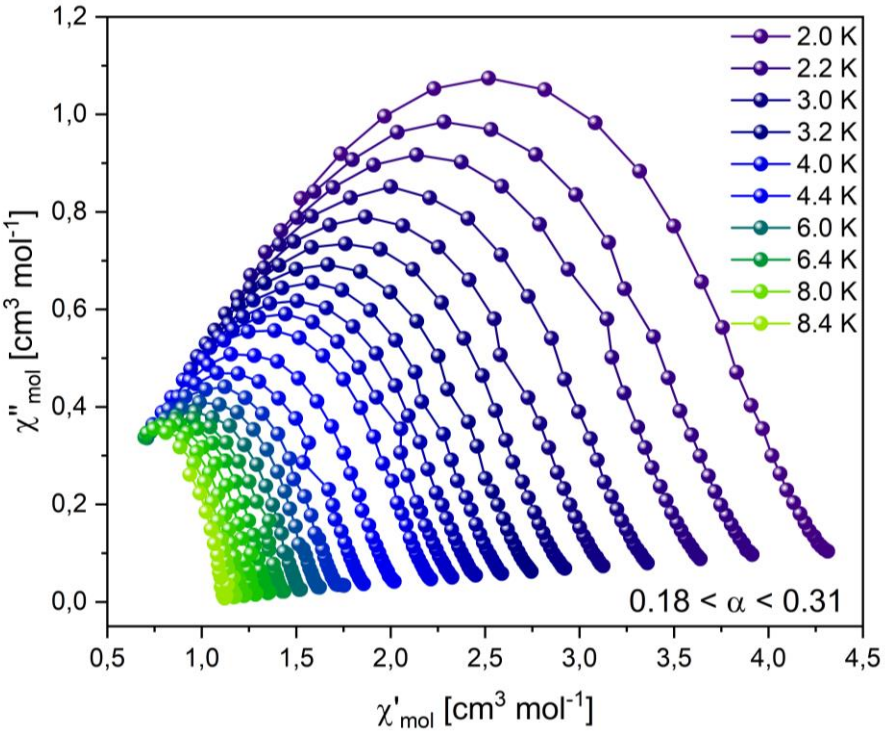

Figure S64. Cole-Cole plot for [Li(12-c-4)$_2$][(η^5-L^{Pb})Er(η^8-COT^{TIPS})] (**10**) (H_{DC} = 0 Oe).

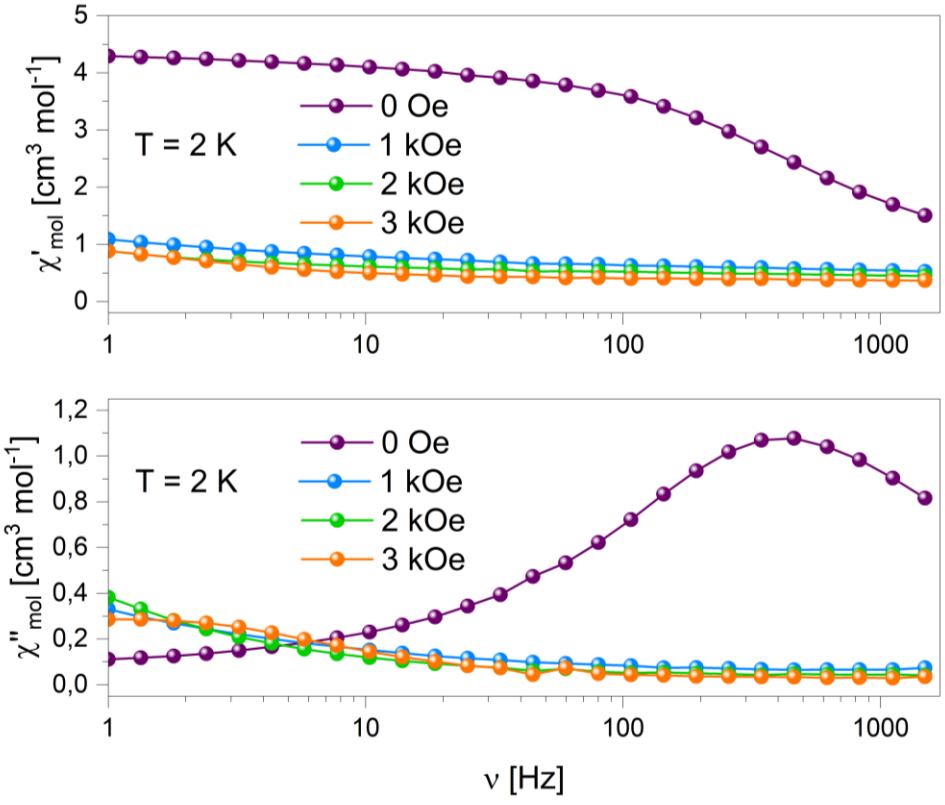

Figure S65. Field-dependent test measurement of [Li(12-c-4)$_2$][(η^5-L^{Pb})Er(η^8-COT^{TIPS})] (**10**).

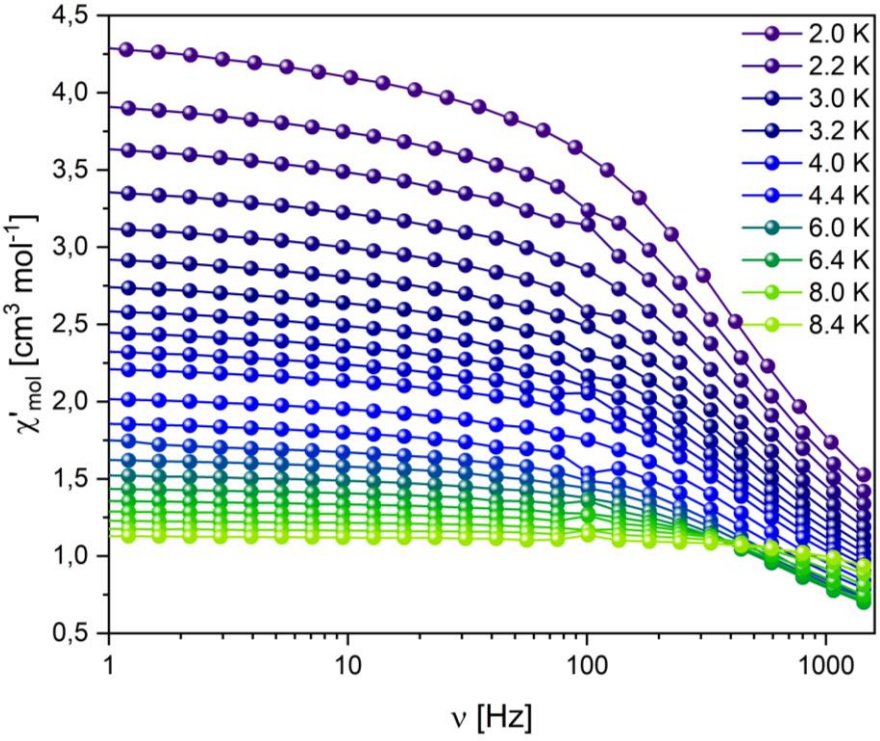

Figure S66. In-phase-component of the mag. susceptibility vs frequency for [Li(12-c-4)$_2$][(η^5-L^{Pb})Er(η^8-COT^{TIPS})] (**10**) (H_{DC} = 0 Oe).

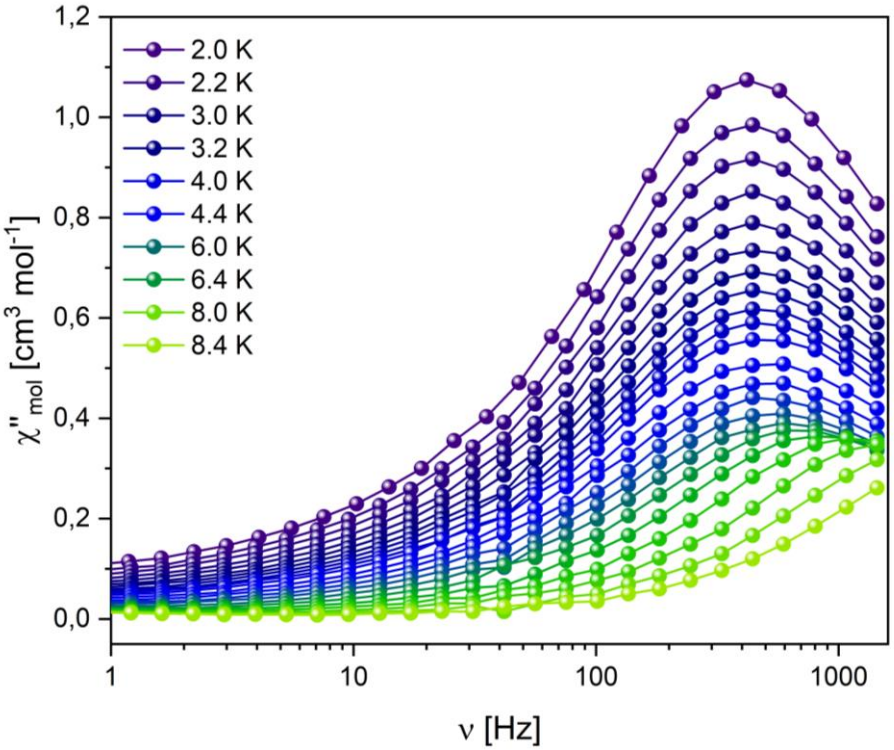

Figure S67. Out-of-phase-component of the mag. susceptibility vs frequency for [Li(12-c-4)$_2$][(η^5-L^{Pb})Er(η^8-COT^{TIPS})] (**10**) (H_{DC} = 0 Oe).

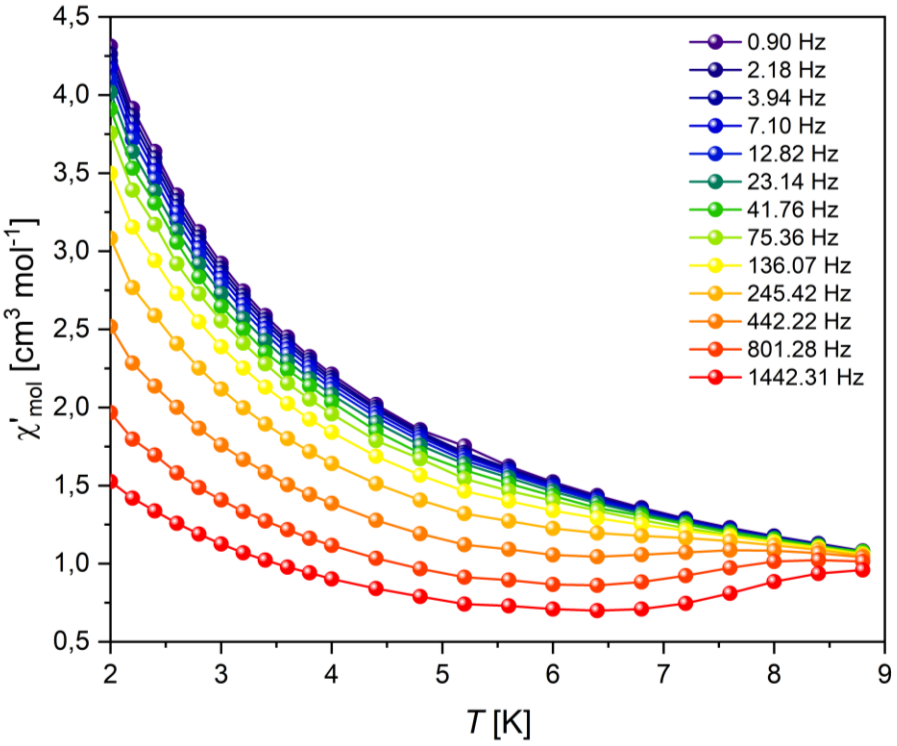

Figure S68. In-phase-component of the mag. susceptibility vs Temperature for [Li(12-c-4)$_2$][(η^5-L^{Pb})Er(η^8-COT^{TIPS})] (**10**) (H_{DC} = 0 Oe).

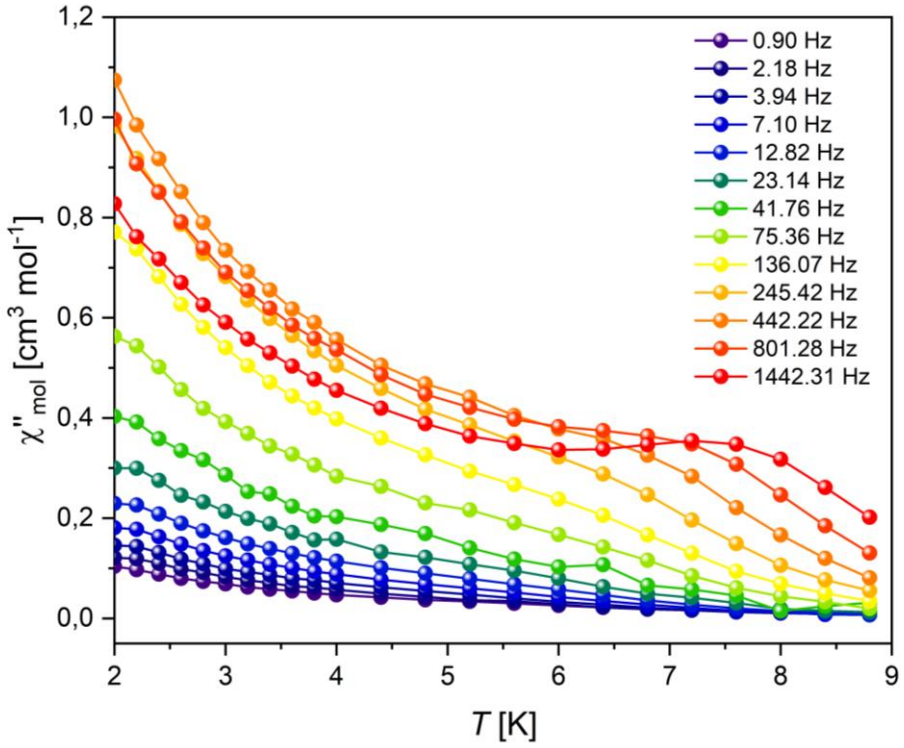

Figure S69. Out-of-phase-component of the mag. susceptibility vs temperature for [Li(12-c-4)$_2$][(η^5-L^{Pb})Er(η^8-COT^{TIPS})] (**10**) (H_{DC} = 0 Oe).

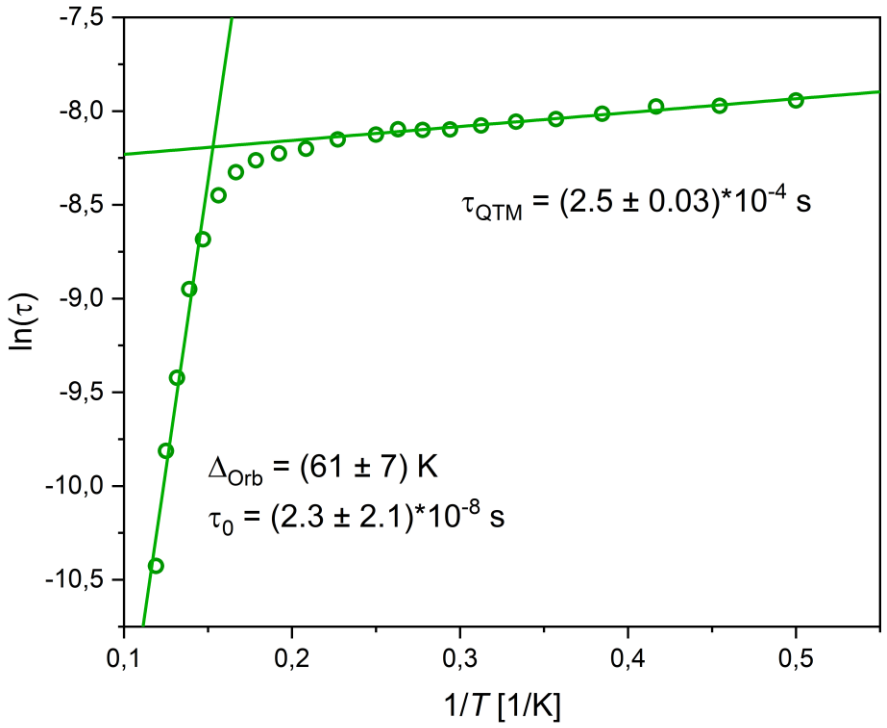

Figure S70. Arrhenius plot for [Li(12-c-4)$_2$][(η^5-L^{Pb})Er(η^8-COT^{TIPS})] (**10**).

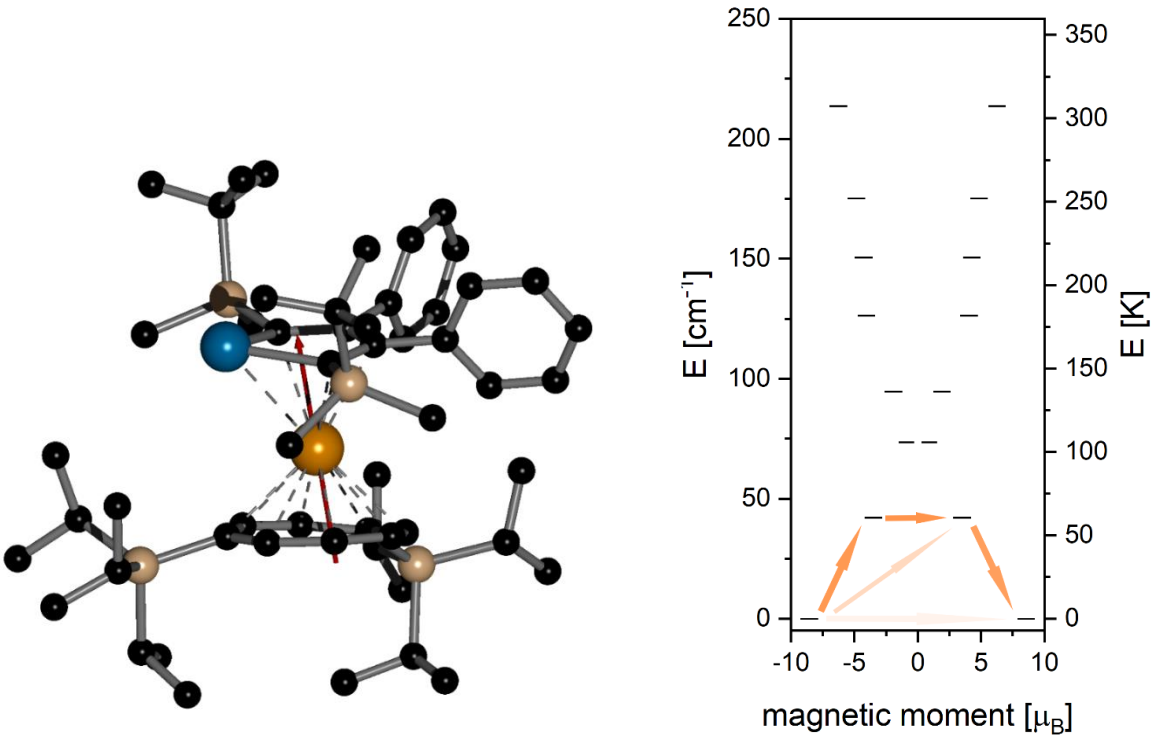

Figure S71. Left: Magnetic anisotropy axis of [Li(12-c-4)$_2$][(η^5-L^{Pb})Er(η^8-COT^{TIPS})] (**10**) Right: *Ab inito* states.

Table S19. Fitting parameters for [Li(thf)(η^5-L^{Pb})Ce(η^8-COT^{TIPS})] (**6**). (H_{DC} = 750 Oe)

T/K	χ_T	χ_S	τ	α
2	2,29E-01	1,38E-21	5,49E-03	3,21E-01
2.2	2,12E-01	1,43E-23	4,85E-03	3,18E-01
2.4	1,99E-01	1,91E-29	4,37E-03	2,99E-01
2.6	1,84E-01	9,66E-04	3,73E-03	2,77E-01
2.8	1,71E-01	1,93E-03	3,00E-03	2,47E-01
3	1,59E-01	2,96E-03	2,47E-03	2,10E-01
3.2	1,49E-01	3,98E-03	1,94E-03	1,74E-01
3.4	1,40E-01	4,22E-03	1,51E-03	1,46E-01
3.6	1,32E-01	4,52E-03	1,19E-03	1,22E-01
3.8	1,25E-01	4,43E-03	9,10E-04	1,01E-01
4	1,18E-01	4,10E-03	7,00E-04	7,72E-02
4.4	1,07E-01	4,56E-03	4,24E-04	4,41E-02
4.8	9,84E-02	7,96E-04	2,50E-04	5,55E-02
5.2	9,15E-02	3,64E-03	1,67E-04	2,21E-02
5.6	8,47E-02	2,89E-04	1,05E-04	2,57E-02
6	7,94E-02	1,01E-03	7,04E-05	2,49E-02

Table S20. CASSCF states, axes, g-tensors for [Li(thf)(η^5-L^{Pb})Ce(η^8-COT^{TIPS})] (**6**).

Doublet state	ΔE/cm^{-1}	ΔE/K	Angle between magnetic z-axes/°	g_x	g_y	g_z	Wavefunction composition
1	0	0	-	0.0725	0.4394	3.7015	∓ 89% |5/2› ∓ 11% |1/2›
2	358.16	515.03	72.65	0.2724	0.7035	3.1321	± 60% |1/2› ∓ 35% |3/2› ± 5% |1/2›
3	602.95	867.04	83.48	0.5680	1.6641	3.1215	± 64% |3/2› ∓ 30% |1/2› ∓ 6% |5/2›

Table S21. Transition probabilities within the lowest three doublet states for [Li(thf)(η^5-L^{Pb})Ce(η^8-COT^{TIPS})] (**6**).

	1	2	3	4	5	6
1		0.1662E-01	0.3737E+00	0.9888E-01	0.1756E+00	0.2477E+00
2	0.1662E-01		0.9888E-01	0.3737E+00	0.2477E+00	0.1756E+00
3	0.3737E+00	0.9888E-01		0.7736E+00	0.2146E+00	0.4829E+00
4	0.9888E-01	0.3737E+00	0.7736E+00		0.4829E+00	0.2146E+00
5	0.1756E+00	0.2477E+00	0.2146E+00	0.4829E+00		0.8541E+00
6	0.2477E+00	0.1756E+00	0.4829E+00	0.2146E+00	0.8541E+00	

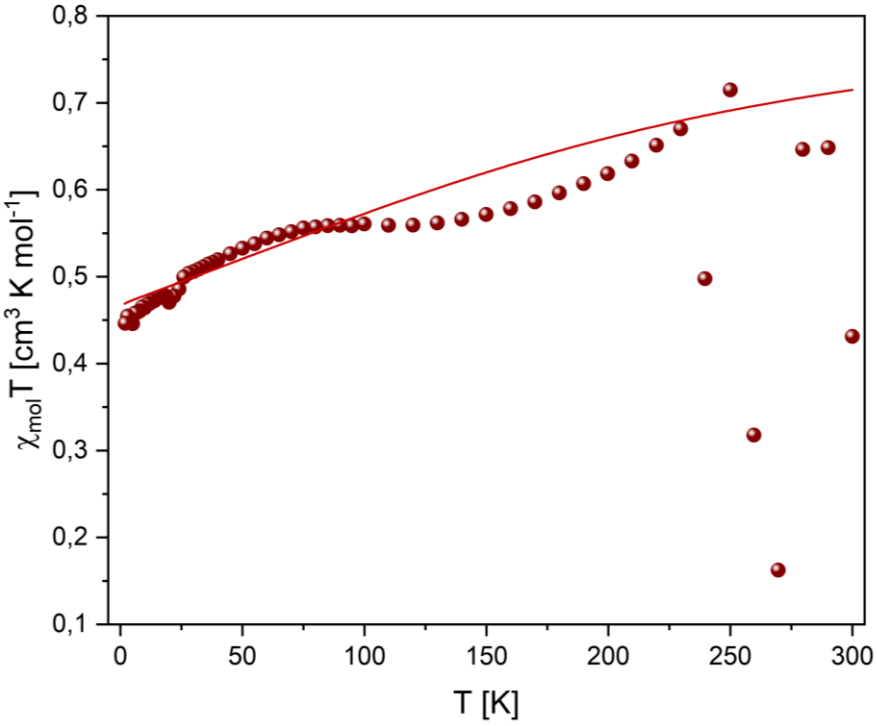

Figure S72. Susceptibility for [Li(thf)(η^5-L^{Pb})Ce(η^8-COT^{TIPS})] (**6**). Due to the small moment of the sample centering of the sample was lost at high T, leading to the observed behaviour.

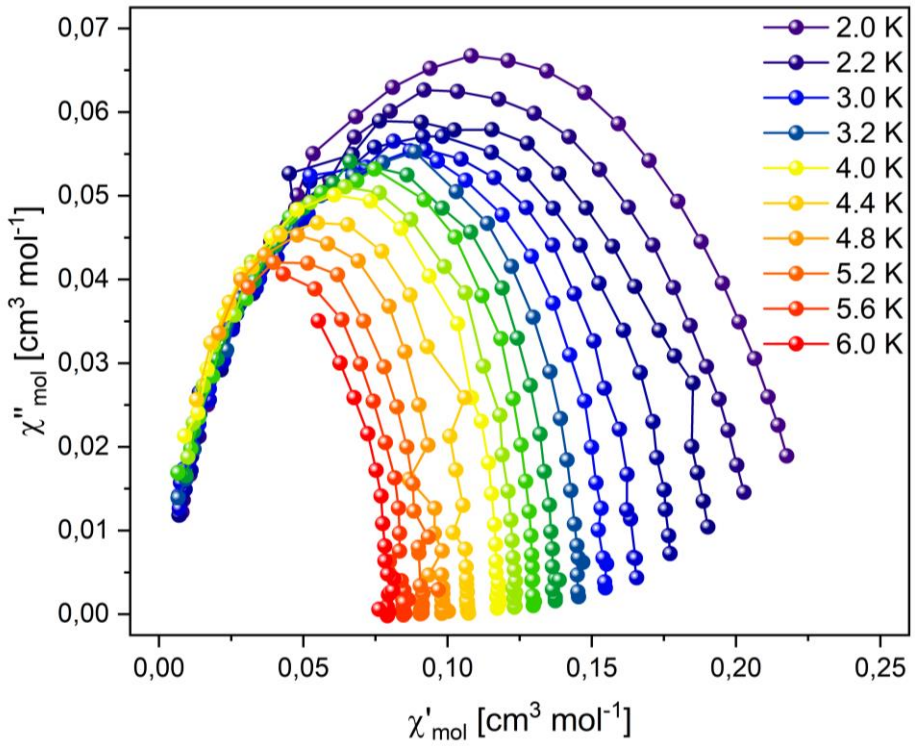

Figure S73. Cole-Cole plot for [Li(thf)(η^5-L^{Pb})Ce(η^8-COT^{TIPS})] (**6**) (H_{DC} = 750 Oe).

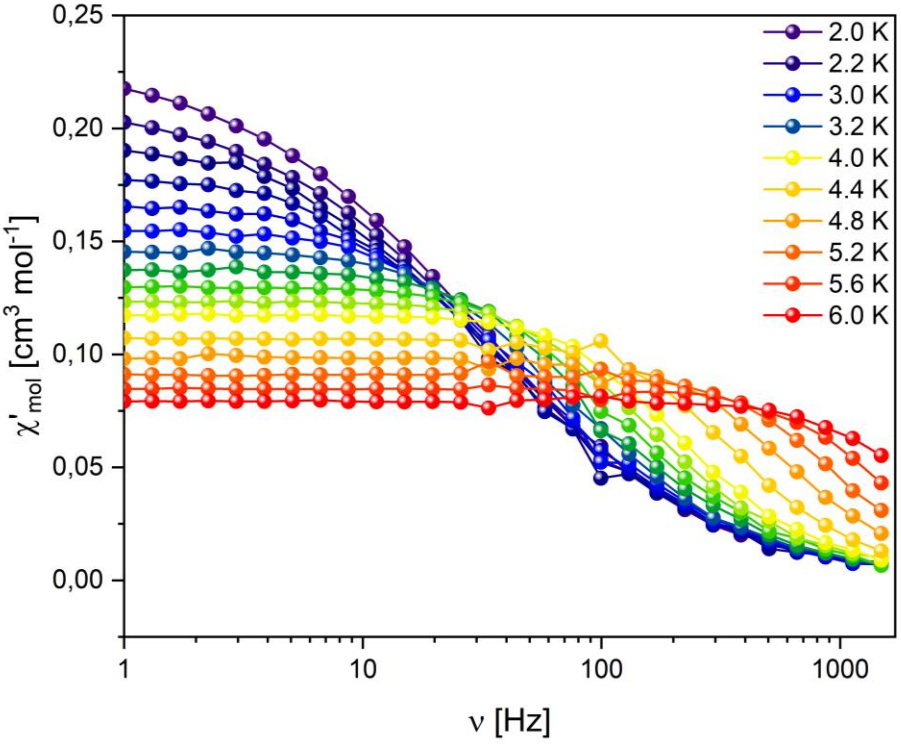

Figure S74. In-phase-component of the mag. susceptibility vs frequency for [Li(thf)(η^5-L^{Pb})Ce(η^8-COT^{TIPS})] (**6**) (H_{DC} = 750 Oe).

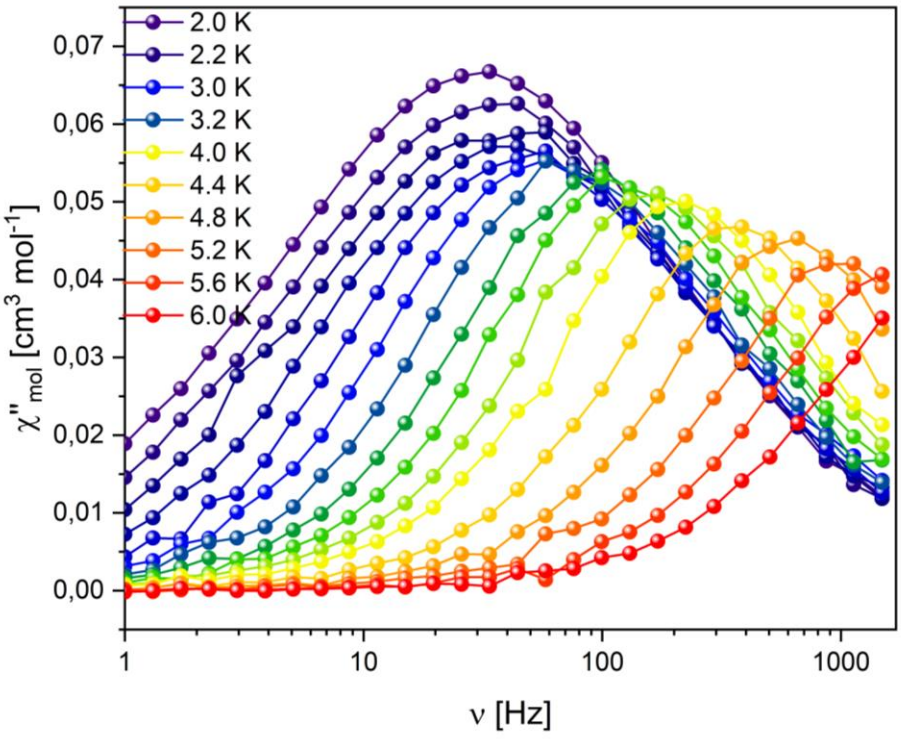

Figure S75. Out-of-phase-component of the mag. susceptibility vs frequency for [Li(thf)(η^5-L^{Pb})Ce(η^8-COT^{TIPS})] (**6**) (H_{DC} = 750 Oe).

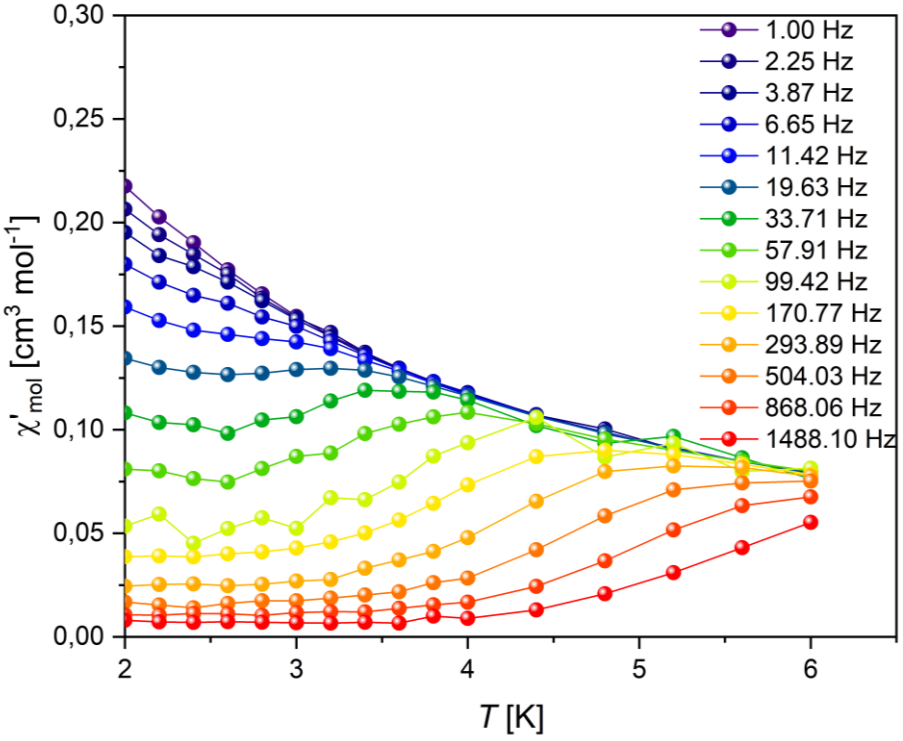

Figure S76. In-phase-component of the mag. susceptibility vs temperature for [Li(thf)(η^5-L^{Pb})Ce(η^8-COT^{TIPS})] (**6**) (H_{DC} = 750 Oe).

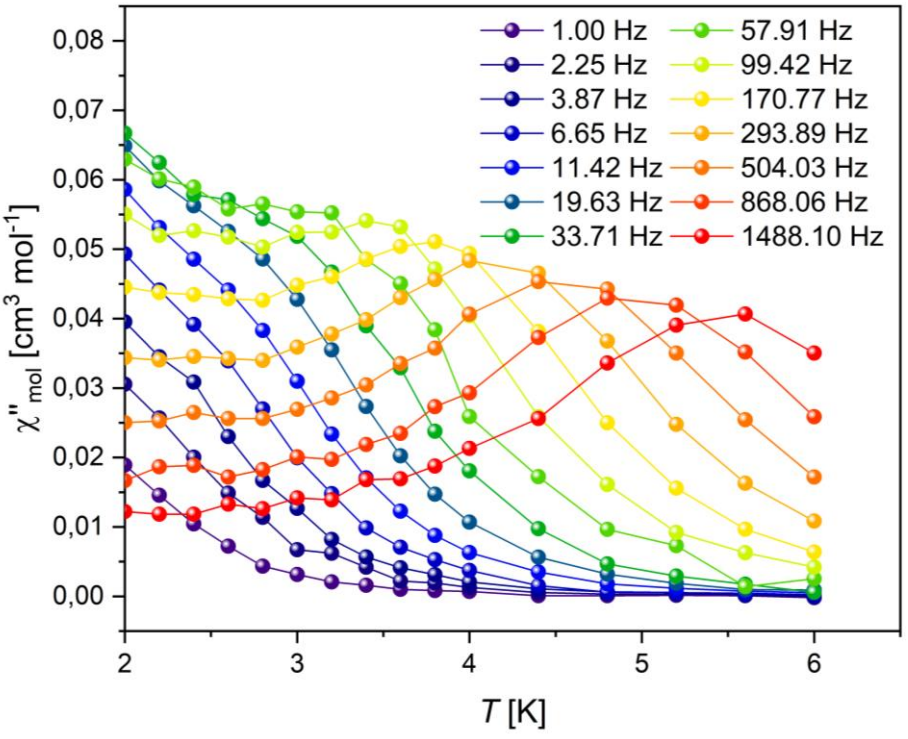

Figure S77. Out-of-phase-component of the mag. susceptibility vs temperature for [Li(thf)(η^5-L^{Pb})Ce(η^8-COT^{TIPS})] (**6**) (H_{DC} = 750 Oe).

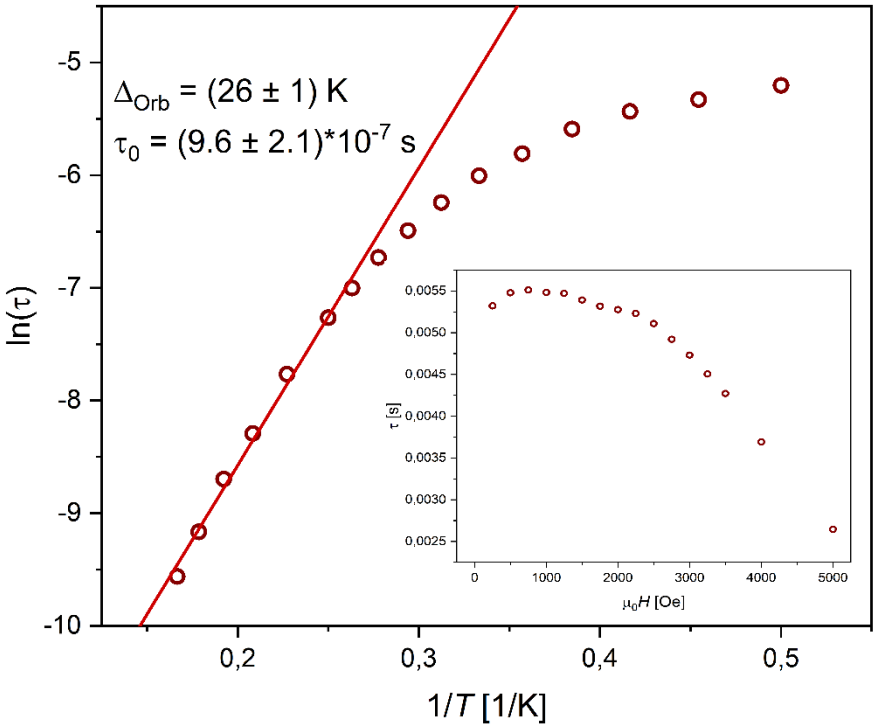

Figure S78. Arrhenius plot (H_{DC} = 750 Oe) and τ vs field for [Li(thf)(η^5-L^{Pb})Ce(η^8-COT^{TIPS})] (**6**).

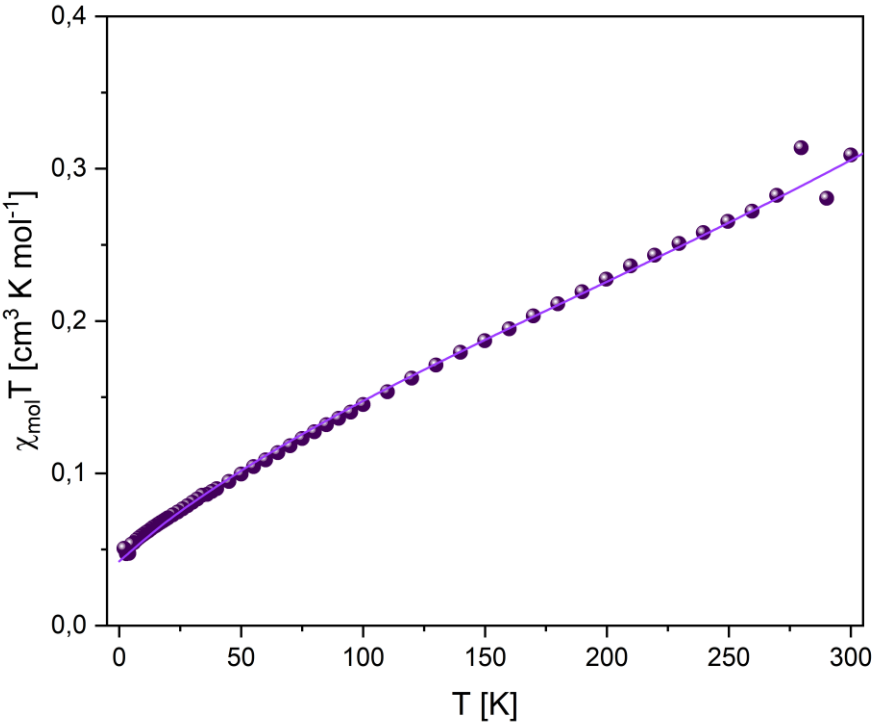

Figure S79. Susceptibility for [Li(thf)(η^5-L^{Pb})Sm(η^8-COT^{TIPS})] (**7**).

Table S22. CASSCF states, axes, g-tensors for [Li(thf)(η^5-L^{Pb})Sm(η^8-COT^{TIPS})] (**7**).

Doublet state	ΔE/cm^{-1}	ΔE/K	Angle between magnetic z-axes/°	g_x	g_y	g_z	Wavefunction composition
1	0	0	-	0.1957	0.2836	1.1093	∓ 69% |5/2› ∓ 17% |1/2› ∓ 13% |3/2›
2	46.20	66.43	34.29	0.2519	0.4909	0.7338	± 55% |3/2› ± 43% |1/2› ∓ 1% |5/2›
3	135.87	195.39	57.57	0.1210	0.2510	1.3694	∓ 40% |1/2› ∓ 31% |3/2› ∓ 29% |5/2›

Table S23. Transition probabilities within the lowest three doublet states for [Li(thf)(η^5-L^{Pb})Sm(η^8-COT^{TIPS})] (**7**).

	1	2	3	4	5	6
1		0.7071E-02	0.1262E-01	0.1735E-01	0.5277E-01	0.3978E-02
2	0.7071E-02		0.1735E-01	0.1262E-01	0.3978E-02	0.5277E-01
3	0.1262E-01	0.1735E-01		0.2580E-01	0.3994E-01	0.6256E-01
4	0.1735E-01	0.1262E-01	0.2580E-01		0.6256E-01	0.3994E-01
5	0.5277E-01	0.3978E-02	0.3994E-01	0.6256E-01		0.1546E-01
6	0.3978E-02	0.5277E-01	0.6256E-01	0.3994E-01	0.1546E-01	

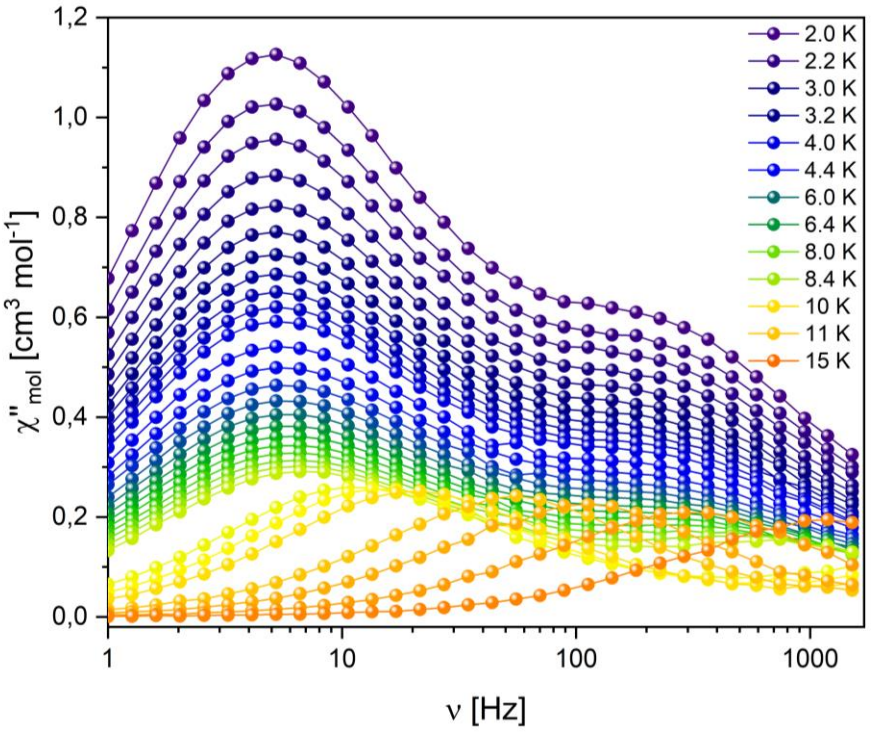

Figure S80. Out-of-phase-component of the mag. susceptibility vs frequency for a sample of $[Li(Et_2O)_{3.4}(thf)_{0.6}][(\eta^5\text{-}L^{Pb})Er(\eta^8\text{-}COT^{TIPS})]$ (**9**) (H_{DC} = 0 Oe). We attribute the observed maximum at approx. 5 Hz (2 K) to the presence of (**8**), formed upon application of a weak static vacuum during sample preparation.

Quantum chemical study of lanthanide plumbole bonding

Density functional theory calculations were performed with the program system TURBOMOLE. The PBE0 hybrid functional[8] together with the def2-TZVP[9] basis set was used. Effective core potentials were employed for the heavy metal atoms. An ECP-60[10] was used for Pb, an ECP-46[11] for La and an ECP-28[10] for Sm and Er. The RI-*J*-approximation was applied for all calculations.[12] Medium sized grids (gridsize 4) were used for the numerical integration of the exchange-correlation part.[13] Self-consistent field thresholds were set to 10^{-7} E_h. Atomic charge contributions to molecular orbitals were calculated via Mulliken population analysis.[14] Magnetically induced current densities were calculated with the GIMIC program.[15-17] For these calculations, the negative charge of $(L^{Pb})^{2-}$ was compensated by using the conductor-like screening model (COSMO) with default parameters.[18] For the preceding calculation of the perturbed density as part of a nuclear shielding calculation, a threshold of 10^{-7} a.u. was used for the response of the orbitals (norm of the residuum) in the coupled-perturbed Kohn-Sham equations. All structures were optimized at level PBE0/def2-TZVP. The conductor-like screening model was employed for the optimization of $(L^{Pb})^{2-}$. Cartesian coordinates of optimized structures are listed in Table S24. Relevant molecular orbitals for compounds **5**, **7** and **8** are depicted in Figures S81-S83. For reasons of comparison, the signed modulus of the current density is depicted for the cyclopentadienyl anion and the hypothetical compound [(Cp)La(COT^{TIPS})] in Figures S84 and S85.

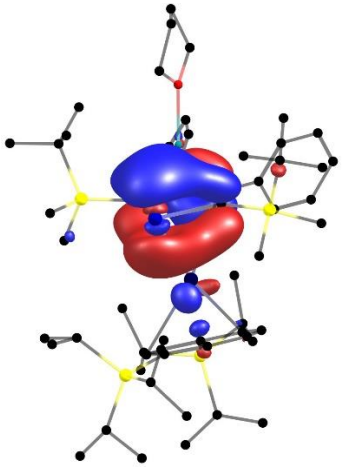

Figure S81. HOMO of [Li(thf)(η^5-L^{Pb})La(η^8-COT^{TIPS})] (**5**)**.** Contours are drawn at 0.04 a.u.. Colors: C Black, O red, Si Yellow, La blue. Hydrogen atoms are omitted for clarity.

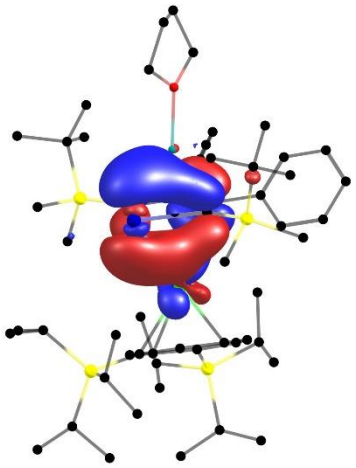

Figure S82. Highest occupied α-orbital of [Li(thf)(η^5-L^{Pb})Sm(η^8-COT^{TIPS})] (**7**)**.** See also Figure S81.

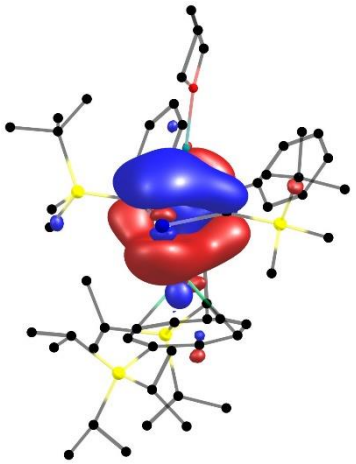

Figure S83. Highest occupied α-orbital of [Li(thf)(η^5-L^{Pb})Er(η^8-COT^{TIPS})] (**8**)**.** See also Figure S81.

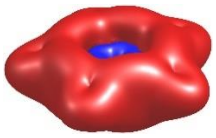

Figure S84. Signed modulus of the current density of the free cyclopentadienyl anion. Contours are drawn at 0.03 a.u.. Diatropic contributions are shown in red, paratropic contributions in blue. The magnetic field is perpendicular to the ring plane. Hydrogen atoms are omitted for clarity.

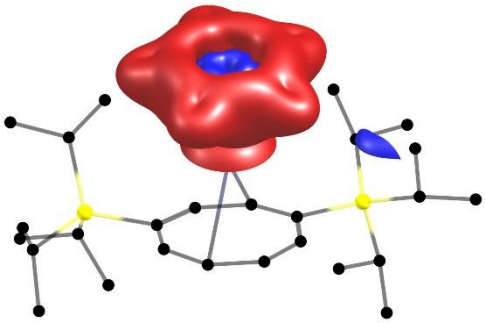

Figure S85. Signed modulus of the current density of the hypothetical compound [(η^5-Cp)La(η^8-COT^{TIPS})]. Colors: C black, Si yellow. See also Figure S83.

Table S24. Cartesian coordinates of the optimized structures (level PBE0/def2-TZVP).

$(L^{Pb})^{2-}$

Pb	0.3218400	1.8599900	0.0338800
C	1.4379700	-0.0736500	-0.0840300
C	-1.3801600	0.4201600	0.0909400
C	0.5271100	-1.1313300	-0.0883500
C	-0.8881000	-0.8891100	0.0036300
Si	3.2724400	-0.0360600	-0.0947400
Si	-3.0720200	1.1168300	-0.0891400
C	1.0121400	-2.5427400	-0.0789400
C	-1.8104400	-2.0540800	-0.0113200
C	4.0250100	0.4475800	-1.8181400
C	4.1679800	-1.6130600	0.4704600
C	3.8930200	1.2877500	1.1142200
C	-3.9354000	0.7108100	-1.7830400
C	-4.3381900	0.6955800	1.2680000
C	-2.9962000	3.0103400	0.0194700
C	1.6114500	-3.1222700	-1.1986300
C	0.8959300	-3.3368600	1.0654400
C	-1.8438100	-2.9572300	-1.0811200
C	-2.6962400	-2.2912300	1.0443200
C	3.7672900	1.9233700	-2.1152000
C	3.3896600	-0.3870600	-2.9268300
C	5.5352500	0.2089600	-1.8262500
H	3.7097800	-1.9874100	1.3905200
H	5.2220600	-1.3998200	0.6756400
H	4.1133400	-2.4173700	-0.2659500
H	3.3841300	2.2412700	0.9501300
H	4.9734800	1.4462000	1.0238900
H	3.6828000	0.9751200	2.1416500
H	-4.5890400	-0.3658200	1.2965000
H	-4.0052200	3.4321600	0.0570200
H	-2.4700600	3.4525000	-0.8302300
C	-4.6921200	-0.6157300	-1.7118600
H	-3.3525500	0.4111800	-3.8540000
C	-4.9408400	1.8034800	-2.1498600
C	-2.8802900	0.6247400	-2.8838200
H	-5.2631600	1.2624000	1.1133600
H	-3.9376100	0.9748100	2.2483400
H	-2.4666700	3.3128500	0.9274800
H	1.7012100	-2.5303200	-2.1020900
C	2.0797700	-4.4283200	-1.1801200
C	1.3658300	-4.6422200	1.0960900
H	0.4250000	-2.9157500	1.9482200

C	-2.7210200	-4.0310700	-1.1010500
H	-1.1691900	-2.8004100	-1.9150900
H	-2.6805900	-1.6163600	1.8929200
C	-3.5772700	-3.3629000	1.0328200
H	2.6978800	2.1570800	-2.0807800
H	4.1417700	2.1819900	-3.1158800
H	4.2716900	2.5757100	-1.3961300
H	3.6072500	-1.4522500	-2.8045700
H	3.7775300	-0.0820300	-3.9091500
H	2.3022500	-0.2665800	-2.9326200
H	6.0444100	0.7755700	-1.0403200
H	5.9657600	0.5249300	-2.7868400
H	5.7817700	-0.8472900	-1.6878100
H	-5.5102600	-0.5714400	-0.9870500
H	-4.0441800	-1.4485700	-1.4312400
H	-5.1351200	-0.8483200	-2.6914300
H	-5.4616300	1.5401000	-3.0815200
H	-4.4573600	2.7713500	-2.3053100
H	-5.7050800	1.9337300	-1.3766700
H	-2.1488000	-0.1581600	-2.6693800
H	-2.3229000	1.5622000	-2.9802400
H	2.5365800	-4.8504300	-2.0703100
C	1.9630000	-5.1979900	-0.0288600
H	1.2669700	-5.2305300	2.0035500
H	-2.7271400	-4.7054800	-1.9522400
C	-3.5982700	-4.2421900	-0.0435000
H	-4.2482000	-3.5180100	1.8725400
H	2.3297800	-6.2189700	-0.0093100
H	-4.2872000	-5.0802600	-0.0569300

[(η^5-L^{Pb})La(η^8-COT^{TIPS})]$^-$

Pb	1.2976900	-1.3788000	0.1813800
La	-0.0934800	0.1548900	-2.5450000
C	1.1271100	0.9110600	0.0118900
C	-0.9607900	-1.0587600	-0.1006100
C	-0.2347200	1.3235000	0.0241600
C	-1.2927800	0.3331600	-0.0355800
C	1.3223600	-1.3993900	-4.4136700
C	-0.0572300	-1.5052600	-4.7693700
C	-1.1423600	-0.6258400	-5.0365800
C	-1.3772300	0.7826200	-5.0576800
C	-0.5165100	1.8773200	-4.7340600
C	0.8379900	2.0325400	-4.3555800
C	1.9247000	1.1539800	-4.1213600

C	2.1222600	-0.2487400	-4.1442600
Si	2.7051800	1.8829000	0.1545000
Si	-1.9838200	-2.5893200	0.1605300
C	-0.6020100	2.7841000	0.0270500
C	-2.7164700	0.7923000	0.0414700
Si	2.2522900	-3.0604800	-4.5433400
H	-0.3896000	-2.5419400	-4.8732300
H	-2.0366200	-1.2069400	-5.2771900
Si	-2.9492200	1.2966400	-6.0038100
H	-1.0168700	2.8484800	-4.7791900
H	1.0975700	3.0758100	-4.1535800
H	2.8180800	1.6903900	-3.7907100
H	3.1377200	-0.4989200	-3.8362900
C	3.4166100	1.9534100	1.9848300
C	2.6497100	3.6693400	-0.5096500
C	4.0700700	1.0179900	-0.8486200
C	-2.8794700	-2.6860600	1.9028600
C	-3.3092800	-2.9802800	-1.1609600
C	-0.8360500	-4.1075700	0.0855300
C	-0.4901200	3.5547600	1.1973800
C	-1.0607900	3.4396300	-1.1279800
C	-3.1808900	1.5243300	1.1530300
C	-3.6544100	0.4840800	-0.9586500
C	1.6167100	-4.3663400	-3.2615600
C	1.8981500	-3.7219700	-6.3278900
C	4.1597700	-2.9429800	-4.2832600
C	-2.4364400	1.5259700	-7.8530000
C	-4.2796900	-0.1032500	-5.9982300
C	-3.6176000	3.0056900	-5.4056400
C	3.9288600	0.5692800	2.4139500
C	2.3577900	2.4086600	2.9979200
C	4.5936000	2.9448800	2.0325400
H	2.1984300	3.6742400	-1.5136600
H	3.6654900	4.0861000	-0.5962000
H	2.0513000	4.3451700	0.1174900
H	4.1311400	-0.0543400	-0.6116000
H	5.0575800	1.4685900	-0.6600700
H	3.8616200	1.1049400	-1.9242700
H	-4.1159500	-2.2360000	-1.1964600
H	-1.4294900	-5.0346200	0.0603100
H	-0.1525200	-4.1658200	0.9457100
C	-4.2510700	-1.9915700	1.8760600
H	-2.4770700	-2.1316900	3.9759800
C	-3.1082400	-4.1609800	2.2833900

C	-2.0017100	-2.0323400	2.9813000
H	-3.7670100	-3.9648300	-0.9695800
H	-2.8434000	-3.0246800	-2.1585600
H	-0.2174700	-4.0820800	-0.8223300
H	-0.1547200	3.0681000	2.1132900
C	-0.8093200	4.9130600	1.2120200
C	-1.3826500	4.7989000	-1.1240600
H	-1.1752100	2.8884600	-2.0679900
C	-4.5119300	1.9281600	1.2550500
H	-2.4810700	1.7663600	1.9534600
H	-3.3357200	-0.0929900	-1.8306300
C	-4.9879200	0.8859600	-0.8635100
H	1.5470400	-3.7798500	-2.3245600
C	0.2153800	-4.9237000	-3.5621300
C	2.5765300	-5.5388800	-2.9930700
C	4.6010600	-2.5602600	-2.8593900
C	4.9436400	-2.1304900	-5.3274200
H	0.8426500	-4.0500600	-6.2754300
C	1.9690300	-2.6471000	-7.4240900
C	2.7334200	-4.9510700	-6.7201200
H	4.4501400	-4.0018200	-4.4305400
H	-3.3602300	1.8197300	-8.3871400
C	-1.9234500	0.2243800	-8.4880000
C	-1.4072500	2.6502100	-8.0480100
C	-4.1604300	3.0083100	-3.9699100
H	-5.1178300	2.4697800	-3.9023100
C	-5.4839000	0.1840600	-6.9112300
H	-3.7447000	-0.9608200	-6.4479300
C	-4.7626600	-0.5516600	-4.6120600
H	-2.7179900	3.6493500	-5.4135500
C	-4.6257900	3.6671500	-6.3607000
H	3.1292000	-0.1879100	2.3934900
H	4.3190600	0.6124800	3.4486200
H	4.7439600	0.2106600	1.7677800
H	1.9903600	3.4228200	2.7792400
H	2.7863400	2.4258200	4.0182100
H	1.4956100	1.7246000	3.0099400
H	5.3939400	2.6740400	1.3262800
H	5.0407900	2.9556900	3.0446700
H	4.2756100	3.9726500	1.8015300
H	-4.9355800	-2.4705800	1.1593100
H	-4.1799900	-0.9282600	1.6122200
H	-4.7244300	-2.0547400	2.8747800
H	-3.6618400	-4.2205900	3.2398000

H	-2.1636700	-4.7087500	2.4137800
H	-3.7059200	-4.6962700	1.5279600
H	-1.8459800	-0.9623800	2.7831500
H	-1.0055000	-2.4991200	3.0397800
H	-0.7143500	5.4802100	2.1412300
C	-1.2549400	5.5460800	0.0480600
H	-1.7360800	5.2724700	-2.0428100
H	-4.8395700	2.4877500	2.1343300
C	-5.4262500	1.6116400	0.2464100
H	-5.6869500	0.6303500	-1.6626700
H	0.1884300	-5.4613600	-4.5239500
H	-0.5534400	-4.1394500	-3.5930600
H	-0.0899000	-5.6414100	-2.7817100
H	2.1805600	-6.1723800	-2.1806100
H	3.5800200	-5.2103100	-2.6904100
H	2.6920500	-6.1870300	-3.8763000
H	4.7865300	-2.5052500	-6.3487500
H	6.0272300	-2.1830800	-5.1203300
H	4.0437500	-3.0962900	-2.0779600
H	5.6744500	-2.7766100	-2.7165500
H	4.4626500	-1.4882900	-2.6601300
H	4.6617900	-1.0673300	-5.3229800
H	2.9951300	-2.2770100	-7.5698200
H	1.3377400	-1.7804500	-7.1844500
H	1.6316700	-3.0568400	-8.3926400
H	2.6161800	-5.7840000	-6.0117600
H	3.8077600	-4.7125000	-6.7712200
H	2.4394500	-5.3231900	-7.7176200
H	-1.0318700	-0.1499200	-7.9620000
H	-1.6419800	0.3866500	-9.5433000
H	-2.6771900	-0.5772100	-8.4690900
H	-1.7703000	3.6213900	-7.6783800
H	-1.1614100	2.7752500	-9.1172800
H	-0.4702000	2.4257200	-7.5165300
H	-5.5772200	3.1155300	-6.3946400
H	-4.3471100	4.0376000	-3.6179500
H	-3.4721400	2.5365700	-3.2551500
H	-6.1163600	0.9875400	-6.5041800
H	-6.1230300	-0.7115000	-7.0015000
H	-5.1850900	0.4802800	-7.9274800
H	-3.9289000	-0.8234200	-3.9501900
H	-5.4215200	-1.4336900	-4.6913100
H	-5.3394400	0.2398600	-4.1113100
H	-4.2483700	3.7382200	-7.3911800

H	-4.8612200	4.6914900	-6.0229600
H	-1.5055900	6.6087700	0.0564100
H	-6.4692000	1.9245900	0.3258200

[(η^5-L^{Pb})Er(η^8-COT^{TIPS})]$^-$

Pb	2.3763867	-1.0019840	0.4766384
Er	-0.5406009	-0.0695930	-0.4459494
C	1.9986375	0.4438478	-1.2289779
C	1.1231708	0.6185146	1.4540524
C	1.4208267	1.6587994	-0.7665910
C	0.9810484	1.7526407	0.5933460
C	-1.4125295	-2.5348813	-0.3982675
C	-2.2195437	-1.7655800	0.4790728
C	-2.9410751	-0.5548557	0.4244692
C	-3.1706628	0.4804147	-0.5177506
C	-2.6193323	0.7036236	-1.8075524
C	-1.7738783	0.0082316	-2.6863984
C	-1.1083664	-1.2286816	-2.6502566
C	-0.9713305	-2.2706440	-1.7176042
Si	2.7671355	0.0254892	-2.8600227
Si	1.0297435	0.4818896	3.2976412
C	1.2468743	2.8450419	-1.6665479
C	0.5096505	3.0664816	1.1192492
Si	-1.1268528	-4.3023946	0.2276566
H	-2.3142571	-2.2092348	1.4642894
H	-3.4282965	-0.3688322	1.3762213
Si	-4.7587810	1.4689151	-0.2146078
H	-2.9099001	1.6586802	-2.2325180
H	-1.5352892	0.5827409	-3.5759767
H	-0.4935669	-1.3805847	-3.5299582
H	-0.2904284	-3.0252332	-2.0885604
C	4.7077383	0.2274342	-2.9079228
C	2.0624533	0.9423101	-4.3597839
C	2.5237138	-1.8131378	-3.2257364
C	2.2670862	1.6298619	4.2628064
C	-0.6741767	0.7257378	4.0960038
C	1.4831342	-1.2867963	3.7918211
C	2.3553363	3.5914087	-2.0667181
C	-0.0018313	3.2663242	-2.1213072
C	1.3550801	4.1802327	1.0852382
C	-0.7391916	3.2302131	1.7147462
C	-0.1863137	-4.3744397	1.9024465
C	-2.8846311	-5.0214220	0.4969511
C	-0.1590172	-5.4369887	-0.9700095

C	-6.1533029	0.5233730	-1.1308493
C	-5.2708946	1.4663882	1.6307177
C	-4.6937113	3.2093761	-1.0103830
C	5.3744367	-0.8613846	-2.0677732
C	5.1851636	1.5784679	-2.3871629
C	5.1872876	0.0801316	-4.3541344
H	0.9698833	0.9168135	-4.3221263
H	2.3784944	0.4624338	-5.2909341
H	2.3580638	1.9929636	-4.3961494
H	2.8010451	-2.4280968	-2.3665436
H	3.1288488	-2.1311034	-4.0802447
H	1.4803821	-2.0280779	-3.4602607
H	-1.0529156	1.7439354	3.9978504
H	1.2869346	-1.4419902	4.8565624
H	2.5332265	-1.5252275	3.6041473
C	1.6531258	2.9953699	4.5693844
H	4.2691761	2.4291082	4.0248460
C	2.6303134	0.9783931	5.5998889
C	3.5489156	1.8238875	3.4560947
H	-0.6333293	0.4837354	5.1634564
H	-1.3974388	0.0476106	3.6322087
H	0.8800153	-2.0055822	3.2353581
H	3.3327306	3.3031080	-1.7044169
C	2.2283656	4.6950109	-2.8952730
C	-0.1388286	4.3692190	-2.9518761
H	-0.8898511	2.7217492	-1.8200049
C	0.9674039	5.3986814	1.6179454
H	2.3374445	4.0787481	0.6412406
H	-1.4178448	2.3859413	1.7496574
C	-1.1308500	4.4453573	2.2562873
H	0.5826723	-3.5973744	1.7947757
C	-1.0357995	-4.0257157	3.1251277
C	0.5417594	-5.6925041	2.1752291
C	1.2917462	-5.0217933	-1.2196108
C	-0.8438083	-5.7947514	-2.2885547
H	-3.2448528	-4.4794380	1.3825858
C	-3.8698096	-4.7165100	-0.6295186
C	-2.8993933	-6.5094218	0.8412262
H	-0.1253586	-6.3640055	-0.3785653
H	-7.0700758	1.1019321	-0.9496878
C	-6.3760064	-0.8823770	-0.5780582
C	-5.9371157	0.4637141	-2.6415843
C	-3.7004229	4.1697128	-0.3651217
H	-4.0374510	4.4818851	0.6271549

C	-6.6591568	2.0574827	1.8781068
H	-5.3421432	0.3957964	1.8666453
C	-4.2671029	2.0739125	2.6045184
H	-4.3370446	3.0126483	-2.0303704
C	-6.0582791	3.8825050	-1.1618411
H	5.0731447	-0.8066775	-1.0176487
H	6.4668564	-0.7466933	-2.1029403
H	5.1377220	-1.8649354	-2.4293100
H	4.8112481	2.4044188	-2.9976891
H	6.2830389	1.6257636	-2.4109539
H	4.8698899	1.7411610	-1.3527686
H	4.8879917	-0.8752603	-4.7945652
H	6.2845393	0.1265198	-4.3936002
H	4.8014952	0.8777318	-4.9943686
H	0.7716016	2.9049580	5.2102236
H	1.3563189	3.5346710	3.6693883
H	2.3827719	3.6207733	5.1033191
H	3.2805439	1.6505742	6.1770880
H	3.1654512	0.0351599	5.4684941
H	1.7458090	0.7780749	6.2132435
H	3.3551203	2.3298411	2.5080713
H	4.0303183	0.8697120	3.2199857
H	3.1125620	5.2546639	-3.1830075
C	0.9773879	5.0888295	-3.3492219
H	-1.1270123	4.6674458	-3.2864130
H	1.6493340	6.2416039	1.5796293
C	-0.2797101	5.5389838	2.2105959
H	-2.1105406	4.5381127	2.7122655
H	-1.8533785	-4.7403292	3.2632985
H	-1.4725086	-3.0272157	3.0713674
H	-0.4245001	-4.0543672	4.0341221
H	1.1063245	-5.6200320	3.1120374
H	1.2507821	-5.9573318	1.3899105
H	-0.1544125	-6.5295536	2.2868065
H	-1.8094577	-6.2795769	-2.1328933
H	-0.2189653	-6.4880111	-2.8648573
H	1.8032223	-4.6833785	-0.3159704
H	1.8643277	-5.8585594	-1.6375625
H	1.3589595	-4.2025020	-1.9372374
H	-1.0178190	-4.9172569	-2.9158460
H	-3.6137400	-5.2461926	-1.5505348
H	-3.8967484	-3.6506439	-0.8626903
H	-4.8841125	-5.0267979	-0.3503184
H	-2.2887595	-6.7400737	1.7175277

H	-2.5247015	-7.1188110	0.0129013
H	-3.9195944	-6.8514123	1.0541928
H	-5.4744634	-1.4926860	-0.6773142
H	-7.1802196	-1.3921753	-1.1220229
H	-6.6514455	-0.8747610	0.4798463
H	-5.8394788	1.4568838	-3.0886532
H	-6.7789876	-0.0368030	-3.1349720
H	-5.0310120	-0.0957118	-2.8875336
H	-6.4856517	4.1533175	-0.1932002
H	-3.5906860	5.0808656	-0.9646589
H	-2.7074839	3.7335417	-0.2469271
H	-6.6626620	3.1416022	1.7375672
H	-6.9754340	1.8697177	2.9108490
H	-7.4218911	1.6362380	1.2191183
H	-3.2818224	1.6135733	2.5245261
H	-4.6034514	1.9440631	3.6398182
H	-4.1460137	3.1469735	2.4374439
H	-6.7847657	3.2498580	-1.6767620
H	-5.9624759	4.8101040	-1.7384966
H	0.8737343	5.9513061	-3.9984890
H	-0.5837596	6.4896869	2.6343237

[Li(thf)(η^5-L^{Pb})La(η^8-COT^{TIPS})] (5)

Pb	3.6770562	6.1543313	11.0019179
La	1.6301719	8.5172776	12.3618177
C	3.4842835	6.3103347	13.2895659
C	1.4491747	5.7357082	11.4247414
Li	2.6338755	4.2632325	12.6876313
C	2.1697900	6.0766938	13.7704583
C	1.1145179	5.7843998	12.8106462
C	2.5588183	10.4190576	10.6054354
C	1.1431087	10.4376108	10.5129312
C	0.0452158	10.5370919	11.3971712
C	-0.1661785	10.6478955	12.7952346
C	0.7521414	10.6361203	13.8777958
C	2.1500279	10.5881450	14.0233974
C	3.2433814	10.5238569	13.1381931
C	3.4074881	10.4549969	11.7408983
Si	5.0425659	6.7258758	14.2405266
Si	0.4193460	5.2862061	9.9274290
O	3.0394984	2.4124944	13.0173108
C	1.8256261	6.1381520	15.2285135
C	-0.2537715	5.4674266	13.3236888
Si	3.4143602	10.6172415	8.9137223

H	0.7871820	10.3627764	9.4902787
H	-0.8824522	10.5098279	10.8348693
Si	-1.8972620	11.2839326	13.2698922
H	0.2681883	10.6645175	14.8486712
H	2.4591555	10.5583315	15.0638903
H	4.1893567	10.4661643	13.6668099
H	4.4550743	10.3678966	11.4830526
C	6.2033636	5.2062945	14.5596698
C	4.7529663	7.6092195	15.8816076
C	6.0741090	7.9012311	13.1877913
C	-0.3970794	3.5288597	9.9247585
C	-0.9359484	6.5408405	9.5159796
C	1.5685097	5.3175778	8.4303570
C	4.0072437	1.7371677	12.1937475
C	2.4050365	1.4746550	13.9013374
C	2.2413882	5.1381559	16.1059229
C	1.0850992	7.1910259	15.7620803
C	-0.4739615	4.3717355	14.1616337
C	-1.3595734	6.2397075	12.9762608
C	3.1020204	9.1084021	7.7667866
C	2.6293097	12.1790118	8.1325634
C	5.3101915	10.8263300	9.0095604
C	-1.7782870	13.1909173	13.2888572
C	-3.1901031	10.8386199	11.9324689
C	-2.3739407	10.7400596	15.0397543
C	6.7828282	4.6977177	13.2405198
C	5.4929235	4.0512716	15.2578933
C	7.3617008	5.6570052	15.4545527
H	4.0429109	8.4294191	15.7460705
H	5.6897321	8.0393163	16.2468419
H	4.3501386	6.9571474	16.6589414
H	6.2929783	7.4921147	12.1986644
H	7.0263539	8.1314733	13.6737799
H	5.5406845	8.8416989	13.0410877
H	-1.7792307	6.5065674	10.2069413
H	0.9905908	5.2040401	7.5097685
H	2.3167796	4.5208548	8.4558917
C	-1.7217654	3.4904135	10.6850366
H	0.1403558	1.4896453	10.4320616
C	-0.6803147	3.1223519	8.4748979
C	0.5530367	2.5022960	10.5348863
H	-1.3243942	6.3527794	8.5103551
H	-0.5366734	7.5601881	9.5168505
H	2.1021204	6.2681204	8.3617336

H	2.7289399	1.6924663	14.9244977
C	4.2398848	0.4000519	12.8651968
H	4.8982722	2.3636063	12.1350051
H	3.5884560	1.6175598	11.1892762
H	1.3236241	1.6100448	13.8351745
C	2.8638693	0.1012484	13.4475211
H	2.8144504	4.3038330	15.7198336
C	1.9394171	5.1882829	17.4575407
C	0.7819513	7.2529818	17.1138334
H	0.7249111	7.9946764	15.1244095
C	-1.7415014	4.0543635	14.6200333
H	0.3671883	3.7615833	14.4698731
H	-1.2355486	7.0993335	12.3250781
C	-2.6320534	5.9306755	13.4335489
H	3.2709894	8.2460297	8.4281176
C	1.6754182	9.0064632	7.2275914
C	4.0822130	8.9788235	6.5987923
C	6.0788062	9.5932931	9.4885371
C	5.8262635	12.0855700	9.7052072
H	1.6196763	11.8517089	7.8467155
C	2.4533668	13.3475697	9.1016899
C	3.3292904	12.6438274	6.8559185
H	5.5469871	10.9454929	7.9418199
H	-2.7839979	13.5431548	13.5568880
C	-1.4324896	13.7749535	11.9206615
C	-0.8088458	13.7152344	14.3463091
C	-2.5582196	9.2362448	15.2168366
H	-3.4732164	8.8889778	14.7302368
C	-4.5503350	11.5012898	12.1547966
H	-2.7758519	11.2857378	11.0185670
C	-3.3730773	9.3487669	11.6616436
H	-1.5055774	11.0344808	15.6445194
C	-3.5699946	11.4936965	15.6230218
H	5.9995722	4.4184767	12.5283246
H	7.4073046	3.8117707	13.4161203
H	7.4110350	5.4474079	12.7541932
H	5.0782392	4.3506189	16.2239482
H	6.2008675	3.2326253	15.4458549
H	4.6810365	3.6464147	14.6469263
H	7.9241291	6.4860809	15.0178069
H	8.0668286	4.8286532	15.6007762
H	7.0159850	5.9700493	16.4427134
H	-2.4560189	4.1750585	10.2533942
H	-1.6083389	3.7437929	11.7396289

H	-2.1502901	2.4807615	10.6319901
H	-1.2072883	2.1597599	8.4573030
H	0.2341467	3.0072667	7.8893359
H	-1.3180740	3.8478752	7.9614473
H	0.7050996	2.6862707	11.6016595
H	1.5327147	2.5092814	10.0459929
H	2.8860652	-0.6165440	14.2677259
H	4.9828506	0.4975257	13.6608428
H	4.5859775	-0.3594125	12.1638978
H	2.1976876	-0.2856440	12.6724722
H	2.2761151	4.3931001	18.1138254
C	1.2096010	6.2508537	17.9703159
H	0.2067899	8.0888978	17.4956369
H	-1.8798310	3.1945943	15.2661829
C	-2.8305398	4.8330492	14.2551791
H	-3.4706279	6.5519973	13.1426972
H	1.4214860	9.8670404	6.6012973
H	0.9268323	8.9379177	8.0185555
H	1.5639860	8.1129516	6.6035486
H	3.8939095	8.0480766	6.0520775
H	5.1256595	8.9632312	6.9163005
H	3.9690338	9.7958512	5.8811367
H	5.4319215	12.9965388	9.2518338
H	6.9190455	12.1353197	9.6384178
H	5.7220881	8.6663099	9.0341335
H	7.1440094	9.6910412	9.2505904
H	6.0095608	9.4610917	10.5702115
H	5.5651671	12.1121985	10.7658457
H	3.4132286	13.7639022	9.4167517
H	1.9130401	13.0525927	10.0028926
H	1.8923823	14.1591982	8.6247545
H	3.3715967	11.8639045	6.0926417
H	4.3562666	12.9651321	7.0532591
H	2.8052660	13.5005976	6.4176916
H	-0.4538355	13.4278861	11.5777948
H	-1.3944763	14.8690425	11.9647268
H	-2.1641515	13.5058129	11.1545109
H	-1.0651676	13.3760749	15.3536159
H	-0.8081654	14.8107865	14.3612972
H	0.2144087	13.3907420	14.1394718
H	-4.4998662	11.2363445	15.1106654
H	-2.6442986	8.9726701	16.2769426
H	-1.7306857	8.6581612	14.8001067
H	-5.0743111	11.0662082	13.0094084

H	-5.1930867	11.3562833	11.2795347
H	-4.4714250	12.5767204	12.3281436
H	-2.4261904	8.8495967	11.4461742
H	-4.0318494	9.1863442	10.8013539
H	-3.8303011	8.8443426	12.5162014
H	-3.4514292	12.5777550	15.5645064
H	-3.7054616	11.2351139	16.6791151
H	0.9731231	6.2952862	19.0269676
H	-3.8243240	4.5873094	14.6105667

[Li(thf)(η^5-L^{Pb})Sm(η^8-COT^{TIPS})] (7)

Pb	3.6521385	6.2665579	10.9886589
Sm	1.6317054	8.5133953	12.3483587
C	3.4808278	6.4025831	13.2735918
C	1.4228998	5.8345422	11.4334279
Li	2.6317179	4.3568663	12.6736376
C	2.1709053	6.1693599	13.7700768
C	1.1070721	5.8675062	12.8223229
C	2.5663343	10.3139122	10.6105177
C	1.1537968	10.3148358	10.5141263
C	0.0461171	10.4109096	11.3859001
C	-0.1719534	10.5265881	12.7791681
C	0.7385222	10.5144509	13.8678738
C	2.1327621	10.4645560	14.0197546
C	3.2330682	10.4110990	13.1454294
C	3.4050792	10.3447390	11.7527583
Si	5.0514750	6.7868349	14.2188538
Si	0.3832910	5.3639616	9.9468017
O	3.0266250	2.4958925	12.9984704
C	1.8449897	6.2027654	15.2337037
C	-0.2539715	5.5361529	13.3444225
Si	3.4267075	10.5557691	8.9267433
H	0.8049539	10.2112783	9.4912615
H	-0.8773262	10.3632885	10.8182120
Si	-1.8970296	11.1942459	13.2505467
H	0.2464840	10.5307554	14.8350574
H	2.4333020	10.4111611	15.0619373
H	4.1723660	10.3377273	13.6825146
H	4.4536015	10.2490114	11.5009348
C	6.1960482	5.2490782	14.5224911
C	4.7826057	7.6571059	15.8700149
C	6.1090006	7.9421556	13.1698171
C	-0.4271732	3.6026966	9.9635010
C	-0.9774731	6.6097389	9.5312567

C	1.5267459	5.3800259	8.4454596
C	4.0056442	1.8193295	12.1895771
C	2.3697706	1.5560048	13.8641869
C	2.2584205	5.1768600	16.0818287
C	1.1164849	7.2470261	15.7985989
C	-0.4610983	4.4330348	14.1760676
C	-1.3677566	6.2982953	13.0016747
C	3.1378396	9.0769204	7.7362642
C	2.6227409	12.1260394	8.1838506
C	5.3188613	10.7882382	9.0350002
C	-1.7318528	13.0984202	13.2655092
C	-3.1987688	10.7838730	11.9110331
C	-2.3829938	10.6731774	15.0241377
C	6.7773738	4.7556383	13.1981940
C	5.4784516	4.0877738	15.2021860
C	7.3542368	5.6779324	15.4286271
H	4.0747881	8.4810484	15.7491077
H	5.7246165	8.0775624	16.2327566
H	4.3823744	6.9978466	16.6427729
H	6.2958007	7.5397509	12.1714863
H	7.0778471	8.1236218	13.6432005
H	5.6154310	8.9065947	13.0465778
H	-1.8151154	6.5778592	10.2292016
H	0.9468660	5.2548895	7.5276239
H	2.2764084	4.5848371	8.4789511
C	-1.7635425	3.5720223	10.7033201
H	0.1091026	1.5744416	10.5147591
C	-0.6870631	3.1689596	8.5170085
C	0.5163147	2.5904836	10.6062619
H	-1.3723462	6.4108682	8.5302679
H	-0.5810500	7.6298099	9.5240931
H	2.0587031	6.3301727	8.3647648
H	2.6757364	1.7646690	14.8947253
C	4.2176337	0.4767376	12.8570492
H	4.9011546	2.4407549	12.1512418
H	3.6057136	1.7075459	11.1764950
H	1.2907179	1.6985031	13.7787185
C	2.8286416	0.1827707	13.4100536
H	2.8204646	4.3470313	15.6708793
C	1.9672299	5.1947199	17.4368120
C	0.8226327	7.2754001	17.1535428
H	0.7679139	8.0677119	15.1783569
C	-1.7253347	4.0977481	14.6306570
H	0.3867293	3.8314429	14.4821804

H	-1.2480643	7.1650607	12.3597581
C	-2.6370116	5.9705250	13.4546083
H	3.3058803	8.1982250	8.3752850
C	1.7189871	8.9797474	7.1761508
C	4.1329877	8.9859420	6.5771859
C	6.1027741	9.5548568	9.4867675
C	5.8167886	12.0360494	9.7635316
H	1.6137652	11.7939003	7.9011237
C	2.4437794	13.2745122	9.1758307
C	3.3063005	12.6223560	6.9104408
H	5.5567297	10.9369187	7.9712483
H	-2.7345732	13.4682058	13.5210208
C	-1.3646568	13.6680570	11.8969098
C	-0.7676216	13.6163086	14.3302337
C	-2.4936109	9.1702051	15.2564789
H	-3.3704946	8.7538044	14.7549560
C	-4.5075268	11.5595971	12.0687854
H	-2.7374395	11.1479595	10.9831517
C	-3.4912188	9.2998302	11.7169987
H	-1.5440862	11.0363907	15.6335566
C	-3.6313157	11.3809963	15.5527825
H	5.9955547	4.4990988	12.4757162
H	7.3894231	3.8588441	13.3623540
H	7.4184667	5.5052242	12.7290685
H	5.0645399	4.3747925	16.1721297
H	6.1822486	3.2629251	15.3788631
H	4.6652308	3.6956418	14.5850539
H	7.9216405	6.5132302	15.0106769
H	8.0553643	4.8437216	15.5602087
H	7.0068073	5.9725998	16.4218188
H	-2.4919262	4.2497862	10.2512707
H	-1.6669547	3.8389904	11.7561166
H	-2.1894852	2.5609484	10.6563149
H	-1.2121730	2.2051999	8.5101078
H	0.2362706	3.0444224	7.9475434
H	-1.3181912	3.8831775	7.9800252
H	0.6487062	2.7944932	11.6718169
H	1.5040014	2.5925852	10.1336590
H	2.8301255	-0.5409815	14.2253655
H	4.9448533	0.5653505	13.6681735
H	4.5732457	-0.2803901	12.1578860
H	2.1754358	-0.1940814	12.6191921
H	2.3025170	4.3804223	18.0699844
C	1.2486352	6.2487618	17.9816399

H	0.2554013	8.1047837	17.5609258
H	-1.8542191	3.2324160	15.2712678
C	-2.8233414	4.8651306	14.2684447
H	-3.4827187	6.5830394	13.1659973
H	1.4646015	9.8573073	6.5743082
H	0.9604425	8.8777839	7.9539656
H	1.6243232	8.1054957	6.5227974
H	3.9574350	8.0690021	6.0035785
H	5.1724306	8.9682221	6.9070575
H	4.0235233	9.8213045	5.8804334
H	5.4148544	12.9532743	9.3300403
H	6.9093556	12.0991987	9.7042181
H	5.7560657	8.6327510	9.0150493
H	7.1663965	9.6703954	9.2495404
H	6.0370183	9.4016643	10.5657524
H	5.5499054	12.0334875	10.8231017
H	3.4019987	13.6964165	9.4880307
H	1.9171061	12.9574295	10.0774920
H	1.8681732	14.0877914	8.7196503
H	3.3463981	11.8588391	6.1307375
H	4.3329905	12.9468247	7.1042098
H	2.7716887	13.4842500	6.4956592
H	-0.3843078	13.3114991	11.5696210
H	-1.3203056	14.7621695	11.9323424
H	-2.0879297	13.3963248	11.1236846
H	-1.0490688	13.2993661	15.3378857
H	-0.7436867	14.7116646	14.3282093
H	0.2517783	13.2671145	14.1463265
H	-4.5349414	11.0289009	15.0493405
H	-2.6028681	8.9461255	16.3236176
H	-1.6233234	8.6212688	14.8923335
H	-5.0676406	11.2336888	12.9481808
H	-5.1536839	11.3946034	11.1996080
H	-4.3496839	12.6362246	12.1588038
H	-2.5823971	8.7196753	11.5461412
H	-4.1478767	9.1408404	10.8544699
H	-3.9988766	8.8797444	12.5890206
H	-3.5858711	12.4653056	15.4299957
H	-3.7626420	11.1768432	16.6211202
H	1.0196813	6.2676859	19.0408043
H	-3.8147040	4.6038300	14.6195692

[Li(thf)(η^5-L^{Pb})Er(η^8-COT^{TIPS})] (8)

Pb	3.6334426	6.3346826	10.9929974

Er	1.7207071	8.4904844	12.3724043
C	3.4519536	6.4980669	13.2857980
C	1.3908609	5.9725580	11.4468209
Li	2.5675758	4.4582300	12.6869697
C	2.1388842	6.2666830	13.7910137
C	1.0699981	5.9928471	12.8422382
C	2.5712934	10.1691306	10.6071198
C	1.1591775	10.0864484	10.5048135
C	0.0542908	10.1609305	11.3823009
C	-0.1607361	10.3218259	12.7736413
C	0.7529642	10.3444921	13.8607829
C	2.1487869	10.3498442	14.0210446
C	3.2436807	10.3339079	13.1401442
C	3.4108942	10.2734437	11.7441610
Si	5.0366554	6.8508225	14.2256743
Si	0.3514259	5.4828384	9.9617037
O	2.9874582	2.5994091	13.0223198
C	1.8225223	6.2637847	15.2567753
C	-0.2864479	5.6247717	13.3537307
Si	3.4210546	10.4811978	8.9265459
H	0.8182725	9.9275259	9.4879019
H	-0.8716216	10.0518864	10.8272317
Si	-1.8584127	11.0598602	13.2367559
H	0.2578399	10.3531951	14.8261829
H	2.4498614	10.3053096	15.0626032
H	4.1876535	10.2961423	13.6711458
H	4.4609063	10.2272122	11.4881033
C	6.1764699	5.3029411	14.5110217
C	4.7868778	7.7107421	15.8850735
C	6.1109056	7.9905076	13.1750450
C	-0.4200544	3.7023060	9.9802730
C	-1.0393786	6.6873727	9.5355876
C	1.4951145	5.5124768	8.4609881
C	3.9689442	1.9288686	12.2114567
C	2.3331391	1.6532072	13.8838942
C	2.2815987	5.2353192	16.0777154
C	1.0542798	7.2634617	15.8485130
C	-0.4673483	4.5024581	14.1653885
C	-1.4187069	6.3569830	13.0091206
C	3.1553736	9.0493815	7.6740185
C	2.5740955	12.0571616	8.2513504
C	5.3091540	10.7493990	9.0318725
C	-1.6061369	12.9556777	13.2341003
C	-3.1774896	10.7111187	11.8964733

C	-2.3685512	10.5867754	15.0169951
C	6.7458179	4.8172660	13.1782874
C	5.4704958	4.1350431	15.1912378
C	7.3441060	5.7238925	15.4094091
H	4.0729752	8.5312195	15.7792967
H	5.7312084	8.1329319	16.2395498
H	4.3993641	7.0437737	16.6577167
H	6.2772312	7.5894385	12.1725247
H	7.0893088	8.1408817	13.6393626
H	5.6466224	8.9696892	13.0613925
H	-1.8708964	6.6455719	10.2401049
H	0.9148785	5.3847687	7.5438441
H	2.2517417	4.7236278	8.4900336
C	-1.7643581	3.6448856	10.7036401
H	0.1557723	1.6851662	10.5323353
C	-0.6548001	3.2592037	8.5320549
C	0.5356263	2.7107127	10.6354715
H	-1.4358764	6.4643981	8.5403477
H	-0.6622305	7.7133306	9.5169742
H	2.0170542	6.4675174	8.3815353
H	2.6352635	1.8615090	14.9155095
C	4.1877872	0.5859424	12.8757631
H	4.8618988	2.5538992	12.1742463
H	3.5687974	1.8170557	11.1984591
H	1.2535887	1.7900191	13.7961377
C	2.8001586	0.2834657	13.4273927
H	2.8718295	4.4377089	15.6443206
C	1.9986587	5.2094046	17.4342411
C	0.7692724	7.2478065	17.2055852
H	0.6684326	8.0748605	15.2410408
C	-1.7253624	4.1206140	14.6013297
H	0.3950346	3.9240222	14.4757497
H	-1.3082644	7.2439805	12.3954932
C	-2.6816631	5.9792920	13.4391202
H	3.2950948	8.1444078	8.2811455
C	1.7564954	8.9902446	7.0594448
C	4.1883581	8.9938025	6.5455428
C	6.1147309	9.5280438	9.4778852
C	5.7942656	12.0037513	9.7578788
H	1.5641157	11.7121717	7.9883586
C	2.4003829	13.1734817	9.2797135
C	3.2137597	12.5971819	6.9730543
H	5.5391950	10.9040168	7.9673131
H	-2.5922984	13.3705910	13.4844158

C	-1.2138716	13.4954579	11.8604475
C	-0.6227844	13.4467728	14.2941131
C	-2.5632244	9.0958352	15.2681381
H	-3.4598605	8.7218925	14.7679069
C	-4.4328567	11.5738699	12.0383884
H	-2.6874656	11.0319708	10.9671238
C	-3.5719081	9.2493650	11.7169448
H	-1.5093711	10.9088873	15.6212786
C	-3.5720288	11.3723254	15.5396486
H	5.9576066	4.5684161	12.4601699
H	7.3555875	3.9169320	13.3308520
H	7.3859962	5.5673376	12.7090228
H	5.0715661	4.4130371	16.1699660
H	6.1792166	3.3109026	15.3506311
H	4.6495879	3.7451385	14.5833659
H	7.9120871	6.5585986	14.9916943
H	8.0426163	4.8860189	15.5310487
H	7.0059950	6.0145434	16.4069442
H	-2.5015964	4.3046030	10.2395294
H	-1.6872146	3.9181699	11.7560749
H	-2.1675015	2.6245053	10.6556794
H	-1.1615136	2.2856531	8.5227159
H	0.2769426	3.1503148	7.9733567
H	-1.2932935	3.9594403	7.9855362
H	0.6411984	2.9117335	11.7045719
H	1.5316156	2.7394001	10.1813492
H	2.8050356	-0.4415705	14.2415729
H	4.9144730	0.6767488	13.6871468
H	4.5478324	-0.1674971	12.1748920
H	2.1495536	-0.0958210	12.6355095
H	2.3699879	4.3942941	18.0459740
C	1.2424822	6.2211032	18.0077278
H	0.1704780	8.0432555	17.6351517
H	-1.8333697	3.2431012	15.2291398
C	-2.8428300	4.8568828	14.2353524
H	-3.5430645	6.5689243	13.1491651
H	1.5341265	9.8927735	6.4827383
H	0.9664567	8.8672765	7.8019267
H	1.6781204	8.1421538	6.3704042
H	4.0095941	8.1133612	5.9182950
H	5.2146598	8.9302083	6.9087347
H	4.1248693	9.8673986	5.8910904
H	5.3798200	12.9154245	9.3247713
H	6.8857462	12.0793187	9.6929207

H	5.7757625	8.5996035	9.0128965
H	7.1742675	9.6571525	9.2296405
H	6.0608312	9.3782479	10.5579364
H	5.5329302	12.0002713	10.8187567
H	3.3572041	13.6130811	9.5707297
H	1.9136841	12.8171798	10.1892277
H	1.7873054	13.9824071	8.8667861
H	3.2417230	11.8540395	6.1730051
H	4.2410009	12.9321592	7.1452880
H	2.6548464	13.4609490	6.5959439
H	-0.2506914	13.0920732	11.5372376
H	-1.1197947	14.5867646	11.8850302
H	-1.9481088	13.2494237	11.0890022
H	-0.9100356	13.1422557	15.3040237
H	-0.5655346	14.5409578	14.2882655
H	0.3847621	13.0663188	14.1078909
H	-4.4951650	11.0741551	15.0367945
H	-2.6892478	8.8932751	16.3377692
H	-1.7237679	8.4950876	14.9145837
H	-5.0154569	11.2977590	12.9204089
H	-5.0855608	11.4378068	11.1690555
H	-4.2063762	12.6391818	12.1128524
H	-2.7078891	8.6061920	11.5434693
H	-4.2440134	9.1310556	10.8597514
H	-4.1017847	8.8710379	12.5948543
H	-3.4595606	12.4511564	15.4122379
H	-3.7161005	11.1813342	16.6088091
H	1.0201854	6.2065967	19.0684166
H	-3.8295839	4.5595464	14.5705802

Cp^-

C	0.0055900	1.1971500	0.0000100
C	1.1402800	0.3646300	-0.0000000
C	-1.1368100	0.3752500	-0.0000000
C	0.6991400	-0.9717800	0.0000100
C	-0.7081800	-0.9652300	-0.0000100
H	2.1743400	0.6953000	-0.0003700
H	-2.1677700	0.7155400	-0.0000700
H	1.3331700	-1.8530600	0.0002700
H	-1.3504000	-1.8405700	-0.0001600
H	0.0106600	2.2828000	0.0002000

[(η^5-Cp)La(η^8-COT^{TIPS})]

La	0.0302200	0.0067400	-2.5713400

C	1.1399500	0.4506200	0.0156700
C	-0.5870200	-1.0415800	-0.0172100
C	-0.0670500	1.1807700	0.0198800
C	-1.1344200	0.2592100	0.0006600
C	1.1832500	-1.3708900	-4.6286700
C	-0.2174600	-1.4190800	-4.8623200
C	-1.3076100	-0.5203000	-4.8672100
C	-1.5266800	0.8654500	-4.6374800
C	-0.6067400	1.9117200	-4.3666300
C	0.7885300	2.0166400	-4.1993900
C	1.8758000	1.1180100	-4.1911900
C	2.0356500	-0.2729000	-4.3522100
Si	2.0163600	-3.0777900	-4.6963800
H	-0.5760500	-2.4303100	-5.0352300
H	-2.2301400	-1.0669100	-5.0360100
Si	-3.3406300	1.3947800	-4.8562100
H	-1.0809700	2.8734600	-4.2080600
H	1.0955100	3.0288400	-3.9547100
H	2.8103100	1.6115900	-3.9425900
H	3.0652900	-0.5629900	-4.1859000
C	1.6139000	-4.0384000	-3.0842200
C	1.3295500	-4.0179000	-6.2167600
C	3.9226700	-3.0120900	-4.8094500
C	-3.6610000	1.6586600	-6.7173800
C	-4.5013800	-0.0050400	-4.2579900
C	-3.6542200	3.0682900	-3.9857600
H	1.9878500	-3.3645900	-2.2982200
C	0.1242500	-4.2534000	-2.8252800
C	2.3488400	-5.3700400	-2.9264200
C	4.6606300	-2.6137600	-3.5298700
C	4.4735400	-2.2499600	-6.0145900
H	0.3364400	-4.3696400	-5.9017700
C	1.1285000	-3.1497700	-7.4592600
C	2.1485300	-5.2575200	-6.5816500
H	4.1565400	-4.0737000	-4.9777800
H	-4.7094100	1.9762200	-6.8013500
C	-3.4938700	0.3864200	-7.5451800
C	-2.7857600	2.7754700	-7.2846600
C	-3.5456600	3.0226800	-2.4630800
H	-4.3832600	2.4760700	-2.0218800
C	-5.9846800	0.3317900	-4.4180100
H	-4.2955500	-0.8326200	-4.9505500
C	-4.2308300	-0.5249000	-2.8484000
H	-2.8436000	3.7132100	-4.3508000

C	-4.9566100	3.7537100	-4.4027600
H	-0.3199800	-4.9134100	-3.5768700
H	-0.4470400	-3.3218300	-2.8396400
H	-0.0371000	-4.7248500	-1.8495300
H	2.2151200	-5.7660400	-1.9136900
H	3.4227100	-5.2897900	-3.1072400
H	1.9540300	-6.1230400	-3.6133800
H	4.0789600	-2.6330300	-6.9575600
H	5.5648800	-2.3377700	-6.0577900
H	4.3204500	-3.1763700	-2.6577300
H	5.7350200	-2.7980100	-3.6386500
H	4.5469700	-1.5526300	-3.2942600
H	4.2333800	-1.1847500	-5.9734400
H	2.0821600	-2.7939100	-7.8575500
H	0.5128900	-2.2718200	-7.2592000
H	0.6448800	-3.7277600	-8.2545200
H	2.2857700	-5.9419100	-5.7424900
H	3.1425100	-4.9827200	-6.9463000
H	1.6582100	-5.8175200	-7.3852700
H	-2.4697200	0.0075300	-7.4860100
H	-3.7080800	0.5818000	-8.6016000
H	-4.1640500	-0.4140700	-7.2212600
H	-2.9422100	3.7294100	-6.7743800
H	-2.9985800	2.9349500	-8.3473400
H	-1.7243900	2.5256700	-7.1978200
H	-5.8355900	3.1999700	-4.0659500
H	-3.5661100	4.0329200	-2.0398100
H	-2.6225700	2.5443200	-2.1238500
H	-6.3031800	1.0856100	-3.6936400
H	-6.6024100	-0.5562300	-4.2458700
H	-6.2241900	0.7093700	-5.4149500
H	-3.1953900	-0.8547800	-2.7248400
H	-4.8721200	-1.3834800	-2.6202900
H	-4.4298600	0.2354400	-2.0896600
H	-5.0371900	3.8710000	-5.4853900
H	-5.0187100	4.7538600	-3.9600300
H	-2.1875900	0.5052400	0.0282200
H	-0.1579100	2.2579500	0.0607200
C	0.8191900	-0.9223800	-0.0057000
H	-1.1467900	-1.9675800	0.0008200
H	2.1364000	0.8698000	0.0521800
H	1.5261600	-1.7409800	0.0186400

References

1. S. M. Cendrowski-Guillaume, G. Le Gland, M. Nierlich and M. Ephritikhine, *Organometallics*, 2000, **19**, 5654-5660.
2. M. Saito, M. Nakada, T. Kuwabara and M. Minoura, *Chem. Commun.*, 2015, **51**, 4674-4676.
3. O. T. Summerscales, F. G. N. Cloke, P. B. Hitchcock, J. C. Green and N. Hazari, *Science*, 2006, **311**, 829-831.
4. G. Sheldrick, *Acta Cryst. A*, 2015, **71**, 3-8.
5. G. Sheldrick, *Acta Cryst. C*, 2015, **71**, 3-8.
6. O. V. Dolomanov, L. J. Bourhis, R. J. Gildea, J. A. K. Howard and H. Puschmann, *J. Appl. Crystallogr.*, 2009, **42**, 339-341.
7. F. Aquilante, J. Autschbach, R. K. Carlson, L. F. Chibotaru, M. G. Delcey, L. De Vico, I. Fdez. Galván, N. Ferré, L. M. Frutos, L. Gagliardi, M. Garavelli, A. Giussani, C. E. Hoyer, G. Li Manni, H. Lischka, D. Ma, P. Å. Malmqvist, T. Müller, A. Nenov, M. Olivucci, T. B. Pedersen, D. Peng, F. Plasser, B. Pritchard, M. Reiher, I. Rivalta, I. Schapiro, J. Segarra-Martí, M. Stenrup, D. G. Truhlar, L. Ungur, A. Valentini, S. Vancoillie, V. Veryazov, V. P. Vysotskiy, O. Weingart, F. Zapata and R. Lindh, *J. Comput. Chem.*, 2016, **37**, 506-541.
8. J. P. Perdew, M. Ernzerhof and K. Burke, *J. Chem. Phys.*, 1996, **105**, 9982-9985.
9. F. Weigend and R. Ahlrichs, *Phys. Chem. Chem. Phys.*, 2005, **7**, 3297-3305.
10. B. Metz, H. Stoll and M. Dolg, *J. Chem. Phys.*, 2000, **113**, 2563-2569.
11. M. Dolg, H. Stoll, A. Savin and H. Preuss, *Theor. Chim. Acta*, 1989, **75**, 173-194.
12. F. Weigend, *Phys. Chem. Chem. Phys.*, 2006, **8**, 1057-1065.
13. O. Treutler and R. Ahlrichs, *J. Chem. Phys.*, 1995, **102**, 346-354.
14. R. S. Mulliken, *J. Chem. Phys.*, 1955, **23**, 1833-1840.
15. J. Jusélius, D. Sundholm and J. Gauss, *J. Chem. Phys.*, 2004, **121**, 3952-3963.
16. H. Fliegl, S. Taubert, O. Lehtonen and D. Sundholm, *Phys. Chem. Chem. Phys.*, 2011, **13**, 20500-20518.
17. S. Taubert, D. Sundholm and J. Jusélius, *J. Chem. Phys.*, 2011, **134**, 054123.
18. A. Schäfer, A. Klamt, D. Sattel, J. C. W. Lohrenz and F. Eckert, *Phys. Chem. Chem. Phys.*, 2000, **2**, 2187-2193.